Draft version September 24, 2025
Typeset using LaTeX **default** style in AASTeX7.0.1

Radio Stars in the Era of New Observatories

Lynn D. Matthews [1]

[1] *Massachusetts Institute of Technology Haystack Observatory, 99 Millstone Road, Westford, MA 01886 USA*

ABSTRACT

An international conference *Radio Stars in the Era of New Observatories* was held at the Massachusetts Institute of Technology Haystack Observatory on 2024 April 17–19. The conference brought together more than 60 researchers from around the world, united by an interest in using radio wavelength observations to explore the physical processes that operate in stars (including the Sun), how stars evolve and interact with their environments, and the role of radio stars as probes of our Galaxy. Topics discussed at the meeting included radio emission from cool and ultracool dwarfs, extrasolar space weather, stellar masers, thermal radio emission from evolved stars, circumstellar chemistry, low frequency observations of the Sun, radio emission from hot stars, applications of very long baseline interferometry techniques to stellar astrophysics, stellar explosive events, the detection of radio stars in the latest generation of widefield sky surveys, the importance of radio stars for understanding the structure and evolution of the Milky Way, and the anticipated applications for stellar astrophysics of future radio observatories on the ground and in space. This article summarizes research topics and results featured at the conference, along with some background and contextual information. It also highlights key outstanding questions in stellar astrophysics where new insights are anticipated from the next generation of observational facilities operating at meter through submillimeter wavelengths.

Keywords: meeting summary, Stars — stars: AGB and post-AGB – stars: winds, outflows – circumstellar matter – radio lines: stars

1. BACKGROUND AND MOTIVATION FOR THE WORKSHOP

The detection and characterization of electromagnetic emission at meter through submillimeter wavelengths (hereafter collectively referred to as "radio" emission) have the ability to provide a broad range of unique insights into the physical processes that govern the workings of stars spanning virtually every type and evolutionary phase (e.g., G. A. Dulk 1985; R. M. Hjellming 1988; J. L. Linsky 1996; S. M. White 2000; M. Güdel 2002; J. M. Paredes 2005). Stellar radio emission can be either thermal or nonthermal in nature and may arise from a range of different mechanisms, including bremsstrahlung (free-free), gyromagnetic radiation, plasma emission, electron cyclotron maser (ECM) instabilities, and spectral lines [including hyperfine atomic transitions, rotational transitions of molecules, and radio recombination lines (RRLs)]. While these various types of radio emission typically comprise only a small fraction of a star's total luminosity, radio wavelength studies provide unique diagnostics of a wide range of phenomena in stars and stellar systems that cannot be probed by any other means.

As illustration of this, during the past decade the current generation of radio telescopes has been pivotal in enabling a rapid pace of exciting discoveries in numerous branches of stellar astrophysics, ranging from the identification of new classes of hot, magnetic stars to unveiling evidence of the ubiquitous role of low-mass companions to shaping evolved star winds, to the discover of radiation belts beyond the solar system and the unveiling of new clues to the longstanding puzzle of how the solar corona is heated. These discoveries are at the same time feeding a growing anticipation for the scientific potential of the next-generation radio facilities currently being built or planned. Motivated by this, a 3-day workshop "Radio Stars in the Era of New Observatories" was convened at the Massachusetts Institute of Technology (MIT) Haystack Observatory in Westford, Massachusetts from 2024 April 17–19 (hereafter "Radio Stars 3" or "RS3"). As described in L. D. Matthews (2013) and L. D. Matthews (2019), previous Radio Stars conferences were hosted by

Email: lmatthew@mit.edu

Haystack Observatory in 2012 and 2017, respectively, each showcasing the latest advances in solar and stellar radio astrophysics.

RS3 sought to bring together stellar astrophysicists (including observers, theorists, modelers, software developers, and instrument builders) from a variety of sub-disciplines to share the latest developments in the study of stars across the Hertzsprung-Russell (H-R) diagram, with a focus on discoveries that exploit the unique potential of the latest generation of radio instruments. Additional underlying goals were taking a forward look at what observations with the next generation of radio instruments are likely to enable for solar and stellar astrophysics and the identification of areas that will require research and development in order to maximally exploit new facilities for solar and stellar science.

2. MEETING OVERVIEW

The RS3 conference was attended by 61 registered participants representing 12 countries. The science program comprised 12 invited talks, 25 contributed oral presentations, and 22 posters. The complete program and presentation abstracts can be viewed on the meeting web site[2]. Copies of many of the presentation slides and posters are also accessible through the meeting web page.

G. Umana (Instituto Nazionale Di Astrofisica, Italy) opened the conference with an invited review that provided a framework for the conference and introduced many of the topics and themes that recurred throughout the meeting. Subsequent oral and invited presentations were organized into twelve additional sessions: (I) Circumstellar Chemistry; (II) Stellar Interactions and Environments; (III) Evolved Star Atmospheres; (IV) Stellar Masers as Tool for Galactic Science and Stellar Astrophysics; (V) Radio Stars with the Highest Angular Resolution; (VI) The Sun as a Radio Star; (VII) Space and Space Weather; (VIII) Ultracool Dwarfs; (IX) Radio Emission from Hot Stars; (X) Radio Star Surveys; (XI) Stellar Explosions; (XII) Looking Back and Looking Ahead. In addition, during several short oral sessions, poster authors delivered brief summaries of their presentations.

The current review is intended to capture a snapshot of the state of stellar radio astronomy by summarizing many of the research topics and highlights presented at the meeting. I also attempt to identify some of the common themes and topical synergies that emerged. In addition, I draw attention to some of the outstanding questions in stellar astrophysics that were identified at the conference and where key insights are anticipated from the next generation of radio wavelength instruments. To maintain cohesiveness, the content is organized by subject area rather than strictly by scientific session. For the benefit of the more general reader, some brief contextual and historical information is included throughout.

3. THE SUN AS A RADIO STAR

For decades, observations of radio emission of the Sun have been providing unique diagnostics of the dynamic solar atmosphere, the Sun's magnetic field, coronal mass ejections (CMEs), space weather, and other phenomena (e.g., G. A. Dulk 1985; D. E. Gary 2023). Multiple mechanisms are known to produce solar radio emission emission, including thermal bremsstrahlung, thermal gyroresonance, nonthermal gyrosynchrotron, (nonthermal) plasma emission, and ECM emission. As illustrated in a series of RS3 presentations, the collective insights gleaned from observations of each of these various types of emission have increased markedly in the past few years thanks to recent advances in instrumentation, data processing techniques, and modeling.

Radio observations of the Sun at different frequencies probe different layers of the solar atmosphere and are thus complementary in advancing our understanding of various solar phenomena. As described below, discussion of the radio Sun at RS3 primarily focused on GHz and MHz frequencies (i.e., centimeter and meter wavelengths). Solar radio emission in the GHz range samples the chromosphere, transition region, and lower corona, and arises from a combination of optically thin thermal bremsstrahlung from the corona, optically thick chromospheric emission (e.g., H. Zirin et al. 1991), together with possible gyrosynchrotron and gyroresonant emission from active regions. Solar emission at MHz frequencies is primarily a diagnostic of the solar corona and arises from thermal bremsstrahlung (from the "quiet" Sun), as well as plasma emission [3] associated with solar activity.

[2] https://www.haystack.mit.edu/radio-stars-2024

[3] Plasma emission is produced when high-speed electrons propagate into dense plasma, creating beam-driven instabilities that lead to the production of Langmuir waves and electromagnetic transverse waves, whose frequency scales as the square root of the plasma density.

3.1. *Advances in Low-Frequency Solar Radio Imaging*

Historically the Sun has been a notoriously difficult source to image using radio interferometers. Among the myriad challenges are the need to sample a wide variety of spatial scales (from a few arseconds, to a degree or more), coupled with the time-varying nature of the solar atmosphere, which generally precludes the use of earth rotation synthesis to improve u-v sampling. In addition, images of high dynamic range are needed to enable the simultaneous study of both weak and strong emission components. The limited angular resolution of most radio images to date has also hindered detailed comparisons with data at other wavelengths [ultraviolet (UV), optical, X-ray], while accurate flux calibration has remained challenging owing to the high signal strengths, which may introduce nonlinearities in the signal chain (e.g., D. Kansabanik 2022a). As a consequence of these factors, many solar radio studies historically focused on the analysis of dynamic spectra rather than images, with an emphasis on the study of bright bursts from the active Sun. However, this situation has evolved dramatically over the past decade (e.g., D. E. Gary 2023), and as showcased in the solar astronomy session at RS3, the past few years have sustained significant improvements in solar radio imaging capabilities.

The session on the Sun opened with an invited talk by D. Oberoi (National Centre for Radio Astrophysics/Tata Institute of Fundamental Research), who provided an overview of recent progress in the domain of low-frequency (<300 MHz) solar physics, with a focus on results from the Murchison Widefield Array (MWA). The MWA is an interferometric array of 128 elements ("tiles"), each comprising 16 dipole antennas, located in the Outback of Western Australia. It operates in the frequency range 80–300 MHz (S. J. Tingay et al. 2013). As described by Oberoi, the MWA (and its 32-tile predecessor) has been instrumental in demonstrating the power of low frequency radio observations for revealing dynamic behaviors on the Sun (in both time and frequency), even during periods where it appears "quiet" at visible, UV, or X-ray wavelengths (e.g., D. Oberoi et al. 2011).

Given the wide bandwidths and high time and frequency resolution of MWA solar data, they are extraordinarily rich in information content, but this also presents challenges. For example, Oberoi noted that imaging each time and frequency slice from just 5 minutes of an MWA solar observations obtained with 0.5 s time resolution could in principle spawn more than half a million images. Additionally, the range of brightness temperatures manifested by phenomena observable in the MWA wavebands—ranging from thermal bremsstrahlung emission from the quiet Sun to plasma emission from active phenomena—span roughly ten orders of magnitude ($T_{\rm B} \sim 10^3$ K to 10^{13} K). At the same time, the range of circular polarization can range from $\sim 0 - 100\%$ (see D. Kansabanik 2022). Consequently, one needs high-fidelity, high dynamic range, spectro-polarimetric snapshot images to fully exploit the scientific potential of these data sets.

An important advantage of the MWA is its excellent instantaneous u-v coverage, which in turn enables snapshot imaging of rapidly time-varying phenomena. A key breakthrough in leveraging this has been the development of automated imaging pipelines which are able to routinely achieve dynamic ranges of a few hundred, to as high as $\sim 10^5$ (S. Mondal et al. 2019). This marks an improvement of 1–2 orders of magnitude compared with previous solar images at similar frequencies. Recently, polarimetric imaging has also been incorporated into these pipelines (D. Kansabanik 2022; D. Kansabanik et al. 2022b, 2023a).

As showcased in the poster presentation of D. Kansabanik (Johns Hopkins University/National Centre for Radio Astrophysics/Tata Institute of Fundamental Research), another general purpose radio array well-suited to solar imaging is MeerKAT, situated in the Karoo region of South Africa. MeerKAT comprises 64 antennas, each 13.5 m in diameter, with baselines up to ∼8 km. Kansabanik's team has recently been exploring MeerKAT's potential to obtain high-fidelity spectroscopic snapshot imaging of the solar corona across the frequency range 880–1670 MHz (D. Kansabanik et al. 2024b; Figure 1). They have already performed MeerKAT commissioning observation with the Sun in the sidelobes of the primary beam (as a means to attenuate the strong solar signal) and are investigating strategies to introduce suitable attenuation in the signal chain to enable accurately flux-calibrated observations for the case where the Sun is within the primary beam.

3.2. *New Insights into the Coronal Heating Problem: WINQSEs*

Another advance highlighted by Oberoi was the progress in our ability to study weak nonthermal emission from the Sun. He reported that recent studies have successfully exploited a continuous wavelet transform-based method to identify and image features with brightnesses of order a *milli-SFU* [4] Such sensitivity levels have been achieved only

[4] A solar flux unit (SFU) is equal to 10^4 Jy.

rarely in the past (e.g., S. Krucker & A. O. Benz 2000), with more typical detection limits being ∼10 SFU in late 1990s (e.g., C. Mercier & G. Trottet 1997) and ∼1 SFU a decade ago (e.g., R. Ramesh et al. 2013). These newly detected emissions have been given the moniker "weak impulsive narrowband quiet Sun emissions" (WINQSEs) and are thought to be the radio counterparts of the nanoflares which have long been postulated to explain the heating of the solar corona by providing a vehicle to extract the required energy from the solar magnetic field (S. Mondal et al. 2021, 2022, 2023aa; R. Sharma et al. 2022; S. Bawaji et al. 2023).

One advantageous features of WINQSEs is that the associated radio emission is coherent, providing a much more readily observable means to explore weaker energies (down to "picoflare" levels) than is accessible with traditional nanoflare studies based on X-ray or UV radiation. Typical brightness temperatures of the WINQSEs lie in the range $\sim 10^3 - 10^4$ K and counterparts have been identified in the extreme UV (S. Mondal 2021). However, Oberoi noted that WINQSEs seem to be ubiquitous even when the Sun is deemed "quiet" based on other such traditional diagnostics. Because the WINQSEs that occur at a given time may number in the thousands, Oberoi and his collaborators have developed machine learning methods for the detection and characterization of these events (S. Bawaji et al. 2023). Surprisingly, WINQSEs appear spatially resolved in images, despite the a priori expectation that they should be compact; this is likely a consequence of scattering (see S. Bawaji et al. 2023).

3.3. *ECM Emission from the Sun*

Among the different emission mechanisms known to contribute to solar radio emission, ECM emission has remained the least well-studied. A poster by S. White (Air Force Research Laboratory) presented results from a recent study to assess the prevalence of ECM emission from solar radio bursts at GHz frequencies (see also S. M. White et al. 2024). This work was motivated by the desire to better understand the impact of solar bursts and space weather on bands where Global Navigation Satellite Systems (GNSS) operate. White's team used multi-frequency data from over 3000 bursts obtained using the Nobeyama Radio Polarimeters between 1998 and 2023. Since optically thick (and incoherent) synchrotron emission has a spectrum that rises with increasing frequency below 5 GHz, cases where the 1.0 GHz flux exceeded the flux at 2.0 or 3.75 GHz were flagged as incompatible with a synchrotron mechanism and identified as likely arising from (coherent) ECM emission. S. M. White et al. estimated that ∼75% of solar bursts at 1.0 GHz and ∼50% of bursts at 2.0 GHz are dominated by coherent emission—a significantly larger fraction than previously believed. For 23 flares, brightness temperatures exceeded 10^{11} K, definitively ruling out an incoherent emission mechanism.

The putative ECM emission is seen to be strongly variable, sometimes lasting for hours after the initial impulsive burst phase. Generally, it is highly circularly polarized (though rarely as high as 100%). White's team also reported evidence that solar ECM emission may be dominated by "spikes" (i.e., forests of short-duration, narrow frequency burst events; see e.g., G. A. Dulk 1985), making them distinctly different from the ECM phenomena associated with solar system planets. To put this in context, the brightest of the bursts studied by S. M. White et al. (2024) would produce mJy-level fluxes at a distance of 10 pc. This work raises the question of whether the ECM emission seen associated with brown dwarfs and magnetically active OB stars (Sections 5, 8.2) is in fact more analogous to the ECM emission seen in solar spike bursts as opposed to that in solar system planets.

3.4. *Solar Coronal Mass Ejections (CMEs) and Space Weather*

Solar CMEs are explosive events that result in the ejection of large quantities of magnetized plasma. They are also the major drivers of space weather in the solar system. In some cases the ejected plasma reaches the Earth's atmosphere and can have a significant effect on the near-Earth environment. The study of CMEs at radio wavelengths is uniquely powerful since radio observations provide the only means available to constrain the magnetic fields of CME plasma via remote-sensing techniques. Such measurements of the magnetic field are critical for understanding the propagation and evolution of these events and for forecasting their geoeffectiveness.

Traditionally, the only means of characterizing the magnetic field of the CME plasma has been through in situ measurements using satellites. However, this is limited to the near-Earth environment where satellites are located, leaving very little advance warning for forecasting possible impacts of these events on Earth. As discussed at the meeting, this has motivated the development of methods to measure CMEs much closer to the Sun using radio techniques, with the ultimate goal of tracking the magnetic field energy all the way from the low corona into interplanetary space.

3.4.1. *Plasma Emission from CME-Driven Shocks*

Some solar CMEs travel at speeds approaching (or even exceeding) the Alfvén speed, driving shocks that accelerate electrons to nonthermal energies, and giving rise to outbursts of plasma emission at both the fundamental frequency and the first harmonic (so-called type II radio bursts; e.g., J. P. Wild 1950; J. Magdalenić et al. 2020). Each harmonic is sometimes seen to be split into two bands (e.g., J. Magdalenić et al. 2020), although the explanation for this has remained controversial. Two competing models attribute this to either independent emission sites (e.g., D. J. McLean 1967) or to emission arising from slightly different plasma densities in the upstream and downstream regions of the shock front, respectively (e.g., N. Chrysaphi et al. 2018). As described by D. Oberoi, recent MWA imaging results (S. Bhunia et al. 2023) have provided rare but compelling evidence that at least in some cases the band splitting is caused by emission from independent emission sites in the shock.

3.4.2. *Gyromagnetic Emission from CMEs*

In addition to plasma emission associated with accompanying type II bursts (Section 3.4.1), CMEs give rise to gyrosynchrotron emission, produced by the interaction of mildly relativistic electrons with the ambient magnetic field. However, owing to its relative weakness, gyrosynchrotron emission can easily be overpowered by the presence of much brighter plasma emission from the active Sun in solar images with limited dynamic range, making it difficult to detect. Indeed, following the first successful detection of the gyrosynchrotron emission from a CME by T. S. Bastian et al. (2001) using the Nançay Radioheliograph, there have been only a handful of subsequent detections reported, and all were rare, highly energetic events with speeds in excess of 1000 km s^{-1}. However, as described at the RS3 meeting, this has begun to change dramatically, thanks to the high dynamic range images now routinely achievable with the MWA (see D. Kansabanik et al. 2023b, 2024a and references therein).

S. Mondal (New Jersey Institute of Technology) reported that the first detection of gyrosynchrotron emission associated with a CME using the MWA was a "regular and unremarkable" event, with a propagation speed of only ∼400 km s^{-1}—significantly slower than the handful of highly energetic events detectable with previous generations of instruments (S. Mondal et al. 2020). As discussed by Mondal, and in a poster presentation by D. Kansabanik, the high dynamic range images now possible with the MWA raise the hope of being able to make such measurements regularly (D. Kansabanik et al. 2023a).

Despite its advantages for CME studies, a drawback of the MWA is that it does not observe the Sun consistently, making it difficult to amass statistics on CME events. However, as discussed by Mondal, the new solar-dedicated backend on the Owens Valley Radio Observatory's Long Wavelength Array (OVRO-LWA) is helping to remedy this. An automated imaging pipeline is now producing daily images of the Sun from OVRO-LWA data, enabling the study of gyrosynchrotron emission from CMEs on a routine basis (S. Mondal et al. 2023b). Mondal also cited one recently discovered case where the OVRO-LWA spectrum of the CME and the quiet solar disk are distinctly different, and moreover, where the spectral energy distribution (SED) of the CME appears to be consistent with *thermal gyroresonance emission*. This represents the first time thermal gyroresonance has been detected from a CME.

Another breakthrough in the study of gyrosynchrotron emission described by D. Oberoi comes from the ability to now use both Stokes I and Stokes V information simultaneously to constrain models (D. Kansabanik et al. 2023b, 2024a). Recently, there has been a positive Stokes V detection of CME for the first time (at ν ∼100 MHz; D. Kansabanik et al. 2024a), a result that challenges current models and their underlying assumptions, namely that the plasma has a homogeneous distribution along the line-of-sight and that the electron distribution can be characterized by an isotropic pitch angle.

3.4.3. *Faraday Rotation Measurements*

At heights of $\gtrsim$10 $R_\odot$ from the solar surface, gyrosynchrotron emission from CMEs starts to become too faint to be detectable. However, in this domain, measurements of the Faraday rotation imposed by the CME plasma on the emission from background sources offers an alternative method for measuring coronal magnetic fields. A poster by D. Kansabanik highlighted work that he and his colleagues have done to explore this topic, including the possibility of exploiting the wide MWA field-of-view for Faraday rotation measurements (see also D. Oberoi et al. 2023). Unfortunately, one current challenge is the low source density of suitable background objects at MWA frequencies (currently ~ 0.05 sources deg^{-2}).

As described in the presentations by S. Mondal and D. Oberoi, a key future goal is to not only measure the magnetic field at specific locations in the corona, but over a wide range of coronal heights by using a combination multi-frequency

measurements from different instruments to create a "movie" of the outward propagation of a CME. For example, the current Karl G. Jansky Very Large Array (VLA) operates at GHz frequencies and can be used to measure the magnetic field at $\sim 5 - 20 R_\odot$ via Faraday rotation measurements (e.g., J. E. Kooi et al. 2017, 2021; S. Mondal et al. 2023a), while the OVRO-LWA is capable of providing complementary detections of gyrosynchrotron from coronal plasma at $\lesssim 5 R_\odot$ (see Section 3.4.2). Crucially, such measurements would supply constraints on the vector magnetic field and significantly advance our ability to forecast space weather.

3.4.4. *Advances in CME Modeling*

While the quality of radio wavelength CME data has improved dramatically in the past decade, the derivation of magnetic field properties from these measurements is strongly dependent on the accurate modeling of the observed emission, which remains challenging. A poster presentation by D. Kansabanik showcased a recent breakthrough in using spectral modeling of MWA measurements of gyrosynchrotron emission to characterize the magnetic field of CME plasma within $\lesssim 10\ R_\odot$ (D. Kansabanik et al. 2023b). His team's work has also demonstrated that polarimetric observations can be used as a tool for resolving the degeneracies that traditionally result from the large numbers of degrees of freedom in gyrosynchrotron models (D. Kansabanik et al. 2024a).

3.5. *Other Solar Phenomena*

3.5.1. *Coronal Holes*

As described by D. Oberoi, recent MWA observations have revealed new information about so-called coronal holes. Owing to their low densities, these regions are expected to appear as dark structures in radio images. However, at MWA frequencies, multiple examples have been found that transition from dark at higher MWA frequencies to bright at frequencies $\lesssim$145 MHz (M. M. Rahman et al. 2019). According to Oberoi, this is likely the result of refraction effects.

3.5.2. *Propagation Effects in the Solar Plasma*

Another powerful application of low-frequency radio observations discussed by Oberoi is to constrain propagation effects (refraction and scattering) in the solar plasma. He cited a multi-frequency MWA study of an active region by R. Sharma & D. Oberoi (2020) that found the measured position of the region to shift as a function of frequency, and where the nonlinearities of these shifts suggest significant inhomogeneities in the plasma. Propagation effects can also be constrained by the study of changes in the surface area of an active source as a function of time, and Oberoi was part of a team that discovered what appear to be quasi-periodic pulsations in intensity in type III solar bursts[5] that are anti-correlated with variations in the size of the region (A. Mohan et al. 2019). These quasi-periodic pulsations are thought to arise from oscillations in the magnetic field.

3.5.3. *Linear Polarization of Solar Bursts*

Perhaps one of the most surprising solar results presented at the RS3 meeting was the announcement by D. Kansabanik of the first robust detection of linearly polarized emission from the Sun at meter wavelengths (S. Dey et al. 2022). As noted above, the meter-wavelength radio emission detected from solar bursts primarily emanates from the corona via the plasma emission mechanism. It has long been assumed that any polarization signatures associated with such bursts would be circularly polarized, since linear polarization is expected be erased by differential Faraday rotation.

Low-frequency polarization studies of solar bursts have been carried out since the 1950s, but nearly all have been based on dynamic spectra from non-imaging instruments. And while there have been a handful of published claims for the detection of linear polarization based on those studies (e.g., K. Akabane & M. H. Cohen 1961; R. V. Bhonsle & L. R. McNarry 1964), these were greatly outnumbered by non-detections (e.g., R. J. M. Grognard & D. J. McLean 1973; A. Boischot & A. Lecacheux 1975), leading to the emergence of a consensus that linear polarization signatures detected from solar bursts were the result of instrumental polarization leakage. Indeed, this interpretation had become so well established that it formed part of the basis for the calibration of solar instruments (cf. P. I. McCauley et al. 2019; D. E. Morosan et al. 2022). However, for the MWA, Kansabanik and collaborators recently developed a new, robust polarization calibration pipeline that does not depend on this assumption (D. Kansabanik et al. 2022, 2023a).

[5] Type III events are short-lived bursts of $\lesssim$10 s duration, often linked with open magnetic field lines.

This work was motivated by the detection of variable Stokes Q emission from a solar burst observed with the MWA, a result that cannot be readily explained by calibration errors.

As described by Kansabanik, multiple lines of evidence point to the MWA-detected linearly polarized signal being real. First, the putatively polarized emission is spatially confined to compact active regions, with no linearly polarized emission seen over the quiet portions of the solar disk. Second, the linear polarization fraction is both large (∼20–25%) and variable in time and frequency. Third, the linear polarization angles are distinct in two observed active regions.

To obtain additional verification, Kansabanik and his team obtained observations of the Sun using two different instruments at the same time and frequency: the MWA and the Giant Metrewave Telescope (GMRT). They detected a type III burst during this campaign, with linear polarization independently detected by both telescopes. Kansabanik also reported that to date, a few additional examples of type I, type II, and type III solar bursts have been examined, and all show evidence of linear polarization. He stressed that a next step is to understand what mechanism is responsible for producing this linearly polarized emission. Such work by his team is ongoing.

3.6. *The Next Decade of Solar Radio Science*

Oberoi noted that owing to both practical and financial reasons, it is unclear that a next-generation dedicated solar radio imaging array will be built in the next decade. Nonetheless, as was amply illustrated by the recent results presented at RS3, the outlook for solar radio science appears to be bright, thanks to the current generation of solar instruments (see, e.g., Table 1 of D. E. Gary 2023), along with continuing efforts to exploit current and planned general-purpose radio instruments for solar science.

To increase the scientific impact of these facilities for solar work, Oberoi advocated for the expanded use of triggered observations to make more efficient use of telescope time. He also suggested building and distributing solar imaging pipelines to the wider science community as a means to make solar radio data more accessible and more widely used. Additional items on Oberoi's "wish-list" for future solar work included: (i) high-fidelity polarimetric imaging of the Sun (both quiescent and active emission); (ii) more sensitive studies of gyrosynchrotron emission and Faraday rotation associated with CMEs; (iii) further study and modeling of slowly varying (hours to days) solar emission, including coronal holes and streamers; (iv) more sophisticated modeling to better understand propagation effects in the solar plasma.

4. STELLAR ACTIVITY

4.1. *Active Binaries*

So-called "active binaries"—a category that includes RS CVn and Algol-type systems—are well-known emitters of non-thermal radio continuum that undergo periods of solar-like magnetic activity, including strong flares (e.g., B. H. Foing 1990). However, as stressed in the presentation by G. Umana, we still lack a full understanding of the physical processes underlying their time-varying radio emission, including the relation between their "quiescent" and "active" phases.

Historically, modeling of the radio wavelength SEDs, coupled with high-resolution imaging using very long baseline interferometry (VLBI) techniques, have served as important means of exploring the physics of active binaries (e.g., R. L. Mutel et al. 1985, 1987). An example of the latest in such efforts was described by W. Golay [Center for Astrophysics | Harvard & Smithsonian (CfA)/University of Iowa], who spoke about recent radio observations of the active binary HR 1099, a chromospherically active, RS CVn type system in which Zeeman Doppler imaging had previously revealed large spots on the subgiant primary star (spectral type K1 IV; S. S. Vogt et al. 1999). Using the VLA, W. W. Golay et al. (2023) measured the radio SED of HR 1099 between 15–45 GHz and found evidence for the presence of a B-field of strength 240±50 G. However, the binary was unresolved by the VLA, leaving open the question of exactly where in the system the radio emission arises. To answer this, Golay and collaborators obtained 6 epochs of data with the Very Long Baseline Array (VLBA) at 22.2 GHz over the course of 3 months, scheduled so as to sample different phases of the binary's 2.8 day orbit. The data rule out the emission arising from the inter-binary region and instead show it is most likely linked to the magnetically active primary (W. W. Golay et al. 2024). Using their individual VLBA epochs, they also divided the data into time slices and fit a linear velocity model in the corotating frame of the binary to search for plasma motions consistent with a stellar CME. Five of six epochs show no evidence for motion, while the sixth (the only epoch containing a flare) shows tentative evidence for motion at a level of 3σ, but the result is inconclusive, leaving the definitive detection of extrasolar CMEs still elusive (see also Section 7.1).

4.2. *The Güdel-Benz Relation*

An empirical relation between the 5 GHz radio luminosity and the soft X-ray luminosity known as the Güdel-Benz relation (M. Guedel & A. O. Benz 1993; A. O. Benz & M. Guedel 1994) has long been known to hold for active stars and solar flares. However, after several decades, the physics underpinning this relation is still not fully understood. Further, as described at the RS3 meeting, some additional puzzles have recently emerged. For example, as described by G. Umana, observations at 144 MHz with the LOw Frequency Array (LOFAR) have led to the identification of a sample of active binaries with *coherent* radio emission that unexpectedly follows the Güdel-Benz relation (H. K. Vedantham et al. 2022). On the other hand, certain recently detected millimeter flare stars appear to deviate from Güdel-Benz (see Section 4.6). Umana predicted that the expanded frequency coverage provided by a combination of the Square Kilometer Array (SKA), the Next Generation VLA (ngVLA), and an upgraded ALMA (see Sections 18.1.4, 18.1.3, 18.1.2, respectively) will help to more comprehensively model the SEDs of these stars to better constrain the plasma properties and the energy densities of the emitting particles. These facilities should also provide the sensitivity to identify radio coronae across a wider range of stellar types than is accessible currently and enable variability studies of large new samples of stars, including searches for variability cycles similar to those of the Sun.

4.3. *VLBI Studies of M Dwarfs*

The typical high levels of magnetic activity of M dwarfs leads to their frequent detection as nonthermal radio emitters. Fortuitously, this nonthermal emission often exhibits sufficiently high brightness temperatures to enable studies of these stars using VLBI techniques, including measurements of their space motions. As an illustration of this, P. Boven (Joint Institute for VLBI European Research Infrastructure Consortium/University of Leiden) described recent astrometric VLBI work on M dwarfs using a technique known as MultiView. MultiView compensates for the phase corruption caused by the Earth's atmosphere through the use multiple phase reference calibrators distributed around the target of interest, coupled with two-dimensional interpolation of phase corrections to the position of the target (M. J. Rioja et al. 2017). At centimeter wavelengths, MultiView enables decreasing by at least an order of magnitude the milliarcsecond-level astrometric errors caused by the ionosphere that would occur if only a single calibrator were used, thereby allowing astrometric accuracy comparable with *Gaia* (see P. Boven et al. 2023).

Boven discussed two examples of VLBI studies of M star systems that exploited MultiView. One was GJ3789A/B, a system originally discovered in the 8.4 GHz astrometric survey of G. C. Bower et al. (2009), but for which the data had remained unpublished because of the unsolved puzzle of their unusual astrometric residuals. Using new follow-up VLBA observations, Boven and colleagues obtained multi-epoch astrometry for GJ3789A/B from which they were able to determine a precise astrometric solution and a set of orbital parameters. The new measurements also show that the system lies at a larger distance than originally thought and that the radio emission originates from the secondary star. However, an outstanding puzzle is that the deprojected radial velocities inferred from the radio astrometric solution are much higher than independently measured radial velocities.

Boven concluded by suggesting that an "ideal" next-generation telescope array for future astrometric VLBI studies of M dwarfs would be comprised of phased arrays of small dishes equipped with wideband receivers. This could provide improved sensitivity (and thus access to more calibrators with close proximity to the target), coupled with the ability to observe both calibrators and science target simultaneously within the field-of-view.

4.4. *Quiescent Coronal Emission from Zero Age Main Sequence Stars*

J. Climent (University of Valencia) presented VLBI measurements of the coronally active zero age main sequence star AB Dor A, a young, rapidly rotating K dwarf that is part of a quadruple system. Motivated by the previous VLBI observations of J. B. Climent et al. (2020), C. E. Brasseur et al. (2024) were able to product a 3D model of the star's coronal magnetic field, and from this, create synthetic radio images over the course of the stellar rotation period. The models are able to reproduce the morphology and extent of the coronal emission seen in 8.4 GHz VLBI maps, which reaches $\sim 8 - 10 R_\star$, making it significantly more extended than the solar corona.

4.5. *Coherent Emission*

In addition to the "quiescent" radio emission from active stars, which is generally attributed to gyrosynchrotron radiation (see above), a growing numbers of such stars are seen to exhibit activity in the form of coherent bursts. These bursts are generally attributed to ECM instabilities and exhibit short duration (pulse-like) emission profiles that are narrow in frequency and display high levels of circular polarization (up to 100%). Importantly, the radio

frequency at which these coherent bursts are observed is directly proportional to the magnetic field strength, providing a means of quantifying the magnetic field. Back in 2021, P. Leto et al. published an empirical relation for early-type magnetic stars (see Section 8.2), linking the nonthermal radio luminosity with the ratio of the magnetic flux to the rotation period. As discussed at the RS3 meeting, this correlation has now been shown to also hold for a wide range of objects with stable, dipole-dominated magnetospheres, including ultracool dwarfs (UCDs; see Section 5) and the planet Jupiter. Indeed, the topic of coherent emission from active stars was raised in multiple presentations and sessions at RS3 (see Sections 3.3, 8.2, 5), highlighting commonalities in the underlying physics across different classes of stars exhibiting coherent bursts, including the presence of strong magnetic fields to aid the production of energetic particles.

4.6. *Flaring at Millimeter Wavelengths*

To date, most of the radio wavelength work on stellar flaring has focused on the centimeter bands. In contrast, as pointed out by C. Tandoi (University of Illinois), stellar flaring in the millimeter regime is relatively unexplored, and until recently, only ∼30 stellar millimeter flares were documented in the literature (see S. Guns et al. 2021 and references therein). However, this has begun to change, thanks in part to datasets available from Cosmic Microwave Background (CMB) experiments, which simultaneously provide the frequency coverage, aerial coverage, temporal sampling, and angular resolution required for blind transient searches, including the identification of stellar flares. For example, Tandoi reported on the detection of 111 millimeter flares from a sample of 66 stars based on data from the South Pole Telescope (SPT; C. Tandoi et al. 2024), including main sequence stars, evolved stars, and interacting binaries. He argued that the emission is most likely to be synchrotron generated by the initial impulsive phase of the flare during which particles are accelerated, although the measured spectral indices of individual sources show a range of values. In cross-comparing with other wavelengths, Tandoi's team found that nearly all of their detected stars are X-ray active, although they do not appear to follow a Güdel-Benz type of correlation between their radio and X-ray fluxes (see Section 4.2). The poster presentation by E. Biermann (University of Pittsburgh) also demonstrated how the high sensitivity and large aerial coverage provided by data from the Atacama Cosmology Telescope (ACT) have been leveraged to perform blind transient searches at millimeter wavelengths and provide a powerful means of identifying flares and transient emission from stellar sources including M dwarfs, RS CVn variables, and even a classical novae (E. Biermann et al. 2025).

As described by G. Umana, the recent detection of millimeter wavelength flares from M dwarfs using ALMA has also opened a new window for understanding stellar activity (M. A. MacGregor et al. 2018, 2020, 2021), Crucially, the ALMA wavelength bands provide access to high-energy (MeV) particles immediately after they are accelerated in the atmosphere. Such particles are not accessible with centimeter-wavelength observations. Building a more comprehensive understanding of the properties of flares detected in the millimeter regime is thus expected to be a rich area for future study.

4.7. *Future Prospects in Active Star Research*

Umana predicted that future research on active stars will benefit enormously from the broad frequency coverage (∼300 MHz to $\gtrsim$100 GHz) that will be provided by a combination of current and planned radio facilities such LOFAR, the upgraded GMRT (uGMRT), the VLA, ALMA, the SKA (both SKA1-Low and SKA1-Mid), and the ngVLA (see Section 18). She stressed the value of this kind of multi-frequency approach, as the lower-frequency bands (up to a few GHz) probe the coherent emission from stellar bursts (enabling characterization of the plasma density and magnetic field strength); the intermediate frequencies (∼10-40 GHz) sample the gyrosynchrotron emission emitted by accelerated particles; finally, the ALMA frequency bands (35–950 GHz), along with the higher-frequency ngVLA bands (up to 116 GHz), supply access to the most strongly accelerated particles (including possible synchrotron emission) while simultaneously providing the sensitivity to study thermal emission from the stellar chromospheres.

5. RADIO EMISSION FROM ULTRACOOL DWARFS (UCDS)

UCDs encompass low-mass objects ranging from late-type M dwarfs to brown dwarfs (i.e., objects with spectral types later than M7). UCDs thus bridge the transition between stars and gas-giant planets, and along this sequence of objects the onset of planet-like auroral/magnetospheric emission is seen. As discussed in the invited review by M. Kao (Lowell Observatory), as well as by several other speakers, radio wavelength studies have emerged as one of the most powerful means of improving our understanding of these objects.

Brown dwarfs were first discovered to be radio emitters by E. Berger et al. (2001), who detected bursting emission in the 4–8 GHz range that violated the Güdel-Benz relation (see Section 4.2) by more than 4 orders of magnitude. Now, more than 20 years later, such behavior has been established as relatively common among brown dwarfs and other UCDs (e.g., P. K. G. Williams et al. 2014). However, it remains a longstanding puzzle as to how UCDs, which are fully convective, can support the strong magnetic fields inferred from their radio emission.

As noted by J. Climent, as of 2023 there were approximately 30 UCDs that had been detected at GHz frequencies (E. Berger et al. 2001; J. Tang et al. 2022 and references therein; M. M. Kao & J. S. Pineda 2022; K. Rose et al. 2023), plus two more at MHz frequencies (see Section 5.1). He stressed, however, that presently these represent only a relatively small fraction of the total number of targets searched (see, e.g., Figure 3 of Y. Cendes et al. 2022). Furthermore, as of the RS3 meeting there had not yet been any confirmed, direct detection of radio emission from bona fide exoplanets (Section 6.1) or star-exoplanet interactions (see Sections 6.1, 6.2), although several of the aforementioned radio-detected UCDs are in the $\sim 12 - 70\ M_{\rm Jupipter}$ mass range.

5.1. *Brown Dwarf Auroral Emission*

Radio-detected brown dwarfs tend to be rapid rotators, and the dominant component of their radio emission is typically rotationally modulated and strongly circularly polarized. These traits are now interpreted as the hallmarks of ECM emission arising from powerful aurorae, linked to kG strength magnetic fields (e.g., G. Hallinan et al. 2015; M. M. Kao et al. 2016; J. S. Pineda et al. 2017). As noted by Kao, the dynamo regions in these objects are thought to be similar to scaled-up analogs of those in exoplanets (see also Section 6).

One recent development in the radio studies of brown dwarfs is the detection of two extremely cold (<1000 K) brown dwarfs at MHz frequencies using LOFAR, one of which represents the first direct discovery of a brown dwarf using radio observations (H. K. Vedantham 2020, 2023). A persistent puzzle, however, is that the inferred strength magnetic fields of these cold brown dwarfs are significantly weaker than predicted by the prevailing dynamo model paradigm.

T. W. H. Yiu (ASTRON/Netherlands Institute for Radio Astronomy) described a recent follow-up study of one of the LOFAR-detected brown dwarfs (the T dwarf binary WISEP J101905.63+652984.2; H. K. Vedantham et al. 2023) in an attempt to identify a spectral cut-off in its periodic emission. For this purpose, Yiu and collaborators obtained observations with the VLA, GMRT, and LOFAR over multiple epochs. Surprisingly, during 10 epochs of LOFAR observations no pulse was detected at a strength comparable to the originally detected level of ∼10 mJy (see H. K. Vedantham et al. 2023). Moreover, 9 of 10 epochs showed no evidence for any type of pulse. There was also no detected radio emission in either the VLA or the GMRT data. Despite this, after combining the available data from all epochs, Yiu et al. identified a new 0.8 hr periodicity in the data, unrelated to the originally detected pulses. The nature of this periodic emission is unclear, although Yiu noted that if it is interpreted as being linked to rotational period, it is interestingly close to the predicted breakup limit for the brown dwarf.

5.2. *Radiation Belts*

In addition to auroral emission (Section 5.1), radio-detected brown dwarfs are seen to display a weaker, quiescent component of radio emission with little or no polarization, and whose origin and nature had remained enigmatic (e.g., P. K. G. Williams et al. 2013). Presentations at the meeting showcased recent observational evidence from two independent groups that this emission arises from *radiation belts*, analogous to those observed in all of the strongly magnetized planets in our Solar System. This is the first empirical confirmation of an idea described at the previous Radio Stars conference by P. Williams (see P. K. G. Williams 2018; L. D. Matthews 2019).

Kao and her collaborators recently used the High Sensitivity Array (HSA), a global VLBI array of radio telescopes spread across Europe and North America, to spatially resolve the radio emission of the UCD LSR J1835+3259 at 8.4 GHz (M. M. Kao et al. 2023). The team obtained three images over the course of a year with angular resolution ∼0.5 mas, revealing a double-lobed, axisymmetric structure with an extent of $\sim 24 R_{\rm Jupiter}$ and a morphology similar to the Jovian radiation belts (Figure 2). This provided compelling evidence that the steady, quiescent emission associated with this system is synchrotron, arising from the presence of radiation belts of magnetically charged particles and a dipole-ordered magnetic field. Additionally, during 2 out of 3 observing epochs, circularly polarized "burst" emission (attributed to an aurora) was detected by Kao's team from a location between the two radio lobes (Figure 2). LSR J1835+3259 is rapidly rotating, with a period of ∼2.8 hr, and this burst emission was seen to be rotationally modulated. The authors derived a magnetic field strength of 3 kG at $\sim 12 R_{\rm Jupiter}$, decaying in strength as a function of radial distance, r, as $\sim r^{-3}$. Kao noted that the origin of such strong magnetic fields remains a puzzle, as it cannot readily be explained by convected thermal energy.

As reported by J. Climent, LSR J1835+3259 was also independently observed at 5 GHz by J. B. Climent et al. (2023) using the European VLBI Network (EVN). The J. B. Climent et al. observations confirmed the double-lobed structure seen by M. M. Kao et al. (2023), but the lower frequency of their observations allowed sampling a distinct population of electrons in the radiation belt. Climent's team also detected a second auroral-like emission component whose properties appear consistent with the earlier model predictions of P. Leto et al. (2021). Climent noted that overall the observed radio emission components in LSR J1835+3259 appear well described by the type of model presented in the poster by R. Kavanagh, namely an oblique rotator coupled with an auroral ring (see Section 15.2).

Kao estimated that ∼30% of T dwarfs have radiation belts, but noted that a persistent puzzle is where their energetic electrons are originating from. Younger, hotter objects are not found to be more likely to exhibit evidence of radiation belts compared with older and colder UCDs, in contrast to earlier predictions. However, binarity *does* enhance the likelihood of detecting radiation belt emission (M. M. Kao & J. S. Pineda 2025). Kao predicted that future observations, especially observations with facilities like the ngVLA (Section 18.1.3) are likely to reveal that radiation belts are far more ubiquitous among different classes of stellar objects than previously thought, including in magnetic massive stars (see Section 8.2). She also pointed out that spatially resolved observations of additional brown dwarfs to directly search for radiation belts (see Section 5.2) would be both challenging and time-consuming and suggested instead that future radio surveys of spatially *unresolved* emission could serve as a useful means of compiling better statistics and improving more generally our understanding of the magnetic field properties of UCDs (M. M. Kao & E. L. Shkolnik 2024).

5.3. *Measuring Physical Parameters of UCDs from VLBI Astrometry*

Another topic discussed by J. Climent was how astrometric VLBI techniques can benefit the study of UCDs. He noted that prior to 2023, among radio-detected UCDs only 3 had been detected using VLBI (J. Forbrich & E. Berger 2009; J. Forbrich et al. 2016a; Q. Zhang et al. 2020). Nonetheless, the results were particularly powerful, enabling dynamical mass measurements, parallax (distance) and proper motion measurements, and in one case, the discovery of an extrasolar planet (S. Curiel et al. 2020; see also Section 13). Climent presented new preliminary results from additional, ongoing VLBI studies of UCDs, including an astrometric monitoring campaign of the substellar T6 dwarf WISEP J112254.73+255021.5. By measuring the radio light curve, Climent and collaborators aim to pin down the rotational period of this object, which has, until now, been a subject of controversy in the literature (cf. P. K. G. Williams et al. 2017).

6. RADIO EMISSION FROM AND EXOPLANETS AND THEIR HOST STARS

During the 2017 Haystack Radio Stars meeting (L. D. Matthews 2019), radio wavelength searches for exoplanets were called out as an exciting new frontier in astrophysics. This area of research has seen substantial growth over the past several years. Although as of the RS3 meeting there still had not been a definitive detection of exoplanet radio emission (see below), several interesting, related developments were reported.

Attempts to detect radio emission associated with exoplanets can largely be divided into two categories: *direct detection* of an exoplanet, or detection of the *signatures of star-planet interaction*. Consensus was that the latter is probably easier and likely to happen sooner—and may even be within the reach of existing facilities, but efforts targeting both approaches were described at the meeting.

6.1. *Efforts to Directly Detect Radio Emission from Exoplanets*

C.-M. Cordun (ASTRON) described her team's effort to detect low-frequency (<40 MHz) emission associated with ECM-generated aurorae in hot Jupiters using LOFAR. Such a detection would represent a major breakthrough by allowing the possibility to directly measure the magnetic field strength of an exoplanet. One of the most promising candidates for detection is thought to be τ Boötis b, a gas giant of ∼6 Jupiter masses orbiting an F-type main sequence star at a separation of 0.049 au. Unfortunately, ionospheric scintillation, human-made radio frequency interference (RFI), contamination from sidelobes of other bright sources, and cosmic noise from galactic background sources all pose challenges for imaging observations at these low frequencies. The deepest images of τ Boötis b obtained to date by Cordun's team reach RMS noise levels of 225 mJy, 80 mJy, and 40 mJy at 15.2 MHz, 27.0 MHz, and 37.7 MHz, respectively. The exoplanet remains undetected, but an important outcome is that the results demonstrate the feasibility of imaging observations at frequencies <40 MHz (C. M. Cordun et al. 2025). An ongoing LOFAR upgrade (see, e.g., E. Orrú et al. 2024) is expected to make the array a factor of two more sensitive and further bolster the chance of detection.

The poster presented by K. Ortiz Ceballos (CfA) described another direct search for exoplanet radio emission, in this case at frequencies between 4–8 GHz, using new and archival observations from the VLA (K. N. Ortiz Ceballos et al. 2024). Ortiz Ceballos and his colleagues examined a total of 77 nearby stellar systems (d <17.5 pc) known to host exoplanets (140 known in total). Radio emission was detected from one target (an M4 dwarf), but based on the radio luminosity and corresponding X-ray luminosity, the emission appears to be stellar in origin. Radio luminosity upper limits for the remaining targets are $L \lesssim 10^{12.5}$ erg s^{-1} Hz^{-1} (3σ), comparable to the lowest radio luminosities of UCDs (see Section 5).

6.2. *Searches for Radio Signatures of Star-Planet Interactions*

While direct radio detections of exoplanets have remained elusive, the past several years have also seen a rapid growth in interest in detecting the auroral-like signatures of star-planet interactions at radio wavelengths. As described by M. Kao, such detections would in principle have a unique advantage over the observations of star-planet interactions at optical or other wavelengths by enabling direct measurements of magnetic field strengths, viz. $\nu_{[\mathrm{MHz}]} \approx 2.8 B_{\mathrm{planet}}[\mathrm{Gauss}]$ (e.g., P. Zarka 1998), and thereby providing crucial tests of magnetic dynamo models for exoplanets (see e.g., R. D. Kavanagh et al. 2021; M. Pérez-Torres et al. 2021; J. S. Pineda & J. Villadsen 2023; C. Trigilio et al. 2023; J. R. Callingham et al. 2024).

The leading dynamo model (U. R. Christensen et al. 2009) unifies planetary and stellar dynamos by assuming that the thermal energy from the deep interior is what determines the energy density in the dynamo region. In this model the strength of the radio emission is expected to be proportional to the apparent size of the emitting object, but additionally depends on the properties of the stellar wind that impacts it (J. Saur et al. 2013). Kao emphasized that a consequence is that the magnetic fields of certain hot Jupiters are predicted to be 10–100 times higher than the one seen in Jupiter itself (R. K. Yadav & D. P. Thorngren 2017; P. W. Cauley et al. 2019). However, despite numerous attempts, these predictions have yet to be observationally confirmed; as of the RS3 meeting, no definitive cases of star-planet interactions had yet been unambiguously detected (e.g., Y. Cendes et al. 2022). Previously, J. D. Turner et al. (2021) reported a tentative detection of radio emission from the τ Boötis system in the 14–21 MHz range, but follow-up observations have so far failed to confirm this detection (e.g., J. D. Turner et al. 2024), suggesting that detectability may depend on the phase of the stellar activity cycle or other, as-yet-to-be determined factors. YZ Ceti is another system where radio emission that may be consistent with star-planet interaction has been reported, although so far the evidence remains inconclusive (J. S. Pineda & J. Villadsen 2023; J. S. Pineda et al. 2024; J. Villadsen et al. 2025).

Kao predicted that when the ngVLA comes online (Section 18.1.3), it will become possible to routinely directly observe satellite-induced aurorae on brown dwarfs and other UCDs through characteristic features in their dynamic spectra (cf. S. Hess et al. 2008). Once such cases are confirmed, these observations will help to anchor modeling of UCD magnetic fields and dynamo theories for both the high- and low-mass ends of the UCD population.

7. EXTRASOLAR SPACE WEATHER

7.1. *Extrasolar CMEs*

7.1.1. *CMEs from Main Sequence Stars*

The quest to directly detect CME-like events and the ejections of energetic particles from stars other than the Sun was discussed at both previous Haystack Radio Stars meetings (L. D. Matthews 2013, 2019). However, as of the time of the RS3 conference there still had not yet been an unambiguous detection of these phenomena beyond our solar system (see also Section 4.1). One challenge has been simultaneously achieving the necessary sensitivity (particularly in the presence of the strong terrestrial RFI environment), in combination with the time and frequency resolution required to identify signatures of such events. Additional factors may include the lack of coordinated, multi-wavelength data, and the fact that many searches to date have targeted M dwarfs, where the magnetic field may suppress associated radio emission at frequencies detectable from Earth-based radio observatories (J. J. Drake et al. 2016; J. D. Alvarado-Gómez et al. 2018). Yet another possibility discussed in the literature is that large-scale overlying magnetic fields in active stars may suppress CME emergence (J. D. Alvarado-Gómez et al. 2018; X. Sun et al. 2022).

I. Davis (California Institute of Technology) described her team's ongoing Space Weather Around Young Suns (SWAYS) project, aimed at overcoming these challenges. SWAYS is a dedicated, multiwavelength effort to monitor space weather from nearby solar-type stars and M dwarfs using the recently commissioned OVRO-LWA (I. Davis et al.

2024b). This instrument comprises 352 dipoles spread over an area spanning 2.5 km and operates in the 13–87 MHz range with 24 kHz spectral resolution (see also Section 3.4.2).

Davis emphasized that at present, the particle environments of active stars are very poorly constrained, which in turn significantly impacts our ability to understand processes such as abiotic chemistry in exoplanet environments and the retention of exoplanetary atmospheres. New efforts are therefore underway to use low-frequency radio emission as a tool for characterizing particle fluxes from stars known to host planets. In particular, the goal is to detect the extrasolar analog of type II and III radio bursts, whose radio emissions are produced by the plasma emission mechanism (see also Sections 3.4, 3.5). An advantageous characteristics of plasma emission is that the frequency at which it arises is related to the plasma density. Additionally, the structure of the emission seen in a dynamic spectrum will depend on the speed of the particles.

For their searches, Davis's team is employing the beam-forming mode of OVRO-LWA, which provides 1 ms time resolution, coupled with simultaneously obtained (and more sensitive) "slow-visibility" mode data with 10 s time resolution to aid in identification of candidate events. Events of interest are de-dispersed in the higher time resolution data in a manner analogous to pulsar searches. In parallel with the OVRO-LWA observations, candidate stars are observed at optical wavelengths using Flarescope, a fully-automated 0.5 m telescope designed to achieve photometric monitoring of bright stars with sub-millimagnitude precision on 5 minute timescales (I. Davis et al. 2023). At the time of the conference, reduction pipelines for the multi-wavelength data were being finalized.

Another effort to detect extrasolar CMEs using low-frequency observations was described by D. Konijn (ASTRON/Kapteyn Institute). He presented a progress report on an effort to identify signatures of such events in data from the LOFAR Two-Metre Sky Survey (LoTSS; T. W. Shimwell et al. 2019). LoTSS is a deep (83 μJy beam^{-1}), widefield (6035 deg^2) survey with high angular resolution (6″) over the frequency range 120–168 MHz and is expected to yield over 5 million sources. At the time of the meeting this already included data for ∼250,000 stars within 100 pc for which dynamic spectra with 8 s time resolution have been produced. Currently searches are being performed on Stokes I data so as not to bias against detection of unpolarized bursts.

Konijn presented one particularly interesting case [originally identified by meeting participant J. Callingham (ASTRON/Leiden University)] in which a bright burst was detected with an apparent drift rate of -0.35 MHz s^{-1} and emission that is 90% circularly polarized. The host star is a high proper motion M-type dwarf lying at $d \sim 40$ pc. The implied ejection speed would be ∼1000 km s^{-1}, making this a tantalizing candidate for a long-sought extrasolar analog to a type II solar burst (see Section 3.4.1). However, some caveats have prevented this event being unambiguously linked to a type II-like event. First, the harmonic is not seen in the data (though it may plausibly lie outside the observed band). Second, the degree of circular polarization is higher than is typical of solar type II bursts. Unexpectedly, linear polarization is also observed—though new results presented at the conference by D. Kansabanik now suggest that this may be unsurprising; see Section 3.5.3.

Konijn also described efforts to search for type III-like bursts in the LoTSS data. No such events have so far been identified, but as these are typically short-duration events ($\lesssim$10 s), a re-processing of the data to 1 s time resolution is underway to enhance the search. Konijn estimates that in total, ∼40 extrasolar type III bursts should be detectable at $\geq 10\sigma$ in the LoTSS survey (see also H. K. Vedantham 2020).

7.1.2. *CMEs from Young Stellar Objects (YSOs)*

An additional program to search for evidence of extrasolar CMEs—in this case associated with young stellar objects (YSOs)—was presented by J. Forbrich (University of Hertfordshire). Forbrich reminded us that highly energetic processes arise even in the earliest stages of star formation, making YSOs among the brightest stellar sources in both radio emission and X-rays. As was reported at the second Haystack Radio Stars meeting (see L. D. Matthews 2019), Forbrich and his collaborators have used high angular resolution observations with the VLA at 4–8 GHz to observe a single field in the Orion Nebula Cluster (ONC) for ∼30 hr, reaching an RMS noise level of 3μJy beam^{-1} and allowing them to identify nearly 700 sources (J. Forbrich et al. 2016b). Parallel X-ray observations were also obtained using *Chandra* (J. Forbrich et al. 2017). At the RS3 meeting, Forbrich described follow-up work to obtain multi-epoch VLBA observations of *all* sources in their sample, providing the means to investigate emission on sub-au scales within the ONC (J. Forbrich et al. 2021). Forbrich stressed that this effort has benefited substantially from recent VLBA upgrades (see Section 18.1.1), including the ability to perform software correlation of multiple sources within the primary beam, eliminating the need to limit focus to just one or two objects per pointing.[6]

Forbrich pointed out that while the rate of occurrence of X-ray megaflares from YSOs is reasonably well constrained (e.g., K. V. Getman et al. 2024 and references therein), the fraction of megaflares generating CMEs is still unknown, as are the parameters that may impact their detectability, such as viewing angle, plasma density, and timescales. His team is therefore using their VLBA data to search for CME signatures within a time window of a few days for targets exhibiting strong X-ray flares. Specifically, expected CME signatures associated with these megaflares are expected to include a rise and fall of the radio flux over several days after the X-ray event, and a spatial offset of the emission from the star on scales $\gtrsim$1 au. However, at the time of the meeting, despite having amassed a volume of VLBA data exceeding 20 TB, there was still no evidence of an unambiguous CME. A caveat noted by Forbrich is that the 5 GHz VLBA band in which they are observing (selected to maximize achievable sample size) is expected to be sensitive only to the most energetic CMEs owing to the high Lorentz factors needed to produce emission at this frequency.

7.2. *Winds from Cool Main Sequence Stars*

S. Bloot (ASTRON/Kapteyn Astronomical Institute) described recent work leveraging LOFAR to study the winds and space weather of M dwarfs. The stars included in her team's sample span the full range of M dwarfs, not just the very latest objects ($\leq$M7) categorized as UCDs (see Section 5). As noted by Bloot, stellar winds are important in the context of these stars, since they can determine the degree to which a planet interacts with its host star, whether orbiting planets can maintain an atmosphere, and whether planets may be able to produce detectable radio signatures. Stellar winds are also of vital importance from a stellar evolutionary perspective, carrying away angular momentum, impacting changes in rotation speed, and returning mass to the interstellar medium. However, the winds of low-mass main sequence stars are in general extremely tenuous, making them difficult to detect, particularly in the case of M dwarfs.

As described by Bloot, historically, the most successful method for characterizing M dwarf winds has been the study of atmospheric absorption lines in the UV toward the interstellar medium (ISM; e.g., B. E. Wood et al. 2002, 2021). Drawbacks of this method are that it requires a detailed understanding of the surrounding ISM and that it is limited to stars lying within $\lesssim$7 pc. The alternative approach used by Bloot and her collaborators instead utilizes free-free absorption at radio wavelengths to place upper limits on the mass-loss rate (see also J. Lim & S. M. White 1996). This in turn provides a direct upper limit on the density of the stellar wind. Since free-free absorption is stronger at lower frequencies, Bloot's team has used LOFAR detections of coherent (ECM) emission from M dwarfs at $\nu \sim$120 MHz, in combination with a simple stellar wind model that includes an estimate of the stellar magnetic field (S. Bloot et al. 2025). At the time of the meeting they had obtained mass-loss upper limits for 19 M dwarfs and were able to reach a sensitivity of 4$\times$ the solar-wind mass-loss rate, independent of distance.

8. RADIO EMISSION FROM HOT STARS

8.1. *Thermal Emission from Hot Massive Stars*

Hot massive stars have winds powered by radiation pressure on lines from metallic elements (J. I. Castor et al. 1975) and the groundwork for the use of thermal radio emission to study their resulting mass-loss rates dates back to the seminal papers by N. Panagia & M. Felli (1975) and A. E. Wright & M. J. Barlow (1975). With an underlying assumption of spherical symmetry,[7] these analytic models lead to the classical prediction that the SEDs of OB stars should follow $S_\lambda \propto \lambda^{-0.6}$, where S_λ is the flux density at a given radio wavelength, λ. A net result is that in the case of free-free opacity, longer wavelengths (lower frequencies) "see" a larger photosphere. Thus observing a range in wavelengths effectively "scans" the geometric layers of the atmosphere/wind. The presentation by R. Ignace (East Tennessee State University) focused on ongoing efforts to address the added complexity of the deviations from spherical symmetry that occur in the envelopes of hot massive stars and how these ultimately shape the winds and outflows.

One example discussed by Ignace is the case of so-called corotating interaction regions (CIRs; e.g., S. R. Cranmer & S. P. Owocki 1996). CIRs are expected to occur when bright or dark spots occur on the surface of a massive star, leading, respectively, to the formation of low- and high-speed streams. Rotation of the star causes these flows to be accelerated at different rates, leading to the formation of corotating structures which then collide. Ignace and his colleagues have explored the question of how far out these regions persist and how radio observations may be able to

[6] Typically the field-of-view of VLBI observations is limited to $\sim 10^{-4}$ times the primary beam size as a result of time and frequency smearing away from the adopted phase center; see A. H. Bridle & F. R. Schwab (1989).

[7] A nonspherical but axisymmetric wind will produce the same SED slope, but with a change in resulting flux level (J. Schmid-Burgk 1982).

provide constraints through the comparison of radio flux variations over time with geometric models (R. Ignace et al. 2020).

In an update from the 2017 Radio Stars meeting (see L. D. Matthews 2019), Ignace pointed to the study by C. Erba & R. Ignace (2022) that models how the combination of synchrotron emission (occurring the presence of a strong magnetic field) and free-free absorption from colliding wind massive binaries can effect changes in their radio SEDs. He also discussed the role of wind clumping in biasing the derived mass-loss rates for hot massive stars. Ignace noted that the presence of clumping will not necessarily change the SED *shape*; however, depending on the porosity, there may be wavelength-dependent variability. Work on this topic remains ongoing.

8.2. *Magnetic Massive Stars*

Approximately 10% of massive (O and B) main sequence stars are now known to possess stable, large-scale, kG level surface magnetic fields (e.g., J. H. Grunhut et al. 2012). Often these fields are found to be simple, axisymmetric dipolar configurations aligned with the rotation axis of the star. As discussed in the invited presentation by B. Das (Commonwealth Scientific and Industrial Research Organisation Space & Astronomy), recent research has increasingly shown that the presence of these magnetic fields significantly impacts the evolution of these stars relative to non-magnetized OB stars, underscoring the importance of studying this class of object from a stellar evolutionary perspective (e.g., Z. Keszthelyi et al. 2020, 2021, 2024). More generally, since magnetic OB stars are bright and their fields very stable, they provide excellent laboratories for studying magnetospheric physics.

Historically, the Hα emission line has been used as a diagnostic of the magnetic properties of OB stars. However, this line becomes undetectable in magnetic OB stars with effective temperatures $T_{\rm eff} \lesssim$15,000 K, which has led to some controversy over whether the cooler end of such stars can even support magnetic fields. Fortunately, as described by Das, radio emission is detectable from magnetic massive stars over a broader range of temperature. Interest in this radio emission is further heightened by the discovery of key similarities with the radio emission observed from UCDs (Section 5).

Similar to UCDs, magnetic OB stars are found to exhibit both quiescent (slowly varying, rotationally modulated) radio emission and pulsed, period emission believed to arise from to an ECM mechanism. The periodicity of the latter emission may be impacted by either the stellar rotational period and/or the orbital period in the case of a binary[8] (e.g., A. Biswas et al. 2023). Additionally, radio flares have been detected from such stars (see Section 8.2.3). Also analogous to UCDs, magnetic massive stars are generally seen to be overluminous in the radio relative to the Güdel-Benz relation (Section 4.2) by up to several orders of magnitude (e.g., P. Leto et al. 2017, 2018).

8.2.1. *Quiescent (Incoherent) Radio Emission*

For the quiescent component of the emission from magnetic OB stars (primary gyrosynchrotron in origin), an early study by J. L. Linsky et al. (1992) proposed an empirical relationship between the radio luminosity, the magnetic field strength, and the stellar mass-loss rate. However, more recent studies using larger samples ($\sim$30–50 stars) have now shown that the radio luminosity is a strong function of both magnetic flux and stellar rotation period—with no dependence on either stellar temperature or mass-loss rate (P. Leto et al. 2021; M. E. Shultz et al. 2022). This result led P. Leto et al. (2021) to propose a new model for the production of radio emission in magnetic massive stars, namely that the (incoherent) radio emission is produced from a "radiation belt" (or "shell"), similar to what is now found for UCDs (see Section 5.2). In this scenario, the radio emission arises interior to the closed magnetosphere, hence the wind in not expected to play an important role. As to what produces the required energetic electrons in this shell, as related by Das, the emerging consensus is that the responsible mechanism is centrifugal breakout (CBO), and S. P. Owocki et al. (2022) have provided a theoretical framework that predicts that the radio luminosity should be proportional to the power provided by CBO in a co-rotating magnetosphere. In this picture, all magnetic massive stars have a region in their magnetosphere where the outward centrifugal force is stronger than the inward gravitational pull. When a critical density of material is reached within the magnetosphere, the magnetic field lines will break open, leading to the escape of plasma from the star. When the magnetic field lines reconnect, part of the energy will go into electron acceleration and in turn, radio emission (similar to the process that occurs in solar/stellar flares). Since these breakouts are not resolved in time by current observations, the resulting radio emission appears quasi-constant. Interestingly, Das noted that this same picture seems to also work for much cooler and lower-mass objects, extending

[8] Das reported that at present no magnetic massive stars are confirmed binaries.

down to the planet Jupiter. However, an outstanding puzzle is that for this scenario to work, the magnetic field must behave as a monopole; if it behaves instead as a dipole, there would be an implied dependence of the radio luminosity on mass-loss rate, which is not observed.

8.2.2. *Coherent Radio Emission*

The presence of coherent, pulsed radio emission from magnetic OB stars was first discovered by C. Trigilio et al. (2000) in the late B-type star CU Vir. This emission was seen to be nearly 100% circularly polarized and was observed close to the magnetic nulls (i.e., when the modulating line-of-sight magnetic field was close to zero). The origin of these pulses was identified as ECM emission (C. Trigilio et al. 2000, 2008), the same mechanism as is believed to be responsible for the auroral radio emission from UCDs (see Section 5.1). As in the case with UCDs, the radio emission frequency is proportional to the magnetic field strength, and emission at higher frequencies is produced closer to the star than emission at lower frequencies (e.g., Figure 3). The emission is also highly beamed, and similar to the case of pulsars, can only be seen with the beam sweeps through the observer's line-of-sight. B. Das & P. Chandra (2021) dubbed these stars "main-sequence radio pulse emitters" (MRPs), and this phenomenon is now believed to be ubiquitous among magnetic massive stars (B. Das et al. 2022b).

As reported by Das, more extensive observations of MRPs over the past several years have uncovered a number of new and unexpected phenomena. For example, observations of the B star HD 133880 by B. Das et al. (2020a) over a wide range of frequencies (300–4000 MHz) using the GMRT and the VLA showed that the RCP and LCP components of the pulses (which are present near the magnetic nulls that appear twice during each rotation phase and arise, respectively, from the two different hemispheres of the star) appear closer together in rotation phase at higher frequencies, as predicted by current working models (C. Trigilio et al. 2011; P. Leto et al. 2016). However, the *shapes* of the observed pulses are different during the two magnetic nulls. In the case of the star CU Vir, B. Das & P. Chandra (2021) observed the star over the entire rotational period (not just near the nulls) and found secondary highly circularly polarized pulses to sometimes occur away from the primary pulses arising at the magnetic nulls.

Das noted that we are likely still missing several pieces of important physical information in understanding magnetic massive stars. One such factor is obliquity—i.e., the misalignment between the rotation axis and the magnetic axis the star. When these two axes are aligned, most of the magnetized plasma is expected to be confined to the equatorial regions. However, a significant misalignment in these axes may result in a much wider angular extent of the plasma, forcing ECM pulses to pass through regions of high-density plasma en route to the observer and explaining the appearance of secondary pulses that do not occur in pairs (see B. Das et al. 2020b, 2024). Das expressed hope that eventually this concept, coupled with observational constraints on the presence of secondary pulses (or lack thereof), can be used to constrain the plasma density in the magnetosphere.

Another trend discussed by Das is the role of stellar effective temperature on the relative strength of coherent versus incoherent radio emission. She noted that for magnetic massive stars with temperatures $T_{\rm eff} \lesssim$18,000 K, the luminosity of the two types of emission is reasonably well correlated, but for hotter stars, the ECM emission seems to be suppressed (B. Das et al. 2022a). The explanation for this is currently unclear; indeed, the incoherent emission itself appears to show no dependence on temperature.

8.2.3. *Radio Flares*

In addition to quasi-stable quiescent emission (Section 8.2.1) and pulsed, coherent emission (Section 8.2.2), magnetic massive stars have been found to exhibit a third category of radio emission: flares. Recent and ongoing work on this topic was presented by E. Polisensky (Naval Research Laboratory).

Because magnetic massive stars possess very stable magnetospheres, previously detected optical and X-ray flares were generally attributed to low-mass companions. However, it was subsequently recognized that flaring could also result from CBO events (R. H. D. Townsend & S. P. Owocki 2005; see also Section 8.2.1). In this picture, the Kepler radius lies interior to the Alfvén radius, leading to trapping of the stellar wind plasma. This trapped plasma is then forced to co-rotate with the star and collapses into a disk (M. E. Shultz et al. 2022). Once centrifugal force overcomes gravity, plasma can move outward to the point that a reconnection event occurs, leading to a flare.

Although the possibility of CBO-induced flaring had been theoretically predicted (e.g., M. E. Shultz et al. 2022), there had been little observational evidence of such flares prior to the study of B. Das & P. Chandra (2021), which reported for the first time *transient* radio emission in the magnetic massive star CU Vir based on 500–800 MHz data from the GMRT. The detected flares exhibited durations of ∼4–8 min and hallmarks of coherent emission ($T_B > 10^{14}$ K, in addition to circular polarization). As described by Polisensky, this study inspired a follow-up search for additional

transient events in magnetic massive stars using data from the VLA Low-band Ionosphere and Transient Experiment (VLITE) Commensal Sky Survey (VCSS; T. Clarke et al. 2015). VLITE commensally operates during most other scheduled VLA experiments conducted at higher frequencies, and at the time of the meeting, it had been operating for over 9 years on a subset of 18 of the VLA antennas, accumulating data at a frequency of $\nu \approx$340 MHz and with a bandwidth of 40 MHz.

Polisensky and his team recently focused on the VLITE data obtained in parallel with observations performed as part of the VLA Sky Survey (VLASS; see M. Lacy et al. 2020), which was conducted at $\nu \sim$3 GHz. Using data from the VCSS, which has a 5σ sensitivity limit of $\sim$50 mJy, they searched for counterparts to 761 catalogued magnetic O, B, and A stars from Shultz et al. (in prep.) and found 3 matches. Each cross-matched detection was seen with a flux density $\sim$100 mJy in only a single data epoch (E. Polisensky et al. 2023). The detected emission was coherent and persisted for of order a few minutes. All three of the detected stars are believed to have centrifugal magnetospheres, and the luminosities of the flares ($> 10^{18}$–19^{19} erg s^{-1} Hz^{-1}) appear to rule out an origin tied to low-mass companions. Polisensky noted that while these data are not yet sufficient to show definitively that magnetic massive stars undergo CBO flares, the three cases so far provide interesting candidates for follow-up monitoring. Searches for new detections were also planned for additional epochs of VCSS data expected to soon be available.

8.3. *Future Work and Unsolved Puzzles*

As reported by Das, current radio facilities are continuing to deliver important new results in the area of magnetic massive star research, including the recent discovery of 20 new such objects in datasets obtained by the Variables and Slow Transients Survey (VAST) with the Australian Square Kilometre Array Pathfinder (ASKAP). However, to gain new insights into many of the unsolved puzzles concerning magnetic massive stars, Das stressed the need for more extensive, multi-frequency radio observations that extend to both higher (>50 GHz) and lower (<200 MHz) frequencies than most current studies, along with spatially resolved VLBI observations. The latter were first attempted in the 1980s (R. B. Phillips & J. F. Lestrade 1988), but with limited success owing to insufficient sensitivities of VLBI arrays of this era. This is expected to change with the planned new VLBI capabilities of the ngVLA (Section 18.1.3).

9. EVOLVED STARS

9.1. *Red Giants and Hypergiants*

Radio observations have long provided a powerful tool for studying cool, mass-losing giants, including red supergiant (RSG) stars (the late-stage descendents of stars with masses $\sim 10 - 30 M_\odot$) and asymptotic giant branch (AGB) stars (descendents of stars with initial masses in the range $\sim$0.8–8.0 $M_\odot$). The cool temperatures of these red giants ($\sim$2000-3000 K for AGB stars and $\sim$3500–4500 K for RSGs) are conducive to the formation of dust and a wide range of molecular species in their atmospheres. These stars are also typically characterized by high rates of mass loss ($\dot{M} \sim 10^{-8}$ to 10^{-4} $M_\odot$ yr^{-1}) through dense, low-velocity winds which produce enormous circumstellar envelopes (CSEs) of gas and dust. These CSEs can in turn be probed through a multitude of molecular lines at centimeter through (sub)millimeter wavelengths (e.g., B. E. Turner & L. M. Ziurys 1988; S. Höfner & H. Olofsson 2018; see also Section 12). Furthermore, some of these molecular lines may exhibit masing behavior, enabling ultra-high angular resolution studies of the outer atmosphere using VLBI techniques (see also Section 11), as well as a means to detect these stars out to significant distances for use as probes of the structure and dynamics of the Galaxy (see Section 16).

The extended atmospheres of AGB and RSG stars, which can have diameters of up to several au, also give rise to thermal continuum emission, detectable across centimeter and (sub)millimeter bands. For AGB stars, this thermal (free-free) emission arises from a region known as the radio photosphere, lying at $\sim 2R_\star$, where $R_\star$ is the classical photospheric radius (M. J. Reid & K. M. Menten 1997), while for RSG stars the thermal continuum (particularly at centimeter wavelengths) arises predominantly from the chromosphere, and samples a cooler component of the chromospheric gas than the emission lines traditionally observed in the optical and UV (J. Lim et al. 1998; E. O'Gorman et al. 2020; L. D. Matthews & A. K. Dupree 2022). As described in the presentation by A. Richards (Jodrell Bank Centre for Astrophysics/University of Manchester), in both AGB and RGB stars, to a first approximation, the observed brightness temperature is correlated with frequency owing to the wavelength dependence of the opacity (M. J. Reid & K. M. Menten 1997); higher frequencies (shorter wavelength) effectively probe deeper layers of the star, hence the stars appear larger at longer radio wavelengths and smaller at shorter wavelengths. However, as highlighted in the poster presentation by B. Bojnordi Arbab (Chalmers University), the relationship between the radius and stellar brightness temperature is complex and not yet fully understood (see also Section 9.3.2).

G. Umana reminded attendees that both the VLA and ALMA currently have the sensitivity to detect thermal radio emission from AGB and RSG stars within a few kpc, and the longest baseline configurations of these two arrays are able to modestly spatially resolve the radio-emitting atmospheres of such stars within $\lesssim$200 pc (e.g., M. J. Reid & K. M. Menten 1997, 2007; L. D. Matthews et al. 2018; E. O'Gorman et al. 2020), although at wavelengths $\lambda \lesssim 3$ mm the angular resolution is rather limited (typically $\lesssim$2–3 synthesized beams across the stellar disk). In the future, however, Umana noted that the combined thermal sensitivity and angular resolution of ngVLA (Section 18.1.3) should make it possible to readily identify the presence of asymmetries, hot spots, and other surface features in a large sample of red giants (see also L. D. Matthews & M. J. Claussen 2018)—and make "movies" of how these features evolve during the course of the stellar pulsation cycle (K. Akiyama & L. D. Matthews 2019). Importantly, the frequency ranges covered by ALMA+ngVLA will be complementary, since owing to the wavelength dependence of the opacity, different wavelengths probe different depths in the atmosphere, enabling the characterization of temperature with depth (e.g., J. Lim et al. 1998; E. O'Gorman et al. 2017, 2020). Additionally, though SKA-Mid (which is expected to have a maximum angular resolution of ∼27 mas; Section 18.1.4) will not match the maximum spatial resolution of ngVLA (∼1 mas), it is expected to contribute crucial radio light curves and multi-frequency measurements of SEDs at $\nu \lesssim 15$ GHz to help constrain atmospheric models of AGB and RSG stars and their mass-loss mechanisms (e.g., K. Marvel 2004). Such measurements are extremely difficult to carry out with current instruments owing to a combination of sensitivity limitations and logistical challenges (cf. M. J. Reid & K. M. Menten 1997).

9.2. *Recent Results from Interferometric Surveys*

C. Gottlieb (CfA) presented an overview the an ALMA Large Project dubbed ATOMIUM (ALMA Tracing the Origins of Molecules In dUst-forming oxygen-rich M-type stars) in which he has been a key team member (L. Decin et al. 2022; C. A. Gottlieb et al. 2022). The overarching goals of ATOMIUM were to improve our quantitative understanding of the physical and chemical processes that govern the inner winds and outflows of oxygen-rich evolved stars, including the formation of dust. As described by Gottlieb, the project targeted a sample of 14 AGB and 3 RSG stars spanning a range in mass-loss rates and other properties using wideband (214–270 GHz) observations with ALMA. The use of multiple ALMA configurations provided access to spatial information on scales ranging from ∼25 mas to $\sim 8''$, aiding the study of the complex and spatially extended CSEs of nearby evolved giants. The ATOMIUM team found a large morphological diversity in the molecular ejecta of their sample stars, which they interpreted as strong evidence for the role of a companion in shaping the ejecta of AGB stars (L. Decin et al. 2020)—i.e., well before the onset of the planetary nebula (PN) stage, where companions have long been assumed to play a key role in shaping the ejecta. The ATOMIUM data also provided a wealth of information for studying the astrochemistry of the circumstellar environments of each source (see Section 12).

A. Richards presented some additional results from ATOMIUM, including a statistical analysis of the derived stellar diameters at $\nu \sim 250$ GHz based on uniform elliptical disk fits to the visibility data. She noted that in terms of their diameters, the stars appear to fall into groups corresponding to their luminosity class. However, two RSGs in the sample (AH Sco and VX Sgr) have 250 GHz brightness temperatures comparable to the majority of the AGB stars, despite the higher effective photospheric temperatures of the RSGs. Additionally she reported that at the frequencies targeted by ATOMIUM, the emission from the AGB stars seem to require a chromospheric contribution in addition to that from the radio photosphere (see Section 9.1).

Richards also previewed some work on the analysis of the SiO masers and high-excitation H_2O masers detectable within the 215–265 GHz band covered by ATOMIUM (see also B. Pimpanuwat et al. 2024 and Section 11). The ATOMIUM data have sufficient spatial resolution to allow tracing the motions of some individual SiO maser-emitting features, revealing evidence for both inflow and outflow. Likewise, the high-excitation H_2O lines, which arise at ∼2–3$R\star$ show evidence of both infall and outflow motions (S. Etoka et al. 2022; A. Baudry et al. 2023).

9.3. *Studies of Individual Stars*

9.3.1. *Red Supergiants (RSGs)*

Betelgeuse—Richards presented new results that have emerged from the recent spatially resolved observations of the nearby RSG star Betelgeuse (α Orionis) at frequencies ranging from ∼6–485 GHz based on observations from ALMA and the enhanced Multi-Element Remotely Linked Interferometer Network (eMERLIN). Many of the new observations were performed in 2023, motivated in part by the desire to obtain an accurate position for the star in advance of its occultation by the asteroid Leona, which occurred on December 12, 2023 (e.g., S. Costantino et al. 2023). At centimeter

wavelengths (ν ~6 GHz) Richards reported that the radio emission exhibits significant variations over time, though the exact cause of the variations is unknown. One possibility raised by Richards is carbon recombination. Consistent with this, recent work presented in the poster from W. Dent (Joint ALMA Observatory) showed evidence of very little ionized carbon in the atmosphere of Betelgeuse. This is based on analysis and modeling by Dent, Richards, and collaborators of a recent detection of the H30α Rydberg line at 231.905 GHz in the atmosphere of Betelgeuse, along with a second line at 232.025 GHz (X30α) that is attributed to a blend of Rydberg transitions from metals with low first ionization potentials (W. R. F. Dent et al. 2024).

At higher frequencies, new images obtained by Richards's team show that the "hot spot" previously seen in the northeast quadrant of the star in 338 GHz data from 2015 (E. O'Gorman et al. 2017) still appears to be at a similar location ~8 yr later, although the contrast between the hot spot and the surrounding emission is less pronounced in the more recent data. New ALMA images presented by Richards also allowed for the first time an estimate of the spectral index of the hot spot; preliminary indications are that at 233–338 GHz it is steeper ($\alpha \sim 1.9$) than the mean spectral index of the star (see below).

Richards reported that in a global sense, the millimeter and submillimeter emission of Betelgeuse is reasonably fitted by a uniform elliptical disk, but divergences from this simple model were seen on various scales; on small scales this is suggestive of the presence of one or more hot spots, while on larger scales there is evidence of an additional layer around the star. The exact nature of the latter component is uncertain. One possibility is emission from dust, although Richards suggested that based on its uniformity, it is perhaps more likely to be a cool free-free-emitting plasma component.

Another finding reported for Betelgeuse by Richards is that the brightness temperatures derived from multi-wavelength radio observations appear to be systematically diminished by of order a few hundred Kelvin subsequent to the so-called "Great Dimming" that occurred in late 2019/early 2020 (E. F. Guinan et al. 2019) and which led to a historically large drop in brightness at visible wavelengths (see e.g., A. K. Dupree et al. 2020). This echoed complementary results presented in the poster by L. Matthews (MIT Haystack Observatory) based on ALMA and VLA measurements (see also L. D. Matthews & A. K. Dupree 2022; L. D. Matthews et al. 2024 and in prep.). The presentations from Richards and Matthews also highlighted how the disk-averaged brightness temperature of Betelgeuse rises from $\sim 6R_\star$ (sampled by centimeter-wave observations) to $\sim 2R_\star$ (sampled by millimeter-wave measurements), but then falls near $\sim 1.2R_\star$, as probed by submillimeter observations. A similar trend was previously reported by E. O'Gorman et al. (2017), but additional measurements from ALMA more clearly define the changes in temperature as a function of radial distance and should help to better constrain future models. Richards pointed out that it is also intriguing that despite changes in brightness temperature over time, the spectral index of Betelgeuse between ~5–500 GHz has remained remarkably stable ($\alpha \sim 1.4$) over more than 20 years (e.g., E. O'Gorman et al. 2015, 2017; L. D. Matthews & A. K. Dupree 2022; Matthews et al. in prep.).

The poster presentation of Matthews also showcased the first spatially resolved images of Betelgeuse at 107 and 136 GHz (λ2–3 mm; Figure 4). The images were created using a regularized maximum likelihood imaging technique that allowed moderately super-resolving the star. Use of this technique has revealed that the radio surface of the star appears markedly different at wavelengths of λ2–3 mm compared with λ0.85–1.3 mm. Given the qualitative similarities between λ0.85 mm images obtained several years apart, the differing appearance in the respective bands cannot be readily be attributed entirely to temporal variations.

Using comparisons with sophisticated 3D modeling, J.-Z. Ma (Max Planck Institute for Astrophysics) presented results aimed at exploring the question of whether Betelgeuse is truly rotating with a projected equatorial velocity of $v_{\rm eq} \sin i \approx 5.5$ km s^{-1}, as had been claimed previously based on evidence from spatially resolved ALMA observations of molecular line (SiO) emission (P. Kervella et al. 2018). Such a rotational velocity is surprisingly high for a RSG star; even if the main sequence progenitor was rapidly rotating, conservation of angular momentum during the transition to the RSG phase (which involves an increase of radius of two orders of magnitude) is predicted to slow rotation to $\lesssim$0.1 km s^{-1}—i.e., two orders of magnitude lower than the observations imply (J.-Z. Ma et al. 2024). One previously proposed explanation is that Betelgeuse resulted from a stellar merger (e.g., J. C. Wheeler et al. 2017; S. Shiber et al. 2024), but Ma and collaborators put forward a competing idea. Ma pointed out that if the bright regions or "hot spots" observed in spatially resolved radio images of RSG stars such as Betelgeuse (see E. O'Gorman et al. 2017 and above) result from convection, then it is predicted that these features should change on timescales of months (commensurate with the convective turnover timescale of the star).

Using 3D hydrodynamic (non-rotating) CO5BOLD simulations of convection in RSG stars (A. Chiavassa et al. 2011; B. Freytag et al. 2012), coupled with chemical modeling as prescribed by the FASTCHEM2 code of J. W. Stock et al. (2018, 2022), Ma and his colleagues produced model images of the continuum and spectral line emission of Betelgeuse, convolved to the angular resolution appropriate for ALMA. They found that the finite spatial resolution (beam smearing) of the ALMA observations can mimic the signatures of rotation and produce spurious rotational velocities of $\geq$2 km s^{-1} in $\sim$90% of their test cases. Ma noted that a follow-up study of Betelgeuse using ALMA's highest resolution configuration is needed to confirm this observationally. He also highlighted the value of future ALMA observations of Betelgeuse with even higher spatial resolution that would enable spatially resolved velocity fields of various molecular lines. Since different molecular lines (e.g., different transitions of SiO) probe different layers of the atmosphere, this would in effect allow velocity field tomography of the star and enable searches for the expected signatures of the different physical processes that impact these various layers (e.g., rotation, shock waves, wind launching; see J.-Z. Ma et al. 2024).

VY CMa—Richards presented a poster led by collaborator R. Humphreys (University of Minnesota) that described recent ALMA spectral line observations of the red hypergiant VY CMa covering 230–250 GHz. VY CMa has been previously extensively studied at multiple wavelengths as an archetype for understanding late-stage stellar mass loss owing to the star's high current mass-loss rate, complex chemistry, and extensive circumstellar ejecta. The new ALMA data (with angular resolution of $\sim$200 mas), combined with archival ALMA measurements and a VLBI-determined distance to the star, have now enabled the derivation of line-of-sight velocities and proper motions (over $\sim$6 yr) of four newly discovered ^{12}CO-rich clumps near the star. The existence of these clumps, along with other clumps previously detected with the *Hubble Space Telescope* (*HST*), imply that the star underwent at least 6 outflow events within a 30 yr period, roughly 60–100 yr ago, resulting in the loss of $\geq 0.07\ M_\odot$ of material (R. M. Humphreys et al. 2024; see also A. P. Singh et al. 2023).

Turning to smaller scales, Richards also drew attention to ALMA Band 9 (670 GHz) observations of VY CMa with 9 mas angular resolution (Y. Asaki et al. 2020). Surprisingly, those observations showed primarily dust, with no clear detection of the stellar continuum; indeed, Richards noted that VY CMa may be the dustiest known Galactic RSG star. Richards and colleagues have also used ALMA to study the H_2O masers around VY CMa and found evidence of both inflow and outflow (Y. Asaki et al. 2020), as well as radial velocity gradients within spoke-like features (A. M. S. Richards et al. 2024). Their data also showed 268 GHz H_2O masers confined to a bow-shock-like structure, suggesting a recent clump ejection. Finally, Richards reported the recent detection of a X30α Rydberg (recombination-like) line arising from high-excitation metals. However, compared with the Rydberg lines recently detected in Betelgeuse (see above), those associated with VY CMa are much more spatially extended and have a much narrower linewidth. Furthermore, the hydrogen H30α line is so far undetected in this source.

9.3.2. *AGB Stars*

A poster by B. Bojnordi Arbab summarized recent work aimed at comparing the predictions of 1-D DARWIN atmospheric models of AGB stars from S. Höfner et al. (2016, 2022) with multi-frequency radio measurements from the VLA and ALMA. He showed examples of predictions for key observable properties of these stars, including brightness temperature variations as a function of radius, as well as flux density variations as a function of time and frequency and discussed how comparisons with multi-frequency radio observations can be used to constrain the role of shocks and associated opacity changes with increasing height in the atmosphere (B. Bojnordi Arbab et al. 2024). Additionally the poster highlighted the prospects for significant future advances in our ability to study the time-varying atmospheres of AGB stars out to tens of kpc with the arrival of SKA-Mid, and especially, the ngVLA—in combination with ALMA—owing to the unprecedented combination of broad frequency coverage, sensitivity, and angular resolution that this trio of facilities will bring (see Section 18).

Other recent ALMA results related to AGB stars were highlighted in the presentation by A. Moullet [National Radio Astronomy Observatory (NRAO)]. Among these was a Band 8–10 (397–908 GHz) study of the nearby carbon-rich AGB star R Lep (Y. Asaki et al. 2023) that produced the highest angular resolution (5 mas) images ever made of a stellar radio photosphere. Additionally, the observations detected and imaged an HCN maser line at 890.8 GHz at comparable angular resolution. Oxygen-rich AGB stars frequently exhibit maser emission from species such as SiO, H_2O, and OH, providing a probe of the dynamic atmospheres of these stars that can be observed with ultra-high angular resolution (see also Sections 11), but these lines are generally not detectable in carbon-rich AGB stars like

R Lep. The Y. Asaki et al. study therefore illustrates the potential of submillimeter HCN masers as a new tool for ultra-high angular resolution studies of carbon AGB star atmospheres using VLBI techniques.

9.4. *Luminous Blue Variables*

Luminous blue variables (LBVs) are representatives of a short-lived and poorly understood post-main-sequence evolutionary phase of very massive stars (initial masses $\sim 60 - 100 M_{\odot}$). LBVs mark the transition from the main sequence to Wolf-Rayet stars and are characterized by strong variability and high rates of mass loss ($\sim 10^{-6} M_{\odot}$ yr^{-1}), which lead to extended circumstellar nebulae (e.g., R. M. Humphreys & K. Davidson 1994; G. Umana et al. 2011). As discussed in the presentation by G. Umana, radio observations provide valuable information on the mass-loss histories of LBVs, including current mass-loss rates and the mass and structure of the circumstellar ejecta.

Among the latest developments in LBV research described by Umana was a recent 1.3 GHz survey of the Galactic Plane with MeerKAT that identified several new LBV candidates and enabled detailed imaging of their extended ejecta (S. Goedhart et al. 2024; Umana et al. in prep.). Radio observations in additional bands enabled identification of the central component (C. Bordiu et al. 2025) and provided spectral information on the ejecta, which in turn aids in identifying a possible non-thermal emission component that may arise from the interaction between the stellar wind and the local environment (see also Section 10). Another new finding reported by Umana was the surprising discovery (using ALMA) of sulfur- and silicon-bearing molecules in the ejecta of LBVs, despite their harsh environments (C. Bordiu et al. 2022). This underscores that these stars can serve as laboratories for the study of molecular chemistry under extreme physical and chemical conditions.

10. STARS INTERACTING WITH THEIR ENVIRONMENTS

10.1. *Modeling Circumstellar Environments*

An invited talk by S. Mohamed (University of Virginia) showcased the results of recent high-resolution simulations of the complex environments of evolved, mass-losing stars, with a focus on AGB stars (see also Section 9.3.2). Modeling such systems is enormously challenging owing to the wide range of relevant physical processes and to the enormous range in scales involved. Driving home the latter point, Mohamed noted that if the stellar core were the size of a marble, the tenuous outer envelope would be a kilometer away.

Mohamed focused in particular on what can be learned from smooth particle hydrodynamics (SPH) simulations in which each particle represents a bit of the fluid being modeled. The particles interact with each other according to a set of specified equations describing the relevant physics [i.e., conservation of mass, energy, momentum, and an equation of state, along with equations describing other physical processes (e.g., dust formation, chemistry, magnetic fields)]. Other necessary ingredients include a numerical solver, boundary conditions, a set of initial conditions, and lastly, a set of parameters and approximations to make the problem tractable. Interpolation between particles using a smoothing kernel is then used to approximate a smooth fluid.

Mohamed showed examples of SPH simulations covering three types of processes of relevance to AGB stars, including stellar interaction with a nearby binary companion, wind-wind interactions, and wind-ISM interactions. She noted that ALMA has been a game-changer for allowing direct confrontation of such models with observations; indeed, researchers have been able to use the increasing body of exceptionally detailed ALMA images of evolved stars and planetary nebulae (PNe) and their circumstellar environments to constrain models of the wide range of physical processes that underlie such objects, and also improve our understanding of stellar evolution and cosmic recycling.

In the case of AGB stars with a binary companion, simulations by Mohamed and her collaborators have shown that as a companion moves through the AGB star's wind it will shape the wind into an Archimedes spiral. Importantly, spacing between the spiral arms will depend on the orbital period, while the mass of the companion impacts the density ratio between the arm and inter-arm regions of the spiral. Detection and measurement of such structures therefore provide a means of inferring the existence of companions of AGB stars that are otherwise difficult or impossible to detect owing to the enormous luminosity of the AGB star itself—and moreover, to constrain the mass and orbit of the companion. One spectacular example of this—the case of the AGB star R Scl (M. Maercker et al. 2012)—was presented at the first Haystack Radio Stars meeting in 2012 (see L. D. Matthews 2013), and additional examples have since been identified with ALMA (e.g., S. Ramstedt et al. 2017; L. Doan et al. 2020).

Recently, E. Aydi & S. Mohamed (2022) modeled the case of substellar/planetary mass companions and found that such companions can have an impact on the mass-loss rate of an AGB star. They also showed that if there are resonances between the orbital period and the pulsation period, multiple spiral structures can form. Mohamed

prognosticated that with future higher sensitivity, high angular resolution (sub)millimeter observations (such as will become possible thanks to ongoing upgrades to ALMA; see Section 18.1.2) it will finally become possible to directly observe some of these predicted structures—not only in AGB star binaries, but even in binaries with lower wind densities where the spiral signatures are expected to be much more subtle (e.g., Wolf-Rayet stars).

Mohamed also discussed the case of the symbiotic binary Mira AB, comprising an AGB star and a white dwarf companion separated by ∼60 au. Given the relatively wide separation of this pair, and the fact that the AGB star does not fill its Roche lobe, the strong focusing of material from the AGB wind onto the companion first observed in the UV and X-rays was initially surprising (M. Karovska et al. 1997, 2005). However, S. Mohamed & P. Podsiadlowski (2012) showed that this could be explained by a process dubbed "wind Roche-Lobe overflow" (WRLOF). In this case, if the wind has a low velocity and its acceleration zone lies at a significant fraction of the Roche lobe radius, material can more readily get channeled into the potential well of the companion, resulting in a higher accretion rate compared with the classic Bondi-Hoyle accretion scenario. Evidence of this has since been seen in ALMA observations of other evolved stars (e.g., S. Ramstedt et al. 2018; L. Doan et al. 2020). Mohamed noted that WRLOF can also play a role in the formation of certain chemically peculiar stars (e.g., C. Abate et al. 2013).

Mohamed explained that realistic SPH modeling of a system as complex as Mira AB requires the inclusion of a broad range of physical processes including the wind acceleration, radiation pressure on the dust, as well as cooling and accretion. In such a case the resulting spiral structure is no longer 3D, but more confined to the orbital plane. Various arcs and cavities are also predicted to form, and such features have been confirmed, for example, through CO observations of the Mira AB system obtained with ALMA (S. Ramstedt et al. 2014). However, the real data include additional surprises, such as the presence of a large bubble not seen in the simulations. Mohamed suggested that this may be a result of the hot wind of Mira A's white dwarf companion.

10.2. *Runaway Stars*

J. van den Eijnden (University of Warwick) spoke on the importance of current and future radio wavelength observations for the identification and study of bow shocks associated with massive (O and B) "runaway" stars. Runaway stars are traveling supersonically through the ISM and have escaped from the clusters in which they originally formed (e.g., M. Stoop et al. 2024). His talk highlighted how such studies complement high-energy (γ-ray) studies of bow shocks and provide insights into how massive stars interact with their local environments. The strong stellar winds of OB stars and the high space velocities at which runaway stars are moving mean that the latter interactions are often strong.

The primary band for identification of bow shocks associated with runaway OB stars is currently the infrared, where the bow shock regions emit owing to thermal radiation from heated dust grains. However, as noted by van den Eijnden, the mechanical energy budget available in these regions ($\sim 10^{50} - 10^{51}$ erg, comparable to that of a supernova explosion, but with emission over a much longer timescale) is also sufficient to power nonthermal high-energy physical processes, including diffuse shock acceleration, whereby charged particles bounce back and forth in a magnetic field; the particles cross the shock front and continue to gain energy with each passage. At radio wavelengths, this leads to the production of synchrotron emission, while at the same time, inverse Compton scattering gives rise to γ- and X-ray emission. However, van den Eijnden stressed that the identification of these nonthermal signatures is challenging; among hundreds of known infrared-emitting bow shocks associated with massive stars, until recently, only a single radio counterpart to one of these bow shocks had been detected (P. Benaglia et al. 2010).

This has finally begun to change thanks to the wide fields-of-view and exquisite surface brightness sensitivity available from facilities such as ASKAP and MeerKAT, and the sample of detected radio bow shocks now stands at ∼10 (J. Van den Eijnden et al. 2022a, 2022b; J. van den Eijnden et al. 2024; and in prep.). Van den Eijnden further noted that this is likely to represent only the "tip of the iceberg". Based on the observed properties of the currently sample, it is predicted that future deep observations with MeerKAT (and eventually SKA-Mid; see Section 18.1.4), are expected to detect synchrotron emission from the bow shock regions of nearly all currently known runaway OB stars and enable determinations of the radio spectral indices (which are lacking for the current sample) and polarization signatures (if present). He also highlighted the value of future synergistic observations with γ-ray observations [e.g., with the planned Cherenkov Telescope Array (CTA)] hold the promise to provide new insights into the stellar wind physics and particle acceleration processes in these sources.

One challenge in interpreting radio continuum observations of bow shocks and extracting meaningful physics is "proving" that the radio emission is at least partly nonthermal. Van den Eijnden reported that one way of doing this

is to combine radio and Hα observations and evaluate whether both the radio flux density and Hα surface brightness can be accounted for by temperatures and electron densities that are consistent with thermal emission. Another is to estimate the electron injection efficiency (J. van den Eijnden et al. 2022b).

Additional work related to stellar bow shocks was presented by V. Yanza Lopez (National Autonomous University of Mexico), who discussed the radio-emitting bow shock at the center of the ultra-compact H II region NGC 6334A. This region has long been known to exhibit both a shell and a compact source that are visible in radio wavelengths (L. F. Rodriguez et al. 1982; P. Carral et al. 2002). However, the central radio source has remained an enigma, showing an arc-like shape, a negative spectral index (indicative of a synchrotron mechanism), and variability on the timescale of years, leading to the suggestion it was associated with a colliding wind region (L. F. Rodríguez et al. 2014).

Using the highest resolution VLA ('A') configuration, Yanza Lopez and her colleagues performed multi-frequency (10, 22, and 33 GHz), multi-epoch observations of the NGC 6334A central source in an attempt to distinguish whether the radio emission is arising from a colliding wind region or a bow shock (V. Yanza et al. 2025). The emission that was observed is spatially resolved, with a mean spectral index $\alpha \approx -0.5$. To explain the observed level of ionization as a colliding wind region would require a binary comprising two massive stars, with approximate spectral types O7 and B0; however, at centimeter wavelengths there are no counterparts to these putative stars. Yanza Lopez's team also examined data at other wavelengths (optical, infrared, X-rays), but still no counterpart was seen. They then considered an alternative scenario in which the radio emission is produced by the bow shock of a runaway massive star. Using archival multi-epoch VLA radio data they measured a proper motion for the compact radio source and derived a space velocity of 123 ± 40 km s^{-1}, consistent with other runaway stars. This favors the bow shock scenario. Nonetheless, a remaining puzzle is that there is no apparent counterpart to the massive star that would have led to the formation of a bow shock. This scenario also cannot as readily explain the observed ionization of the surrounding shell. Yanza Lopez noted that tentatively, both issues could be resolved by assuming the progenitor is a B0 star (identified in a *Herschel* 70 μm image) that has since moved away from the center of the shell structure.

11. STELLAR MASERS

A. Bartkiewicz (Toruń Institute of Astronomy, Nicolaus Copernicus University) presented an invited overview of the role of cosmic molecular masers for studying various phases of stellar evolution. She described how owing to its inherently beamed nature, maser emission is able to escape from dense regions and deeply embedded sources, providing a diagnostic of the kinematics and physical conditions near star-forming regions and evolved stars. The non-thermal, high brightness temperature nature of the maser emission also means that it can be observed at ultra-high angular resolution using VLBI techniques (see below).

11.1. *Masers in High-Mass Star-Forming Regions*

Bartkiewicz pointed to the recent review by J. S. Urquhart (2024) and the study of J. Kang et al. (2024) as illustrations of how different molecular lines observed at radio wavelengths (both thermal lines and maser lines) can uniquely probe distinct phases in the process of massive star formation ($M_\star \gtrsim 8 M_\odot$). She also highlighted the recent work by D. Ladeyschikov (2024) suggesting that H_2O masers appear even earlier in the process of massive star formation than methanol masers and tend to trace outflow processes.

One point emphasized by Bartkiewicz is the value of multi-epoch monitoring of masers over timescales of months to years as a means of tracing gas kinematics and documenting ongoing evolution of sources (e.g., A. Bartkiewicz et al. 2020, 2024a, 2024b). For example, in the nearest massive star-forming regions, multi-epoch observations using VLBI techniques can achieve spatial resolution of < 0.1 au, sufficient to record gas clumps spiraling along magnetic field lines (e.g., L. D. Matthews et al. 2010; L. Moscadelli et al. 2022). However, spatially unresolved maser monitoring with single-dish radio telescopes can also provide unique and valuable information. For example, Bartkiewicz cited recent studies demonstrating that methanol maser flares at 6.7 GHz can be used to identify episodic accretion onto high-mass protostars (e.g., A. Kobak et al. 2023; R. A. Burns et al. 2023). This phenomenon had been predicted by previous theoretical studies (D. M. A. Meyer et al. 2017, 2021). For the case of the high-mass protostar G358-MM1, VLBI follow-up by R. A. Burns et al. further revealed that the methanol masers trace a Keplerian disk with a four-arm spiral structure that appears to be feeding material onto the protostar.

Also on the topic of methanol masers, a poster by S. Paulson (Tata Institute of Fundamental Research) focused on the Galactic mid-infrared-emitting bubble N59, known to host eight 6.7 GHz methanol masers. Such masers are signposts of narrow time window during the process of massive star formation ($t \sim 0.4-2\times10^4$ yr; S. P. Ellingsen 2007;

S. J. Billington et al. 2020). Using multiwavelength observations of N59, including archival radio observations obtained with the James Clerk Maxwell Telescope (JCMT), the Atacama Pathfinder EXperiment (APEX) telescope, and the VLA, S. T. Paulson et al. (2024) performed a comprehensive analysis of this region that led to the identification of multiple H II regions and massive YSOs in the region, together with a cluster of OB stars.

11.2. *Masers in AGB and Post-AGB Stars*

The study of masers in evolved stars serves a unique role in investigating their mass-loss process, since the masers enable probing regions within a few $R_\star$, where dust formation occurs and where the wind is accelerated. They also complement other multi-wavelength observations. Bartkiewicz showed spectacular high-resolution images of the AGB star W Hya from the recent study of K. Ohnaka et al. (2024), obtained contemporaneously in visible light with the Very Large Telescope (VLT)/Spectro-Polarimetric High-contrast Exoplanet REsearch (SPHERE)-Zurich Imaging Polarimeter (ZIMPOL) and in two vibrationally excited H_2O lines with ALMA. The overlap between the polarized intensity maps and the H_2O emission suggests that both dust and the H_2O emission (which is most likely masing), both originate at $\sim 2-3R_\star$ from cool, dense pockets of gas within the inhomogeneous atmosphere of the star.

Another recent, novel result obtained through the study of masers was made by W. Homan et al. (2020) using ATOMIUM data (Section 9.2). In the AGB star π^1 Gru, W. Homan et al. found that on scales of $\lesssim$0$''$.5 the SiO masers appear to trace the effects of a second, previously unknown companion on the inner wind, revealing an apparent flow of gas accelerating from the AGB star surface onto the companion.

M. Lewis (Leiden Observatory) reported on the use of data from the Bulge Asymmetries and Dynamical Evolution (BAaDE) survey of SiO masers (see Section 16) to study the statistical properties of the SiO maser-emitting stars themselves. She reminded us that among the molecular maser species commonly found in oxygen-rich AGB stars, the SiO masers arise closest to the stellar core and that while SiO masers are detected in evolved stars spanning a broad range of infrared colors, they are most prevalent in Mira-type variables with thin to moderately thick circumstellar envelopes, and less common in the subclass of very red OH-IR stars with thick envelopes. In her presentation Lewis focused on the analysis of the SiO maser properties of subset of 28,000 AGB star candidates observed by the BAaDE project using the VLA with a bandpass tuned to encompass 7 lines from various SiO transitions and isotopologues between 42.3–43.5 GHz. Detections of the ^{28}SiO v=1,2 $J=1-0$ lines were the most common, being seen in over 50% of the sample, while the ^{29}SiO v=1, $J=1-0$ line was the rarest, occurring in just 0.1% of the targets. In a handful of cases, all seven maser lines were detected in a single star (see M. O. Lewis et al. 2024).

Lewis has been analyzing the line ratios of the various detected maser lines, and highlighted in particular the importance of the $F_{^{28}\mathrm{SiO}\ v=1}/F_{^{29}\mathrm{SiO}\ v=0}$ flux ratio. She noted that in most cases this ratio is $\sim$10, but her team has identified an interesting subset of stars for which brightness of the ^{29}SiO isotopologue is equal to or greater than that of the ^{28}SiO line. The cause of these unusual ratios is not yet entirely clear, but the effect appears to be time-variable (M. O. Lewis et al. 2020b).

Another aspect of the BAaDE SiO masers studied by Lewis and colleagues is variability. Incorporating multi-wavelength data, including optical light curve data from the Optical Gravitational Lensing Experiment (OGLE; P. Iwanek et al. 2022), Lewis and her team found a very strong correlation between SiO maser detectability and pulsation period, with the longer-period stars ($P \gtrsim$450 days) having the highest detection fraction ($\sim$80%; Figure 5). Examining the SiO maser data as a function of light curve phase, they also found that all maser transitions they observed show a statistically significant correlation with stellar phase: maser detection rate is highest at maximum brightness of the infrared light curve (when the stellar radius is the smallest), with the ^{28}SiO v=3, $J=1-0$ line being the most sensitive to phase. This is consistent with the predictions of theoretical modeling that suggested that this transition arises from high-density environments (J. F. Desmurs et al. 2014).

Bartiewicz also stressed the importance of temporal information and multi-epoch observations for studying masers in evolved stars, noting that observing cadences of at least every few weeks are desirable. She presented one recent example from the East Asian VLBI Network (EAVN) Synthesis of Stellar Maser Animations project, which produced a 37-epoch study over 3 years of the H_2O masers in the AGB star BX Cam (S. Xu et al. 2022). Unfortunately, studies of this kind, particularly when they involve high-resolution imaging, are extremely time-consuming and can be difficult in practice to schedule at telescopes. However, the scientific value of such data sets is extraordinarily rich (see also I. Gonidakis et al. 2013) and Bartiewicz emphasized the value of undertaking additional studies of this kind for larger samples of evolved stars.

Maser monitoring that spans many years (or even decades) has a unique role to play in our understanding of stellar sources, and as an example, Bartkiewicz cited the recent study by S. Etoka et al. (2024) using the Nançay Radio Telescope to monitor OH masers (at 1612 MHz) in a sample of late AGB and post-AGB stars over timescales of more than a decade. The short-lived post-AGB phase of stellar evolution is notoriously difficult to study, but the results of the Nançay survey in combination with near infrared photometry, are establishing that with statistical samples it becomes possible to study the AGB to post-AGB transition in real time.

11.3. *Masers in (Proto)-Planetary Nebulae (PNe)*

So-called "water fountain" sources are highly evolved sources (descended from low-to-intermediate mass stars) that are found to be accompanied by high-velocity jets (velocities up to ∼500 km s^{-1}) traced by the 22.2 GHz H_2O maser line. First reported by H. Imai (2007), water fountain sources are rare but important objects that are key to understanding the short-lived post-AGB evolutionary phase during which an AGB star undergoes its transition to a PN. As reported by Bartkiewicz, X.-J. Ouyang et al. (2024) recently discovered high-excitation OH masers at 4.6 and 6.0 GHz in the water fountain source IRAS 18460−0151, providing a new window into the kinematics and physical conditions of these sources. Other noteworthy recent developments in the study of water fountain sources include the discovery of a second known case with associated SiO masers by K. Amada et al. (2024), which the authors argue to be a hallmark of a unique evolutionary phase, and the discovery by L. Uscanga et al. (2023) of a sudden, rapid growth in the measured outflow velocity in the previously known water fountain source IRAS 18043−2116. The outflow velocity in IRAS 18043−2116 was found to be $v_{\rm out}$ ∼540 km s^{-1}, setting a record for this type of object.

A small fraction of PNe are known to be associated with molecular maser emission from H_2O and/or OH, and this presence of maser emission is thought to be a hallmark of youth (e.g., A. Zijlstra et al. 1989). Bartiewicz drew attention to the recent discovery of variability in the 1612 MHz OH maser line in the PN IRAS 07027−7934 (R. A. Cala et al. 2024), which has significantly weakened since the original discovery by A. A. Zijlstra et al. (1991). R. A. Cala et al. suggested that this may be related to the expansion of a photoionized region during the early stages in the onset of the PN phase. These authors also found evidence that, unexpectedly, low-mass, C-rich central stars may be common to PNe hosting OH and H_2O (i.e., oxygen-rich) masers and hypothesized that this may be reflective of their status as post-common envelope binary systems.

12. CIRCUMSTELLAR CHEMISTRY

B. McGuire (MIT) presented an invited review on the topic of the astrochemistry of circumstellar environments. He defined the objective of astrochemistry as achieving an understanding on a molecule-by-molecule, chemical reaction-by-reaction basis, the steps required to form all of the known complex molecules throughout the Universe (including those fundamental to life). Progress toward this goal requires evaluating the chemical inventories in different environments in space and using that information as part of understanding the physical processes and underlying chemistry that this resulted from.

McGuire reported that as of April 2024, the inventory of molecular species detected outside of our Solar System[9] had surpassed 300. It is noteworthy that 95% of these have been detected through radio observations, typically of rotationally excited transitions. Also, of the 300+ molecules, roughly 30% were discovered for the first time in the circumstellar environments of red giants, and a significant fraction of those were in either the RSG star VY CMa (see also Section 9.3.1) or the carbon-rich AGB star IRC+10216 (see below). An interesting aspect of the CSE of VY CMa is that it includes a number of lines from "real" metals, including TiO and TiO_2 (T. Kamiński et al. 2013; E. De Beck et al. 2015) and VO (R. M. Humphreys et al. 2019). Furthermore, McGuire noted that for line-rich sources, on average 30–40% of molecules typically remain unidentified in current studies. And while most of these are likely to be vibrationally excited states or isotopologues of known molecules that have not been measured, some are almost certainly new species awaiting discovery.

12.1. *Carbon-Rich AGB Stars: IRC+10216*

As described by McGuire, the carbon-rich AGB star IRC+10216 was discovered as an infrared source in the mid-1960s (E. E. Becklin et al. 1969), and soon thereafter began yielding detections—through radio observations—of a range of new molecular species seen for the first time outside the solar system, including CS (A. A. Penzias et al.

[9] https://bmcguir2.github.io/astromol. See also B. A. McGuire (2022).

1971), SiS (M. Morris et al. 1975), and C_2H_2 (S. T. Ridgway et al. 1976). This trend of discovery has continued almost linearly ever since, with the total number of molecules known in the circumstellar environment of this star totaling 67 as of the time of the meeting (B. A. McGuire 2022). McGuire stressed that access to large aperture, single-dish antennas has been crucial to these efforts, with the Institut de Radioastronomie Millimétrique (IRAM) 30 m antenna contributing the largest number of the molecular detections in this source to date, followed by the Yebes 40 m antenna. To underscore the importance of IRC+10216 for advancing astrochemistry, McGuire recounted that 100% of molecular species outside the solar system containing the elements Na (3 molecules), Mg (14 molecules), K (2 molecules), Ca (1 molecule), and Fe (2 molecules) were discovered for the first time in IRC+10216, along with 12 of the 13 known Si-containing molecules.

Expounding on the significance of few of these, McGuire pointed out that the overall scarcity of Fe-rich molecules in circumstellar environments (with the exception of the CSE of IRC+10216, where FeCN and FeC have been detected; L. N. Zack et al. 2011; L. A. Koelemay & L. M. Ziurys 2023) is somewhat puzzling given that this element it is fairly common in space. Consequently, knowledge of such molecules in the gas phase—where we can study their chemistry—is particularly valuable. Ca is another molecule of interest owing to its importance for human biology, but historically its origin has been difficult to study in space, as it is typically found in grains, not in the gas phase. Thanks to the recent detection of CaNC in IRC+10216 (J. Cernicharo et al. 2019), we are just now beginning to be able to study it in the gas phase through rotational line spectroscopy.

McGuire also showcased some of the recent results on IRC+10216 by PhD student M. Siebert (University of Virginia). Based on past work, IRC+10216 is well known to be surrounded by a complex array of molecule-rich circumstellar shells. The numerous Si-rich species surrounding this star are of particular interest, arising predominantly from the inner $\lesssim 10''$ of the CSE (e.g., J. P. Fonfría et al. 2014; L. Velilla-Prieto et al. 2019). Mg-containing molecules are also important, as these seem to require UV radiation (and the subsequent formation of certain ions) as a catalyst for their formation. These latter molecules are found predominantly in a shell with radius $\sim 15''$, which corresponds to the radius at which dust no longer obscures the UV background radiation. However, McGuire described work by M. A. Siebert et al. (2022) that revealed that there also seems to be some UV-driven chemistry going on interior to this radius, as is needed to explain the presence of higher energy transitions of species such as CN and H_2CN. Modeling by M. A. Siebert et al. led to the suggestion that the observed abundances of these species requires the presence of UV radiation from a solar-type companion, coupled with a clumpy outflow containing gaps that allow exposure of the circumstellar gas to UV radiation. In effect, astrochemistry has provided strong but indirect evidence for the presence of a companion to this star. The existence of such a companion had been previously hinted at by *HST* observations (H. Kim et al. 2015) and by the characteristic spacing of molecular shells around this star (M. Guélin et al. 2018).

12.2. *Oxygen-Rich AGB Stars*

C. Gottlieb summarized some of the wealth of astrochemical data obtained for the circumstellar environments of evolved stars through the ATOMIUM project (e.g., A. Baudry et al. 2023; see also Section 9.2). The wide bandwidth covered by the ATOMIUM survey (214 to 269 GHz; Figure 6) enabled efficient identification of a wide range of molecular species, and in total, ∼300 rotational lines from 24 different molecules were observed, along with ∼30 unidentified lines (S. H. J. Wallström et al. 2024). Gottlieb noted that these data are now being used to understand the physiochemical processes that convert diatomic and triatomic molecules into grains within the inner winds of oxygen-rich evolved stars (C. A. Gottlieb et al. 2022; S. H. J. Wallström et al. 2024). This marks an important advance, as prior to ATOMIUM, only a handful of oxygen-rich evolved stars (e.g., VY CMa; IK Tau) had been the subject of dedicated line surveys (L. M. Ziurys et al. 2007; L. Velilla Prieto et al. 2017).

12.3. *Astrochemistry in the Environments of Massive Protostars*

In addition to discussing the astrochemistry of the environments of very old stars, McGuire also touched on the roles of astrochemistry (and radio wavelength observations specifically) for studying massive protostars and the process of high-mass star formation (see also Sections 7.1.2, 11.1). Historically, a persistent challenge has been penetrating the dust and surrounding molecular cloud in which such sources are enveloped. McGuire highlighted the work of A. Ginsburg et al. (2018) who discovered a set of (initially unidentified) molecular lines that trace a Keplerian disk around the high-mass young stellar object Orion Source I (see also L. D. Matthews et al. 2010). With the help of McGuire, A. Ginsburg et al. (2019) later identified these as various vibrational levels of the salt molecules KCl and NaCl and their various isotopologues. Importantly, these molecules trace the disk that can be observed without contamination

from the surrounding molecular cloud. Furthermore, these lines are bright and readily observable. However, despite this, we do not fully understand how these molecules formed and how they give rise to the vibrationally hot lines that are observed. In particular, it is not yet known whether they form in situ or are liberated from grains. McGuire noted that answers to these questions would provide valuable new information about the immediate environments of massive protostars.

Also on the topic of the astrochemistry of star-forming regions, A. Burkhardt (Worcester State University) presented new survey results from a continuation of the ARKHAM (A Rigorous K-band Hunt for Aromatic Molecules) survey conducted using the Green Bank Telescope (GBT; A. M. Burkhardt et al. 2021). This new work has expanded to ∼10 the number of sources in star formation regions with detections of the aromatic molecule benzonitrile (C_6H_7CN) and established that the star-forming region TMC-1 is not unique in containing aromatic molecules. The results have implications for the long-debated question of whether aromatic molecules form in the atmospheres of evolved carbon stars, or in situ in star-forming regions ("top-down" versus "bottom-up" formation, respectively). At the time of the meeting the next major release of the ARKHAM survey was forthcoming.

12.4. *Future Astrochemistry Work*

McGuire concluded his presentation by emphasizing that the combined sensitivity, instantaneous bandwidth, and spatial and spectral resolution of the ngVLA are expected to be a game-changer for astrochemistry (e.g., B. A. McGuire et al. 2018a, 2018b; Section 18.1.3). The wavebands covered by the ngVLA will enable the penetration of dust to probe the inner few arcseconds around nearby AGB stars like IRC+10216. As described by A. Moullet, the ongoing Wideband Sensitivity Upgrade (WSU) at ALMA is also expected to be extremely valuable for astrochemistry by enabling ALMA to far more efficiently observe wide swaths of spectrum in a given target with high spectral resolution (Section 18.1.2).

13. VLBI ASTROMETRY AS A TOOL FOR STELLAR ASTROPHYSICS

An invited talk by G. Ortiz-León (Instituto National de Astrofisica, Mexico) summarized the importance of VLBI astrometry as a tool for the study of stellar systems. Ortiz-León began by highlighting the steady progress in achievable astrometric accuracy over the years, from the level of $\sim 1'$ reached by Hipparcus in 150 BC to the $\sim 10\mu$m levels that are now realized. For stellar astrophysics, such accuracy enables the derivation of fundamental stellar parameters (including masses and ages) and the precise orbital characterization of binary and planetary companions.

While the space-based *Gaia* mission has now provided astrometric measurements of >1 billion stars (Gaia Collaboration et al. 2023), Ortiz-Léon pointed out that there are certain classes of stellar sources that are not readily accessible to *Gaia*, including highly extincted young stars, close binaries (separations $<0''.2$; D. Chulkov & O. Malkov 2022), and red giants (AGB and RSG stars) whose large angular diameters and dusty envelopes add large uncertainties to *Gaia* measurements (M. Andriantsaralaza et al. 2022). As described by Ortiz-León, these are among the areas where VLBI astrometry—which can currently achieve accuracies of $\sim 10\mu$m for parallaxes and $\sim 1\mu$m for proper motions (M. J. Reid & M. Honma 2014)—is particularly valuable. A caveat, however, is that because of sensitivity limitations, VLBI remains limited to bright sources, including nonthermal continuum emitters such as YSOs, M dwarfs, and UCDs, and evolved stars with nonthermal (maser) lines (see Sections 5, 11).

One recent project discussed by Ortiz-León is known as Dynamical Masses of Young Stellar Multiple Systems with the VLBA (DYNAMO–VLBA), which has observed ∼20 protostellar systems using the VLBA. For the case of Oph-S1, a young binary in the Ophiuchus region, Ortiz-León and colleagues used 35 epochs of VLBA observations to model the astrometry and binary orbit and obtain dynamical mass estimates of the binary components (J. Ordóñez-Toro et al. 2024). Another DYNAMO–VLBA result was featured in the poster presentation of J. Ordóñez-Toro (UNAM). She described work using the VLBA to study the young triple stellar system EC 95 located in the Serpens star-forming region. Previous radio observations of this system with the VLA and VLBA had played important roles in determining its distance and the nature of its binary components (e.g., C. Eiroa et al. 2005; G. N. Ortiz-León et al. 2017). The multi-epoch VLBA observations presented by Ordóñez-Toro (32 epochs spread over 12 years) expanded on this work by enabling precision measurements of the binary orbit, along with the the masses of the primary and secondary components (J. Ordóñez-Toro et al. 2025; Figure 7). Her group had also obtained radio measurements of the third component of the system during 4 epochs, and efforts to determine its mass were ongoing.

Another result showcased by Ortiz-León is the study by S. Curiel et al. (2024) of the close, ultracool binary LP 349-25. Thanks to their multi-epoch VLBI astrometry, S. Curiel et al. were able to obtain detailed orbital parameters,

along with dynamical masses for both components, revealing that the secondary is a brown dwarf ($M \approx 67\ M_{\rm Jupiter}$) rather than a hydrogen-burning star. In addition, through comparison with theoretical tracks, they were able to derive ages, effective temperatures, and radii for both components and show that the secondary is significantly less evolved (by ∼60 Myr) than the primary.

Ortiz-León and her collaborators are also using their astrometric results to search for previously unseen planetary mass companions in low-mass stars within 10 pc. In the case of the system TVLM 513-46546, the study by S. Curiel et al. (2020) obtained an astrometric detection of a planetary mass companion ($M \approx 0.4\ M_{\rm jup}$) to an M9 UCD—one of only a handful known and the first to date detected using radio wavelength astrometry. For a second example, the low-mass binary GJ 896, both M dwarf components were detected in the radio and the VLBI astrometric data revealed the presence of an additional Jupiter-like companion in the system (S. Curiel et al. 2022). The authors were also able to map the 3D orbital architecture of all three components, revealing a surprisingly large mutual inclination angle (148°) between the two orbital planes.

Ortiz-León emphasized that the future is expected to be bright for further astrometric exoplanet searches using VLBI techniques (see also Section 6.1). For example, with an expected astrometric accuracy of $\sim 1\mu$m, the ngVLA (see Section 18.1.3) will have the potential to detect lower mass exoplanets and also planets associated with more distant stars than in now possible with VLBI, including planetary mass objects that fill a unique parameter space that is not accessible to *Gaia* or other search methods (see C. Melis 2019).

14. STELLAR EXPLOSIONS

14.1. *Novae*

14.1.1. *Background and Recent Work*

Classical novae are explosive events that occur in binary systems containing a white dwarf component that accretes material from its companion (either a main sequence star or a red giant), leading to thermonuclear runaway on the white dwarf's surface. Characteristic ejection velocities and ejection masses of such events are ∼500-5000 km s^{-1} and $\sim 10^{-7}$ to $10^{-3}\ M_\odot$, respectively, with the latter depending both on the accretion rate and the white dwarf mass. Energies of these events are typically $\sim 10^{45}$ erg (one millionth that of a supernova). The importance of radio wavelength observations for understanding the physics of classical novae was reviewed by L. Chomiuk (Michigan State University).

Chomiuk noted that the longstanding picture to explain the electromagnetic emission observed from novae is one whereby residual nuclear burning is sustained on the white dwarf's surface for a period of days to weeks at close to the Eddington luminosity (10^{38} erg s^{-1}). In this scenario, the radio emission from novae is expected to be thermal free-free ($S_\nu \propto \nu^2$), with properties similar to an expanding H II region. Initially, the source will be optically thick, and hence brighter at higher radio frequencies. Higher frequencies then become increasingly optically thin until an $S_\nu \propto \nu^{-1}$ spectral index is seen (e.g., R. M. Hjellming et al. 1996). Because higher ejection masses take longer to become optically thin, by studying radio light curves it becomes possible to infer the mass of the ejecta (e.g., E. R. Seaquist & M. F. Bode 2008).

Chomiuk described how radio light curves of novae pose challenges to this model, and have provided some of the first clues that the "expanding H II region" picture is too simplistic. One of the first hints was the appearance of a second peak in the radio light curve of some novae. Examples can be seen in the compilation of radio-detected novae (36 in total) published by L. Chomiuk et al. (2021b). Estimates for the brightness temperature of the emission during the two peaks systematically point to values of $T_B > 5 \times 10^4$ K for the initial peak, implying that the emission is non-thermal (synchrotron) in nature, while the second peak is thermal. In total, ∼25% of the novae in the sample compiled by L. Chomiuk et al. show evidence for synchrotron emission. She noted that this development is not surprising in light of other clear indicators for the role of shocks in novae, such as the now routine detection of novae as GeV γ-ray sources (e.g., A. A. Abdo et al. 2010; M. Ackermann et al. 2014; L. Chomiuk et al. 2014, 2021a).

VLBI observations, which are sensitive only to nonthermal emission, allowed Chomiuk and collaborators to pinpoint the regions where shock-induced synchrotron emission originates (L. Chomiuk et al. 2014), and helped lead to the emergence of a working model whereby the envelope of the nova expands slowly, primarily along the orbital plane of the binary. Later, nuclear burning on the white dwarf powers the emergence of a fast, bipolar wind, which interacts with the denser equatorial disk/envelope and leads to synchrotron-producing shocks along the interaction region (see also M. M. Nyamai et al. 2021). Chomiuk cautioned that these complexities, along with the possible presence of

clumping in the thermal emission, lead to uncertainties of at least a factor of a few in ejection masses derived from radio observations.

The value of VLBI observations for nova studies was also highlighted in the presentation by M. Williams (New Mexico Institute of Technology), who presented results of a recent study of nova V1674 Her (an intermediate polar). V1674 Her erupted in 2021 and was seen to fade from its peak optical brightness by two magnitudes in ∼1.1 days, indicative of extremely rapid evolution; indeed, it is the most rapidly evolving nova seen to date (K. V. Sokolovsky et al. 2023). Its detection in γ-rays suggested it was a good candidate for the presence of nonthermal emission that could be followed up with VLBI. Motivated by this, Williams's team observed V1674 Her with the VLBA during 4 epochs (21, 24, 36, and 71 days after eruption; M. Williams et al. 2023). Based on the morphology of the imaged radio emission, V1674 Her appears different from other VLBI-imaged novae (cf. L. Chomiuk et al. 2014; M. Giroletti et al. 2020; U. Munari et al. 2022) in that it lacks the prototypical double-lobe structure, suggesting that the shock that formed in this system may be one-sided (or else that one side is hidden from view). Using the revised equipartition theory of R. Beck & M. Krause (2005), Williams and colleagues were able to estimate from the VLBA measurements the brightness temperature and magnetic field strength during each epoch, enabling a tracing of the evolution of the shock. They also derived a shock expansion velocity of ∼5300 km s^{-1}.

Other areas of active, ongoing research on novae as highlighted by Chomiuk include exploring how the properties of the radio light curves of novae correlate with the properties of the γ-ray light curves and understanding how and where dust forms in nova ejecta. It has been proposed that the same shocks responsible for the production of γ-rays and synchrotron emission may also lead to dust formation (A. M. Derdzinski et al. 2017). Supporting this suggestion, Chomiuk pointed to the cases of novae (including V357 Mus and V1324 Sco) where the synchrotron peak in the radio light curve corresponds in time with a dip in the visual light curve that is believed to result from dust formation.

While Chomiuk's review primarily focused on classical novae (i.e., those with a main sequence companion star), I. Molina (Michigan State University) provided details of a recent study of the recurrent symbiotic nova V745 Sco, in which the companion is a red giant. Molina noted that for novae with main sequence companions, the mass transfer is primarily through Roche lobe overflow, while in the case of a red giant companion, wind accretion dominates, leading to the production of a denser and more copious circumstellar medium. V745 Sco is one of 10 recurrent novae known in our Galaxy and one of only four with a red giant companion.

V745 Sco underwent its last outburst in 2014, during which it was observed with the VLA in several bands, including 1.2, 4.6, and 28.2 GHz. All frequencies were seen to peak at the same time and at comparable flux densities, in contrast to classical novae where lower frequencies peak later and exhibit lower flux densities (e.g., L. Chomiuk et al. 2021b). Molina estimated the brightness temperature of the V745 Sco radio emission and found $T_B > 5 \times 10^4$ K, indicative of synchrotron emission. However, she and her colleagues found simple models for the synchrotron emission unable to reproduce the behavior of the radio light curves (I. Molina et al. 2024). Instead, the observed evolution of the spectral index points to a picture where the radio emission starts off optically thick (α=1.3), but then rather abruptly becomes optically thin ($\alpha \approx 0$). This could occur if the absorbing screen disappears suddenly, allowing the shock to break out abruptly, unveiling emission at all radio frequencies at once. Molina noted that this idea is supported by X-ray observations which suggest a rapid decrease in the column density of absorbing material (L. Delgado & M. Hernanz 2019). One possible instigator, explored by I. Molina et al., is a modulation of the optical depth by the presence of an equatorial density enhancement, as seen in the hydrodynamic simulations of V745 Sco by S. Orlando et al. (2017).

14.1.2. *Future Work*

In terms of future work on novae, Chomiuk noted that on the theoretical side, more detailed modeling is needed to fully account for the observed radio light curves, including complexities such as variations in mass-loss geometry. She also pointed to the anticipated power of the ngVLA (Section 18.1.3), which would allow observing both the thermal and nonthermal radio emission from novae concurrently, as well as significantly increasing the number of novae each year whose thermal and non-thermal radio properties can be studied in detail (see J. D. Linford et al. 2018). In the nearer term, M. Williams pointed out that ongoing VLBA upgrades (see Section 18.1.1) will improve the ability to study nova through improved sensitivity and better imaging capabilities, including at Ka band where imaging with the VLBA has heretofore not been possible.

14.2. *Supernovae*

Invited speaker D. Dong (NRAO) reminded the audience that there is a considerable diversity in the types and properties of progenitor systems that can give rise to supernovae (SNe; e.g., A. V. Filippenko 2005). That includes

a wide range in mass-loss rates, leading to significant variants in the types of explosions they can create and the ejecta they leave behind. Understanding the origin of this diversity is relevant from the standpoint of studying stellar evolution, but also for understanding the important role that SNe play in shaping their galactic environments and driving new generations of star formation (see e.g., I. Heywood et al. 2022; C. Zucker et al. 2022). However, systematically understanding these relationships and connecting the properties of SNe to their progenitors requires access to large sample sizes. As noted by Dong, historically this has meant studies based on samples identified in optical surveys, which to date comprise $\sim 10^4$ SNe. Unfortunately, those SNe samples have certain limitations. Optically identified SNe span a relatively narrow range in peak luminosity ($\sim$ orders of magnitude; e.g., N. Smith et al. 2007), and optical data are also limited by the timescales (days to months) and spatial scales (up to $< 10^{15}$ to $< 10^{17}$ cm) to which they are sensitive. On the other hand, as stressed by Dong, the inclusion of radio-emitting SNe, whose emission arises predominantly from synchrotron emitted by the forward shock (e.g., R. A. Chevalier 1998), can significantly expand the luminosity range of SNe samples and enable the study of larger-scale phenomena, including stellar mass loss on the timescales of centuries to millenia before the supernova explosion.

As of 2020, $\sim$100 radio-detected SNe were known, the bulk of which had been targeted for radio wavelength follow-up subsequent to optical discovery (M. F. Bietenholz et al. 2021). Characterization of the radio light curves of this sample was already seen to increase by three orders of magnitude the peak luminosity range known to occur among SNe. However, this type of follow-up study is time-consuming and resource-intensive. Fortunately, as reported by Dong, one of the outcomes of the latest generations of widefield radio wavelength surveys such as VLASS (see also Section 15) has been the discovery of several dozen or more radio-detected SNe, both through cross-matching against optical detections (M. C. Stroh et al. 2021) and through the direct detection of new SNe in the radio (Dong et al., in prep). These SNe are preferentially luminous ones owing to the depth of the VLASS survey, but importantly extend by 1–2 orders of magnitude to longer mass-loss timescales compared with pure optically selected samples. Dong noted that present-day widefield radio surveys, including VLASS, VLITE, VAST, and others (see Section 15) are sensitive to SNe luminosities of $\gtrsim 10^{27}$ erg s^{-1} Hz^{-1}. However, next-generation surveys with facilities like the Deep Synoptic Array (DSA) 2000 are expected to reach $\sim 10^{25}$ erg s^{-1} Hz^{-1}, while pointed observations with ngVLA or SKA (Section 18) could reach as low as $\sim 10^{23}$ erg s^{-1} Hz^{-1}.

Another topic addressed by Dong is the question of what determines the radio luminosity of a supernova. He noted that decreasing the energy of the explosion itself results in a sharp decrease in the radio luminosity—an assumption that has been little discussed in the literature to date. Historically, low luminosities have instead been attributed primarily to low densities alone. In addition, geometric effects can become important in the optically thick regime. In such a case, assuming a spherical geometry, free-free absorption can in principle absorb all of the radio emission. However, an aspherical geometry (e.g., resulting from a binary interaction) can lead to the presence of shock-heated, low-density regions along the poles where free-free absorption is no longer relevant (D. Z. Dong et al. 2021).

15. RADIO STAR SURVEYS

Most of the work done on radio stars over the past half century has targeted individual stars for study based on known properties at other wavebands. And while some limited attempts have been made to identify stellar sources in existing radio surveys, distinguishing them from extragalactic background sources can be challenging. However, as was apparent from the number of related presentations at the RS3 meeting, we are now entering an exciting new era for radio survey-enabled stellar science.

15.1. *Survey Limitations and Biases*

As emphasized by G. Umana, essentially all current radio star surveys are subject to particular biases depending on the search method used. For example, looking for radio variability results in a bias toward detection of flare stars; targeting circular polarization favors detections to stars with coherent emission; proper motion detections require radio emission to be persistent; selection based on source classification requires extensive databases of supporting ancillary information and good a priori knowledge of the source physics; sky surveys that omit low Galactic latitudes are biased against detection of types of stellar sources that are concentrated toward the Galactic Plane. For these reasons, the combined results from multiple survey approaches are crucial to obtaining a more comprehensive understanding of stellar radio emission. Several meeting presentations highlighted important strides in reducing previous limitations and biases.

One example described by Umana is the GLObal view of STAR formation in the Milky Way (GLOSTAR) survey in the Galactic Plane with the VLA, which combined higher sensitivity and angular resolution than past centimeter wave

surveys of the Plane. This survey successfully identified more than 100 new PN candidates and nearly 600 new radio star candidates (A. Y. Yang et al. 2023). GLOSTAR also illustrated the power of using databases of multiwavelength measurements to distinguish between different classes of sources.

A longstanding major challenge in identifying stellar sources in large radio sky surveys is contamination by active galactic nuclei (AGN). However, Umana pointed out that we can take advantage of lessons learned from current and ongoing sky surveys with various SKA precursors such as LOFAR, ASKAP, and MeerKAT to address this challenge (see, e.g., T. W. Shimwell et al. 2017; T. Murphy et al. 2021; S. Goedhart et al. 2024).

One tool at our disposal to help distinguish stellar sources from background objects is circular polarization (see Section 15.2). Another effective discriminant is short-term variability; for example, searching with a 15 minute cadence in ASKAP pilot survey data, Y. Wang et al. (2023) were able to identify 38 transients, including 7 previously unknown radio stars (plus one known radio star). Proper motions can also be used to find stars in widefield radio surveys with sufficiently long time baselines, as was recently demonstrated by L. N. Driessen et al. (2023) using data from the VLA Faint Images of the Radio Sky at Twenty-cm (FIRST) survey and the Rapid ASKAP Continuum Survey (RACS), combined with proper motion information from the *Gaia* Data Release 3. Their search identified 2 new radio stars, plus several previously known radio stars and 43 candidate variable radio stars. Additional results are discussed below.

15.2. *Centimeter Wavelength Surveys*

T. Murphy (University of Sydney) provided an overview of a range of stellar science results emerging from surveys being conducted by ASKAP, a telescope array in Western Australia comprising 36 12 m dishes and operating at frequencies from 700–1800 MHz. Attributes of ASKAP data products that make them particularly well-suited to mining for stellar science include ASKAP's wide field-of-view (30 square degrees) and the availability of both circular polarization and temporal information. At the time of the conference, a year's worth of ASKAP data amassed from several different survey projects had been made publicly available to the worldwide community (e.g., D. McConnell et al. 2020; T. Murphy et al. 2021; S. W. Duchesne et al. 2023).

As noted above, circular polarization is a useful tool for distinguishing stellar sources from background objects. The reason is that only a few class of celestial objects–namely pulsars and certain classes of stars—exhibit significant circular polarization ($>$ a few percent). In contrast, active galactic nuclei (AGN), whose source counts dominate centimeter-wave continuum surveys, typically have circular polarization fractions of $\ll$1%. Murphy stressed that such polarization information is a game-changer compared with earlier generations of radio surveys that lacked such information and where distinguishing stars from AGN was extremely challenging.

As one example, Murphy highlighted the recent work by J. Pritchard et al. (2021, 2024) who identified ∼70 radio stars in ASKAP survey data, of which two-thirds had not been detected previously. A comparison between model predictions and derived brightness temperature limits allowed constraining the radio emission mechanisms and suggests that radio emission from active binaries such as RS CVn and Algol systems (see also Section 4.1) tends to be consistent with gyrosynchrotron, whereas certain other types of stars (including K and M dwarfs) require a coherent mechanism. Another important finding was that each epoch of data revealed new radio stars. Furthermore, the majority of the radio stars detected in each epoch were stars that were not radio-bright in the previous one. An analysis of these data showed that for K and M dwarfs within 25 pc, the median fraction of stars that undergo radio-bright bursting or flaring events at a given time is $\gtrsim$10% (J. Pritchard et al. 2024). This rate is notably lower than inferred previously from samples of stars that were pre-selected based on activity levels at shorter wavelengths (∼25%; cf. S. M. White et al. 1989; J. Villadsen & G. Hallinan 2019). Nonetheless, an extrapolation of these results suggests that future all-sky surveys with SKA-Mid are expected to result in the detection of ∼58,000 stars from just a single hour of data.

L. Driessen (University of Sydney) presented the Sydney Radio Star Catalogue (SRSC), a new radio star catalogue for ν <3 GHz based primarily, though not exclusively on ASKAP data, along with recently published data from other SKA precursor instruments (L. N. Driessen et al. 2024 and references therein). The SRSC contains ∼850 radio stars representing types across the entire H-R diagram that were identified using a range of techniques, including circular polarization searches, proper motions, variability searches, and cross-matching with multi-wavelength data (Figure 8). A significant fraction of the SRSC stars (∼600) had not been identified as radio stars prior to ASKAP.

While a few small catalogues of radio stars have been published over the years (e.g., H. G. Walter et al. 1990; A. E. Kimball et al. 2009), as noted by Driessen, there has not been a major radio star catalogue published since the compilation of H. J. Wendker (1978, 1987, 1995), which was last updated in 2001 (see H. J. Wendker 2015). Driessen stressed that new and more extensive catalogues have the potential to provide insights into a range of topics

in stellar astrophysics research, including the overall fraction of radio-bright stars of different types, variability/flare rates of different stellar types, stellar rotation rates, and magnetic field properties of cool stars. In turn, such statistics are relevant to a range of more general problems including exoplanet habitability, the tying together of optical/radio reference frames, and Galactic foreground removal for extragalactic and cosmological studies. At the time of the meeting, work was underway to further expand the SRSC to include centimeter-detected radio stars from other surveys, as well as new ASKAP detections. Contributions to the catalogue are also welcomed from the community (see https://radiostars.org).

Using soft X-ray data from from eROSITA, Driessen and her collaborators have explored how well the SRCS sample conforms to the "new" Güdel-Benz relation of P. K. G. Williams et al. (2014) and find that the bulk of the stars lie *below* this relation (i.e., for a given radio flux they are less bright in X-rays than predicted). One explanation could be that a portion of the radio emission from many of the SRCS sample stars arises from a coherent mechanism, but work is ongoing to better understand this result.

Another outcome of the survey data from ASKAP has been the identification of interesting individual sources worthy of follow-up study. One example is the T8 brown dwarf WISE J062309.94−045624.6 (Figure 9), which was the subject of a poster by K. Rose (University of Sydney; see also Section 5). This object was identified through its strongly circularly polarized emission (∼66%) in the ASKAP RACS-mid survey at 0.9–2.0 GHz and is the coolest dwarf yet detected in the radio. Consistent with other radio-bright UCDs (Section 5), the high level of circular polarization suggests that coherent emission generated via the ECM instability dominates the radio signal. Follow-up observations with MeerKAT and Australian Telescope Compact Array (ATCA) showed WISE J062309.94−045624.6 to have rotationally modulated coherent emission and enabled a determination of a lower limit on the magnetic field strength of $B > 0.71$ kG (K. Rose et al. 2023). A complementary poster by R. Kavanagh (ASTRON) showed how the complex structure present in the periodic radio light curve of this object can be characterized using a purely geometric model. In this model, the magnetic field is dipolar with a large obliquity (i.e., the angle between the rotational and magnetic field axes), and the emission is beamed along two active field lines (R. D. Kavanagh et al. 2024). This work is expected to have future applications to other types of objects as well, including M dwarfs, magnetic massive stars (Section 8.2), or possible future radio-detected exoplanets.

Results of the largest non-targeted search for stellar radio transients at centimeter wavelengths undertaken to date were summarized in a poster presented by C. Ayala (California Institute of Technology). This study was based on data from VLASS, which covered 33,885 deg^2 at 2–4 GHz and reached a sensitivity of $\sim 140\mu$Jy (1σ). Ayala and his colleagues identified a sample of point sources that were undetected in a first epoch of data but detected at $> 7\sigma$ in a second epoch obtained 2 years later and then cross-matched these with known stellar sources from the *Gaia* catalogue[10]. After correcting for proper motions and assigning a probability of false detection they found a final sample of 80 stellar radio transients. The classes of sources detected included tight binaries, pre-main sequence stars, and M dwarfs, and in the majority of cases the radio emission appears linked with magnetic activity (C. Ayala et al. 2024; see also I. Davis et al. 2024a).

15.3. *Future Stellar Science from Radio Surveys*

Knowledge gained from current generations of radio star surveys is poised to help design and optimize future radio star surveys with up-and-coming facilities, e.g., insuring that such efforts are, by design, multi-epoch, full polarization surveys that include the Galactic Plane fields. As suggested by M. Rupen (National Research Council, Canada), building cross-referencing to other databases and catalogues into these surveys could help to increase their value and usage given the enormous anticipated data volumes. He also cautioned that compiling and processing such enormous future catalogues will require investing in dedicated teams of people.

Rupen suggested that source stacking, as is being recently employed by the Canadian Hydrogen Intensity Mapping Experiment (CHIME) collaboration, could be another potential tool for identifying relatively weak stellar sources in survey data. Also important will be well-developed source extraction algorithms, together with reliable, automated classification tools. Finally, to maximize the scientific return of upcoming radio surveys, L. Driessen emphasized the need for "outreach" to astronomers working at other wavelengths, as well as making radio wavelength data products more accessible and their unique value more widely appreciated.

[10] https://irsa.ipac.caltech.edu/Missions/gaia.html

16. RADIO STARS AS PROBES OF THE GALAXY

As we were reminded by L. Sjouwerman (NRAO), surveys of radio stars are useful not only for studying the properties of the stars themselves, but for also gaining insights into our Galaxy. A poster by Sjouwerman summarized recent results from the BAaDE Survey, a large, long-term project that has been using targeted VLA and ALMA observations of SiO masers in a large sample of evolved stars in the inner Milky Way/bulge region to provide information on the structure and evolution of the Milky Way (e.g., L. O. Sjouwerman et al. 2024). The radio measurements provide a powerful complement to other surveys owing to their ability to penetrate regions obscured in the optical and infrared, as well as the provision of important velocity information. BAaDE also complements the Bar and Spiral Structure Legacy (BeSSEL) program, another Galactic structure survey using masers (e.g., A. Brunthaler et al. 2011); since BeSSEL focuses on methanol and H_2O masers from high-mass star-forming regions, it primarily traces disk and spiral arm regions—but it cannot trace the bulge. Some of the recent BAaDE highlights featured on Sjouwerman's poster included sample spectra showing commensal detections of up to 7 SiO transitions in individual BAaDE target stars (see M. O. Lewis et al. 2020c; L. O. Sjouwerman et al. 2024; Section 11.2), a determination of the distinct Galactic distributions of oxygen-rich and carbon-rich AGB stars (M. O. Lewis et al. 2020a), a map of the Milky Way's structure as traced by BAaDE stars, and a new Galactic position-velocity diagram derived from SiO maser measurements of ∼15,000 targets over a full range of Galactic longitude (T.-Y. Xia et al. 2024). The latter sample has been used to measure the gravitational potential of the Milky Way bar and enables for the first time comparison with Galactic positions-velocity curves derived using gas (H I or CO) measurements.

A complementary poster by R. Weller (University of New Mexico) described a recently launched effort to tie together the dynamics of the disk with the older bulge and bar regions of the Milky Way using the SiO maser-emitting RSG stars in the BAaDE sample. Up to 20% of RSG-classified stars in their sample were found to be SiO maser emitters.

Accurate distance determinations are a crucial piece of using the measurements accumulated by the BAaDE project for Galactic science, and the poster presentation of R. Bhattacharya (University of New Mexico) featured an exploration of supervised machine learning as a tool to improve our ability to obtain distance estimates for large samples of Galactic AGB stars from the BAaDE sample. Using SEDs derived from infrared measurements of nearly 15,000 stars and assuming that stars with similar intrinsic properties (e.g., initial mass, temperature, metallicity, etc.) should have similar SEDs and similar luminosities, Bhattacharya and colleagues created a set of distance-calibrated SED templates and compared the inferred distances with direct distance measurements available for the subset of stars from *Gaia* or VLBI parallaxes (R. Bhattacharya et al. 2024). The results appear promising and are expected to aid in mapping the structure and dynamics of the inner Galaxy in addition to determining mass-loss rates and luminosities for large samples of AGB stars.

One additional topic addressed by M. Lewis was the use of the BAaDE SiO sample to derive a new period-luminosity (P-L) relation specific to maser-bearing stars. This is valuable for helping to overcome the extinction effects that impact traditional P-L relations. This was done using a sample of sources believed to lie in the Galactic Center region and with independently known distances. Applying this newly derived relation to their sample they were able to derive new P-L distances to over 6000 stars (see M. O. Lewis et al. 2023). This is complementary to the work presented in the poster by Bhattacharya (see above). Access to new and better distance estimates is expected to help with ongoing work on the SiO maser luminosity function by Lewis and collaborators. These new distance estimates are also crucial to achieving BAaDE's science goals of of measuring the structure and dynamics of the Galaxy (e.g., T.-Y. Xia et al. 2024).

Follow-up VLBI observations provide an important means of tying down the calibration of indirect, statistical distance determination methods for BAaDE stars. As described in the presentation by Y. Pihlström (University of New Mexico), VLBI methods are able to produce proper motion measurements for SiO maser stars within the bulge even in cases where parallax measurements are not possible; these in turn help to assess the Galactic orbits of these stars. However, one impediment to VLBI follow-up studies of targets near the Galactic Plane is the lack of calibration sources suitable for use at frequencies of $\gtrsim$43 GHz. To circumvent this issue, Pihlström and her collaborators have been developing a technique termed "shared astrometry", whereby the positions of multiple maser sources (each with its associated error ellipse) are used collectively used to pin down the positions of targets of interest, effectively building a frame of reference sources (e.g., L. H. Quiroga-Nunez et al. 2022). Because of proper motions, sources move relative to one another over time, hence a second step ties together the reference frames from different epochs. To date the shared astrometry approach has been tested via both Monte Carlo simulations and pilot VLA observations, and the results appear promising. While this method is too observationally intensive to apply to large samples, Pihlström

stressed that it could still serve as a means to calibrate other distance derivation methods used for BAaDE stars (see above).

17. DEGENERATE STARS AND STELLAR SYSTEMS

17.1. *X-Ray Binaries*

A poster by E. Pattie (Texas Tech University) featured radio observations of the relativistic jets associated with accreting black holes and neutron star binaries. Using archival ALMA and VLA data, Pattie and his colleagues have derived power spectra and high-cadence light curves for a sample of such systems, with the goal of comparing the observed characteristics of black hole binary and neutron star binary systems to assess their levels of similarity or differences in terms of their jet launching mechanisms (see E. C. Pattie et al. 2024; E. Pattie & T. Maccarone 2025). Unexpectedly, they find that both types of binary systems exhibit similar levels of variability despite large differences in radio luminosity, suggesting that their underlying jet structures and launching mechanisms may be similar.

17.2. *Cataclysmic Variables*

P. Barrett (George Washington University) presented new observations at 220 GHz and 354 GHz of the magnetic cataclysmic variable AR Sco, obtained with the Submillimeter Array (SMA; P. E. Barrett & M. A. Gurwell 2025). AR Sco is sometimes referred to as a "white dwarf pulsar". Synchrotron emission dominates the radio emission from this system at centimeter wavelengths, but the SMA observations have filled in a missing gap in the previous SED and point to a break in the synchrotron emission near $\nu \sim$200 GHz (Figure 10). A periodigram analysis of the SMA measurements at 220 GHz shows modulation at approximately twice the spin frequency of the white dwarf component of the binary and implies that the synchrotron emission originates from matter accreted onto the white dwarf's magnetic dipole rather than the photosphere of the red dwarf companion. A key conclusion of this study is that AR Sco is a magnetic propeller.

17.3. *White Dwarf Binaries*

R. Ignace discussed the possibility of using radio wavelength observations to search for the extensive disks postulated to occur around double degenerate white dwarf mergers. Unlike most accretion disks, these putative disks would not be thermally supported (which leads to a change in scale height with radius), but would instead be very flat with a steep density gradient, resulting in a signature kink or "knee" in the radio SED (R. Ignace 2024). Ignace pointed out that analogous signatures have already been seen in the disks of Be stars and interpreted as a truncation of their disks caused by a companion (R. Klement et al. 2017).

18. FUTURE PROSPECTS

18.1. *New and Upgrade Facilities of Relevance for Stellar Science*

18.1.1. *The Very Long Baseline Array (VLBA)*

Planned upgrades to the 31-year-old VLBA that are of potential relevance for stellar science were described in a poster by J. Linford (NRAO). These included both near-term (next 1–2 years) and longer-term ($\lesssim$10 years) efforts, leading up the the ngVLA era (see Section 18.1.3). Examples include new synthesizers that will allow greater tuning flexibility, new digital back-ends (enabling wider bandwidths, higher bit sampling rates, and improved timing stability), and a possible new suite of ultra-wide band (X–Ka band, i.e., 8-40 GHz) receivers. Linford reported that a prototype of the latter receiver has already been tested at the VLBA Owens Valley site. Other recent developments highlighted by Linford included improvements in high-frequency (86 GHz) pointing and the possibility of performing real-time correlation rather than the requirement to ship disk packs from individual stations to the central correlator in Socorro, New Mexico.

18.1.2. *ALMA 2030 and the Wideband Sensitivity Upgrade (WSU)*

Thanks to its combination of exquisite sensitivity (6600 m^2), unique dry, high-altitude site, broad frequency coverage (35 to 950 GHz), and the ability to image emission on angular scales from $\sim 1'$ down to as fine as $\sim$5 mas, ALMA, which began full science operations in 2014, has opened vast new discovery space for many areas of astrophysics. Stellar astrophysics is no exception, and numerous examples of its contributions to this subject were highlighted at the meeting (see above).

As described in talks by G. Umana and A. Moullet, a series of major developments is presently underway at ALMA under the umbrella of a program known as the Wideband Sensitivity Upgrade (WSU) to make ALMA even more powerful. The vision for the WSU was put forth in a document known as the ALMA 2030 Development Roadmap (J. Carpenter et al. 2019, 2022), and its top priority is expanding ALMA's IF bandwidth by at least a factor of two (to 16 GHz per polarization)—and up to a factor of 4—across ALMA's entire frequency range. Additional WSU improvements will include a new, more flexible ALMA correlator, improvements to the ALMA archive (to deal with larger data volumes), receiver upgrades, and improvements in digital efficiency across the entire signal chain. Essentially, with the exception of the antennas, the WSU will overhaul all components of ALMA by the end of the current decade.

Some of the anticipated benefits of the WSU for stellar astrophysics were highlighted in Moullet's presentation. For instance, among the first bands to be fully upgraded will be Band 6, which is one of most important bands for astrochemistry (Section 12). The improved spectral grasp will enable the simultaneous observations of lines within a spectral range of up to 32 GHz without sacrificing spectral resolution, and it will become possible to simultaneously process up to 1.2 million spectral channels, or 50× more than currently. For AGB and RSG stars this will make it possible, for example, to simultaneously observe a full suite of CO isotopologues in a single observation and enable simultaneously measuring multiple time-varying maser lines during the course of the stellar pulsation cycle (see Section 16). In the case of protostars, it will become possible to simultaneously observe at high spectral resolution lines arising in *all* components of the protostellar environment (e.g., jet, outflows, warm inner envelope, disk, disk wind, cold envelope; see Ł. Tychoniec et al. 2021).

As Moullet described, higher continuum sensitivities at ALMA resulting from the WSU will also improve the ability to perform polarization measurements of protostars, evolved stars, and PNe. Moreover, for spatially resolved imaging of such sources, the higher bandwidths will result in improved *uv* coverage, and therefore improved imaging fidelity and dynamic range (see J. Carpenter et al. 2022). This will enhance the ability to identify subtle features in the circumstellar environments of evolved, mass-losing stars, better constrain gas/dust coupling in these environments, and benefit searches for signatures of companion stars in radio data (see e.g., E. Aydi & S. Mohamed 2022; J. H. Kastner et al. 2024).

The anticipated improvements in digital efficiency and receiver performance at ALMA will result in a factors of ∼1.5–2.2× improvement in *spectral line* sensitivity as well. This will provide access to weaker molecular transitions and lines in more distant stars. In combination with the available ultra-high spectral resolution (∼10 m s^{-1}), improved measurements of Zeeman-induced circular polarization patterns in stellar sources (cf. W. H. T. Vlemmings et al. 2019) should also become possible.

18.1.3. *Next Generation VLA (ngVLA)*

The game-changing potential of the planned ngVLA for stellar science was spotlighted in a number of the presentations at the RS3 meeting (see above). As G. Umana described, the ngVLA's goal is to provide a factor of 10 improvement in both sensitivity and angular resolution compared with the VLA or ALMA for the study of thermal emission across the frequency range 1.2–116 GHz. The ngVLA will comprise an array of 214 18 m dishes concentrated in the Southwestern United States and northern Mexico. The array will include a dense core to provide high surface brightness sensitivity at ∼1,000 mas resolution, spiral-shaped arms of antennas for high-fidelity imaging at ∼10 mas scales, and longer arms to provide baselines for imaging at ∼1 mas scales. In addition, a continent-scale long baseline array is proposed as part of the ngVLA and would replace the current VLBA (see Section 18.1.1) and achieve angular resolutions as high as ∼0.1 mas. A more detailed description of the ngVLA design and examples of how it is expected to advance stellar science can be found in E. Murphy (2018). The ngVLA was only new radio facility in the United States that was specifically recommended in the Astro2020 Decadal Survey (Committee for a Decadal Survey on Astronomy and Astrophysics 2023). However, at the time of the RS3 meeting, the estimated cost of the ngVLA was projected to be ∼2.3 billion and full funding for the project had not yet been secured.

18.1.4. *Square Kilometer Array (SKA)*

Another future interferometric array facility that received prominent mention at the RS3 conference was the SKA. As described by G. Umana, at the time of the meeting the first phase of this project (known as SKA-1; R. Braun et al. 2019) was about 80% funded and construction was projected to be completed around the year 2030. In the mean time, a taste of what is to come from the SKA for stellar science was already given at the meeting through results already available from various SKA precursor telescopes, including MeerKAT, ASKAP, and the MWA (see above).

The SKA will operate at lower frequencies compared to the ngVLA (Section 18.1.3), although there will be a significant region of overlap. SKA-Low, to be sited in Western Australia, will operate at 50–350 MHz, while SKA-Mid, to be located in the Karoo region of South Africa, will cover 350 MHz–15.4 GHz. SKA-Low will be made up of more than 130,000 log-periodic antennas spread between 512 stations (equivalent collecting area of 419,000 m^2) and provide baselines of up to 74 km. SKA-Mid will comprise 197 parabolic antennas of diameter 13.5 m on baselines of up to 150 km and have a total collecting area of 33,000 m^2.

The SKA's frequency coverage will make it less ideally suited compared with the ngVLA for spatially resolved stellar imaging (see C. L. Carilli et al. 2018; K. Akiyama & L. D. Matthews 2019) and astrochemistry (see B. McGuire 2019). On the other hand, the SKA's enormous sensitivity, coupled with its primary operating mode as a survey instrument, are expected to yield large numbers of new detections of radio stars, coupled with a wealth of information on the radio light curves and SEDs of stellar radio sources (see, e.g., K. Marvel 2004; G. Umana et al. 2015; Section 9.1).

18.2. *Going to Space*

An invited talk by M. Knapp (MIT Haystack Observatory) summarized some of the unique advantages of pursuing future solar and stellar radio science from space. These include access to frequencies not observable through the Earth's atmosphere (i.e., $\lesssim$15 MHz), access to longer baselines, and, in the case of heliophysics, the ability to perform in situ measurements of plasma.

Knapp noted that the radio spectra of planets in our solar system obtained by the Voyager 2 satellite (P. Zarka 1992) have long informed our search for radio emission from planets *beyond* the solar system, including the push to go to space to enable direct detection of these emissions. She then provided a brief overview of several recent and planned space missions with relevance to solar and stellar science. For example, the Sun Radio Interferometer Space Experiment (SunRISE) will form a low-frequency interferometer in space (comprising 6 toaster-sized CubeSat spacecraft) to allow studies of energetic particles produced by CMEs and other solar bursts (J. C. Kasper et al. 2019). Launch is planned for 2025 or later. The CubeSat Radio Interferometry Experiment (CURIE) is another space mission designed to study low-frequency radio emission from CMEs (see Section 3.4), in this case utilizing a two-element interferometer (D. J. Sundkvist et al. 2016). [11] Both of these missions are expected to be able to follow CMEs as they propagate out from the Sun, and where the plasma frequency falls to low-frequency bands that can only be accessed from space.

Adding the list of proposed small spacecraft was the Auroral Emission Radio Observer (AERO)[12], led out of MIT Haystack Observatory, which planned to operate at 100 kHz–5 MHz (P. J. Erickson et al. 2019). A notable feature of AERO is that it would make use of a vector sensor antenna, which has the ability to fully characterize incident electromagnetic waves and measure the direction of arrival of auroral radio emission and image source regions, and at the same time obtain polarimetric information.

Knapp also described several space mission concepts that are in their early planning stages, including Farside Array for Radio Science Investigations of the Dark ages and Exoplanets (FARSIDE; J. O. Burns et al. 2019), a low radio frequency interferometric array proposed for the far side of the Moon which would comprise 128 dipole antennas spread across 10 km, operating from 150 kHz–40 MHz. Building the array on the lunar far side would shield it from terrestrial RFI, as well as other solar system noise sources, enabling near-continuous searches for radio signatures of CMEs and energetic particles from nearby stars, along with searches for exoplanet magnetospheres. An even more ambitious project, FarView, proposes to build a dipole array on the lunar far side through in situ mining of materials (R. S. Polidan et al. 2024). Lastly, Knapp introduced a project she is leading, a concept for free-flying space-based radio observatory known as Great Observatory for Long Wavelengths (GO-LoW). GO-LoW would comprise a large constellation of reconfigurable antenna nodes located at a stable Lagrange point (L4 or L5) and operating between 300 kHz–15 MHz. The number of spacecraft is driven by the goal of obtaining sufficient sensitivity to observe exoplanet magnetic fields in the solar neighborhood, including those of terrestrial planets. GO-LoW would be in the spirit of NASA's Great Observatory concept in that it would open an entirely new area of the electromagnetic spectrum to exploration (M. Knapp et al. 2024). Knapp speculated that a realistic timeline for building such an array may by $\sim$20–30 yr in the future.

[11] CURIE launched subsequent to the RS3 conference, in July 2024.

[12] At the time of the meeting, two identical spacecraft, AERO and VISTA were envisioned. The mission concept was later scaled back to a single spacecraft (AERO), but as of mid-2025 AERO had not been selected for development funding.

18.3. *Closing Perspectives*

R. Mutel (University of Iowa) closed the RS3 conference by offering some perspectives and forward-looking remarks. He reminded us that in spite of the capabilities of current radio instruments, the majority of Milky Way stars are still undetectable as "radio stars". Thus the stars that we do detect and study in the radio are often "unusual". (As one example, with current telescopes, the radio Sun would be undetectable out beyond a few pc). However, these limitations continue to fuel the desire to build new and better radio telescopes that enable observations over a broad range of radio frequencies.

Mutel informally polled meeting attendees to compile a list of some of the key outstanding questions in solar/stellar astrophysics that are likely to be prime targets for being answered in full or in part by future radio wavelength measurements. The resulting list (sorted by topic) included:

• *The Sun and Space Weather:*—(i) *How is the solar corona heated?* The question of the source of the coronal heating dates back more than 65 years (E. N. Parker 1958), but there is still no fully agreed upon answer. S. White noted that nanoflares are now a prime candidate (see Section 3.2), but it is not yet clear that they alone are sufficient. (ii) *Can we learn to reliably predict space weather (including CMEs)*? See e.g., Section 3.4 for some discussion of this point.

• *Exoplanets:*—(i) *Do all exoplanets have significant magnetic fields?* (ii) *How close are we to directly detecting exoplanets using radio techniques (i.e., astrometric VLBI)?* While there are still no exoplanets directly detected using radio techniques (Section 6.1), Mutel flagged this is a burgeoning field and predicted that as new, more sensitive instruments come online, this is likely to be one of the big discoveries in the next decade.

• *Star formation:*—(i) *What is the role of the magnetoplasma (especially in solving the angular momentum problem)?* Mutel stressed that it is clear that in many YSOs infall/outflow/jets are modulated by magnetic effects, yet many star formation studies do not account for the pressure of the magnetic field. (ii) *Can we build a comprehensive picture of the complex astrochemistry in star-forming regions?* This is a complex topic (see Section 12.3), but Mutel noted that an upgraded ALMA (see Section 18.1.2) should help to build a more comprehensive understanding over the next decade.

• *Ultracool Stars:*—*Why are the magnetic fields of many UCDs so strong?* Despite years of study (e.g., Section 5), it remains unclear what type of dynamo operates in UCDs (e.g., J. Robrade & J. H. M. M. Schmitt 2009). Mutel predicted that radio astronomy will play a key role in solving this puzzle.

• *Evolved Stars:*—(i) *What is the Galactic distribution of evolved stars?* Some new insights were presented at the meeting thanks to a combination of new databases and analysis approaches (Section 16) and more are forthcoming. (ii) *Why are PNe morphologies so complex and how do they evolve from main-sequence stars?* Some new clues have recently come from detailed ALMA observations of AGB stars (Section 9.2) and new observations of masers in PNe and water fountain sources (Section 11.3). (iii) *What accounts for the recent behavior of Betelgeuse?* See Section 9.3.1.

• *Active Stars:*—(i) *Why are "active" (solar-type) stars so much more active than the Sun?* (ii) *Why is there not a continuous range in radio luminosity for solar-type active stars, but rather an apparent "jump" in the activity levels?* See, e.g., M. Guedel et al. (1995) and Figure 6 of M. Güdel (2002). Possibilities mentioned by Mutel are that it is related to how the electron acceleration scales, or else differences in the large-scale magnetic field strength. (iii) *Where is the energetic plasma in interacting binaries?* Typically it is unclear whether the radiating plasma is associated with the active star, the less active star, or somewhere in between (but see Section 4.1). Generally interactive binaries like Algols and RS CVn and W Ursa Majoris systems are ∼10,000× more luminous than the Sun, requiring intense magnetic fields with very energetic particles, but generally we do not know exactly where they are arising from. Mutel suggested that better astrometric VLBI (with phase referencing), and comparisons with *Gaia* optical astrometry, should be able to answer this question in the future.

There was general agreement that solving the above questions will require the aid of new and better instruments (more sensitive; better angular resolution). However, as the volume and complexity of data continue to increase over the next decade, Mutel stressed that better analysis tools will play an equally important role [e.g., machine learning, high-performance computing, artificial intelligence (AI)].

Indeed, the dramatic growth in the use of machine learning and AI in scientific research represents one of the major changes since the previous Haystack Radio Stars conference in 2017 (L. D. Matthews 2019). Although these topics

were not prominently featured at RS3, their emergence as tools in stellar research was highlighted in a handful of presentations (e.g., Sections 3.2, 16). Applications of both machine learning and AI to stellar research are expected to grow significantly in the coming years owing to the rapidly expanding data volumes anticipated from new generations or instruments, for example, as aids to stellar source identification and extraction in large surveys (e.g., Section 15.3). Another dramatic change compared with a decade ago is the emerging importance for stellar science of a new set of low-frequency imaging arrays, including LOFAR, MWA, ASKAP, MeerKAT, and uGMRT—alongside the VLA, ALMA, and the VLBA, all of which remain in heavy use for stellar science at radio wavelengths.

Mutel closed with some remarks on the question of justification for the >$1 billion+ price tags of some of the currently proposed new radio telescope arrays (Section 18.1). He invoked the concept of the observable "hypervolume", whose four axes are the spectrophotometric, temporal, astrometric, and morphological domains (M. Harwit 1975; G. Djorgovski 2014), noting that certain types of objects will inhabit a part of this hypervolume that if not searched, will not be discovered. Examples of recent discoveries in radio astronomy that were not made until a new part of parameter space was sampled include fast radio bursts (no one had previously searched at such a fast time domain; D. R. Lorimer et al. 2007) and UCDs (which were not expected to be detectable radio sources until someone actually looked; E. Berger et al. 2001). The meeting organizers look forward to seeing what similarly paradigm-shifting discoveries await at the next Radio Stars Conference later this decade, as we approach the 50th anniversary of the first ever conference dedicated to radio stars (P. A. Feldman & S. Kwok 1979).

ACKNOWLEDGMENTS

The author gratefully acknowledges the contributions of the other members of the RS3 Local Organizing Committee (H. Johnson, D. Crowley, N. W. Kotary, D. Tonnelli, J. Tsai) and the RS3 Scientific Organizing Committee (R. Ignace, M. Rupen, L. Sjouwerman, S. White). Financial support for the RS3 conference was provided by award AST-2332009 from the National Science Foundation (NSF). The author's scientific contributions to the meeting were supported by grants from the NSF (AST-2107681) and from the Space Telescope Science Institute (HST-GO-16655.008-A). The author also wishes to acknowledge helpful comments from an anonymous referee.

REFERENCES

Abate, C., Pols, O. R., Izzard, R. G., Mohamed, S. S., & de Mink, S. E. 2013, A&A, 552, A26, doi: 10.1051/0004-6361/201220007

Abdo, A. A., Ackermann, M., Ajello, M., et al. 2010, Science, 329, 817, doi: 10.1126/science.1192537

Ackermann, M., Ajello, M., Albert, A., et al. 2014, Science, 345, 554, doi: 10.1126/science.1253947

Akabane, K., & Cohen, M. H. 1961, ApJ, 133, 258, doi: 10.1086/147021

Akiyama, K., & Matthews, L. D. 2019, arXiv e-prints, arXiv:1910.00013, doi: 10.48550/arXiv.1910.00013

Alvarado-Gómez, J. D., Drake, J. J., Cohen, O., Moschou, S. P., & Garraffo, C. 2018, ApJ, 862, 93, doi: 10.3847/1538-4357/aacb7f

Amada, K., Imai, H., Hamae, Y., et al. 2024, in IAU Symposium, Vol. 380, Cosmic Masers: Proper Motion Toward the Next-Generation Large Projects, ed. T. Hirota, H. Imai, K. Menten, & Y. Pihlström, 359–361, doi: 10.1017/S1743921323002739

Andriantsaralaza, M., Ramstedt, S., Vlemmings, W. H. T., & De Beck, E. 2022, A&A, 667, A74, doi: 10.1051/0004-6361/202243670

Asaki, Y., Maud, L. T., Fomalont, E. B., et al. 2020, ApJS, 247, 23, doi: 10.3847/1538-4365/ab6b20

Asaki, Y., Maud, L. T., Francke, H., et al. 2023, ApJ, 958, 86, doi: 10.3847/1538-4357/acf619

Ayala, C., Dong, D., Hallinan, G., et al. 2024, in American Astronomical Society Meeting Abstracts, Vol. 243, American Astronomical Society Meeting Abstracts, 359.33

Aydi, E., & Mohamed, S. 2022, MNRAS, 513, 4405, doi: 10.1093/mnras/stac749

Barrett, P. E., & Gurwell, M. A. 2025, ApJ, 986, 78, doi: 10.3847/1538-4357/add725

Bartkiewicz, A., Sanna, A., Szymczak, M., et al. 2020, A&A, 637, A15, doi: 10.1051/0004-6361/202037562

Bartkiewicz, A., Sanna, A., Szymczak, M., et al. 2024a, A&A, 686, A275, doi: 10.1051/0004-6361/202449491

Bartkiewicz, A., Szymczak, M., Kobak, A., & Aramowicz, M. 2024b, in IAU Symposium, Vol. 380, Cosmic Masers: Proper Motion Toward the Next-Generation Large Projects, ed. T. Hirota, H. Imai, K. Menten, & Y. Pihlström, 207–209, doi: 10.1017/S1743921323002466

Bastian, T. S., Pick, M., Kerdraon, A., Maia, D., & Vourlidas, A. 2001, ApJL, 558, L65, doi: 10.1086/323421

Baudry, A., Wong, K. T., Etoka, S., et al. 2023, A&A, 674, A125, doi: 10.1051/0004-6361/202245193

Bawaji, S., Alam, U., Mondal, S., Oberoi, D., & Biswas, A. 2023, ApJ, 954, 39, doi: 10.3847/1538-4357/ace042

Beck, R., & Krause, M. 2005, Astronomische Nachrichten, 326, 414, doi: 10.1002/asna.200510366

Becklin, E. E., Frogel, J. A., Hyland, A. R., Kristian, J., & Neugebauer, G. 1969, ApJL, 158, L133, doi: 10.1086/180450

Benaglia, P., Romero, G. E., Martí, J., Peri, C. S., & Araudo, A. T. 2010, A&A, 517, L10, doi: 10.1051/0004-6361/201015232

Benz, A. O., & Guedel, M. 1994, A&A, 285, 621

Berger, E., Ball, S., Becker, K. M., et al. 2001, Nature, 410, 338, doi: 10.1038/35066514

Bhattacharya, R., Medina, B. M., Pihlström, Y. M., et al. 2024, ApJ, 969, 109, doi: 10.3847/1538-4357/ad463e

Bhonsle, R. V., & McNarry, L. R. 1964, ApJ, 139, 1312, doi: 10.1086/147866

Bhunia, S., Carley, E. P., Oberoi, D., & Gallagher, P. T. 2023, A&A, 670, A169, doi: 10.1051/0004-6361/202244456

Biermann, E., Li, Y., Naess, S., et al. 2025, ApJ, 986, 7, doi: 10.3847/1538-4357/adce70

Bietenholz, M. F., Bartel, N., Argo, M., et al. 2021, ApJ, 908, 75, doi: 10.3847/1538-4357/abccd9

Billington, S. J., Urquhart, J. S., König, C., et al. 2020, MNRAS, 499, 2744, doi: 10.1093/mnras/staa2936

Biswas, A., Das, B., Chandra, P., et al. 2023, MNRAS, 523, 5155, doi: 10.1093/mnras/stad1756

Bloot, S., Vedantham, H. K., Kavanagh, R. D., Callingham, J. R., & Pope, B. J. S. 2025, A&A, 695, A176, doi: 10.1051/0004-6361/202452722

Boischot, A., & Lecacheux, A. 1975, A&A, 40, 55

Bojnordi Arbab, B., Vlemmings, W., Khouri, T., & Höfner, S. 2024, ApJ, 976, 138, doi: 10.3847/1538-4357/ad83b8

Bordiu, C., Rizzo, J. R., Bufano, F., et al. 2022, ApJL, 939, L30, doi: 10.3847/2041-8213/ac9b10

Bordiu, C., Riggi, S., Bufano, F., et al. 2025, A&A, 695, A144, doi: 10.1051/0004-6361/202450356

Boven, P., Vedantham, H. K., Callingham, J., & van Langevelde, H. J. 2023, in 15th European VLBI Network Mini-Symposium and Users' Meeting, 50

Bower, G. C., Bolatto, A., Ford, E. B., & Kalas, P. 2009, ApJ, 701, 1922, doi: 10.1088/0004-637X/701/2/1922

Brasseur, C. E., Jardine, M. M., & Hussain, G. A. J. 2024, MNRAS, 530, 2442, doi: 10.1093/mnras/stae996

Braun, R., Bonaldi, A., Bourke, T., Keane, E., & Wagg, J. 2019, arXiv e-prints, arXiv:1912.12699, doi: 10.48550/arXiv.1912.12699

Bridle, A. H., & Schwab, F. R. 1989, in Astronomical Society of the Pacific Conference Series, Vol. 6, Synthesis Imaging in Radio Astronomy, ed. R. A. Perley, F. R. Schwab, & A. H. Bridle, 247

Brunthaler, A., Reid, M. J., Menten, K. M., et al. 2011, Astronomische Nachrichten, 332, 461, doi: 10.1002/asna.201111560

Burkhardt, A. M., Loomis, R., Shingledecker, C. N., et al. 2021, in 2021 International Symposium on Molecular Spectroscopy, doi: 10.15278/isms.2021.RC07

Burns, J. O., Hallinan, G., Lux, J., et al. 2019, arXiv e-prints, arXiv:1911.08649, doi: 10.48550/arXiv.1911.08649

Burns, R. A., Uno, Y., Sakai, N., et al. 2023, Nature Astronomy, 7, 557, doi: 10.1038/s41550-023-01899-w

Cala, R. A., Gómez, J. F., & Miranda, L. F. 2024, in IAU Symposium, Vol. 380, Cosmic Masers: Proper Motion Toward the Next-Generation Large Projects, ed. T. Hirota, H. Imai, K. Menten, & Y. Pihlström, 343–346, doi: 10.1017/S1743921323001965

Callingham, J. R., Pope, B. J. S., Kavanagh, R. D., et al. 2024, Nature Astronomy, 8, 1359, doi: 10.1038/s41550-024-02405-6

Carilli, C. L., Butler, B., Golap, K., Carilli, M. T., & White, S. M. 2018, in Astronomical Society of the Pacific Conference Series, Vol. 517, Science with a Next Generation Very Large Array, ed. E. Murphy, 369, doi: 10.48550/arXiv.1810.05055

Carpenter, J., Brogan, C., Iono, D., & Mroczkowski, T. 2022, ALMA Memo Series, 621

Carpenter, J., Iono, D., Testi, L., et al. 2019, arXiv e-prints, arXiv:1902.02856, doi: 10.48550/arXiv.1902.02856

Carral, P., Kurtz, S. E., Rodríguez, L. F., et al. 2002, AJ, 123, 2574, doi: 10.1086/339701

Castor, J. I., Abbott, D. C., & Klein, R. I. 1975, ApJ, 195, 157, doi: 10.1086/153315

Cauley, P. W., Shkolnik, E. L., Llama, J., & Lanza, A. F. 2019, Nature Astronomy, 3, 1128, doi: 10.1038/s41550-019-0840-x

Cendes, Y., Williams, P. K. G., & Berger, E. 2022, AJ, 163, 15, doi: 10.3847/1538-3881/ac32c8

Cernicharo, J., Velilla-Prieto, L., Agúndez, M., et al. 2019, A&A, 627, L4, doi: 10.1051/0004-6361/201936040

Chevalier, R. A. 1998, ApJ, 499, 810, doi: 10.1086/305676
Chiavassa, A., Pasquato, E., Jorissen, A., et al. 2011, A&A, 528, A120, doi: 10.1051/0004-6361/201015768
Chomiuk, L., Metzger, B. D., & Shen, K. J. 2021a, ARA&A, 59, 391, doi: 10.1146/annurev-astro-112420-114502
Chomiuk, L., Linford, J. D., Yang, J., et al. 2014, Nature, 514, 339, doi: 10.1038/nature13773
Chomiuk, L., Linford, J. D., Aydi, E., et al. 2021b, ApJS, 257, 49, doi: 10.3847/1538-4365/ac24ab
Christensen, U. R., Holzwarth, V., & Reiners, A. 2009, Nature, 457, 167, doi: 10.1038/nature07626
Chrysaphi, N., Kontar, E. P., Holman, G. D., & Temmer, M. 2018, ApJ, 868, 79, doi: 10.3847/1538-4357/aae9e5
Chulkov, D., & Malkov, O. 2022, MNRAS, 517, 2925, doi: 10.1093/mnras/stac2827
Clarke, T., Kassim, N. E., Polisensky, E., et al. 2015, in The Many Facets of Extragalactic Radio Surveys: Towards New Scientific Challenges, 19, doi: 10.22323/1.267.0019
Climent, J. B., Guirado, J. C., Azulay, R., et al. 2020, A&A, 641, A90, doi: 10.1051/0004-6361/202037542
Climent, J. B., Guirado, J. C., Pérez-Torres, M., Marcaide, J. M., & Peña-Moñino, L. 2023, Science, 381, 1120, doi: 10.1126/science.adg6635
Committee for a Decadal Survey on Astronomy and Astrophysics. 2023,
Cordun, C. M., Vedantham, H. K., Brentjens, M. A., & van der Tak, F. F. S. 2025, A&A, 693, A162, doi: 10.1051/0004-6361/202452868
Costantino, S., Costa, C., & Noschese, A. 2023, The Astronomer's Telegram, 16374, 1
Cranmer, S. R., & Owocki, S. P. 1996, ApJ, 462, 469, doi: 10.1086/177166
Curiel, S., Ortiz-León, G. N., Mioduszewski, A. J., & Arenas-Martinez, A. B. 2024, ApJ, 967, 112, doi: 10.3847/1538-4357/ad3df6
Curiel, S., Ortiz-León, G. N., Mioduszewski, A. J., & Sanchez-Bermudez, J. 2022, AJ, 164, 93, doi: 10.3847/1538-3881/ac7c66
Curiel, S., Ortiz-León, G. N., Mioduszewski, A. J., & Torres, R. M. 2020, AJ, 160, 97, doi: 10.3847/1538-3881/ab9e6e
Das, B., & Chandra, P. 2021, ApJ, 921, 9, doi: 10.3847/1538-4357/ac1075
Das, B., Chandra, P., & Petit, V. 2024, ApJ, 974, 267, doi: 10.3847/1538-4357/ad71c5
Das, B., Chandra, P., Shultz, M. E., et al. 2022a, MNRAS, 517, 5756, doi: 10.1093/mnras/stac3123
Das, B., Chandra, P., & Wade, G. A. 2020a, MNRAS, 499, 702, doi: 10.1093/mnras/staa2499
Das, B., Mondal, S., & Chandra, P. 2020b, ApJ, 900, 156, doi: 10.3847/1538-4357/aba8fd
Das, B., Chandra, P., Shultz, M. E., et al. 2022b, ApJ, 925, 125, doi: 10.3847/1538-4357/ac2576
Davis, I., Hallinan, G., Ayala, C., Dong, D., & Myers, S. 2024a, arXiv e-prints, arXiv:2408.14612, doi: 10.48550/arXiv.2408.14612
Davis, I., Hallinan, G., & Saini, N. 2023, in American Astronomical Society Meeting Abstracts, Vol. 241, American Astronomical Society Meeting Abstracts, 346.07
Davis, I., Hallinan, G., Saini, N., & OVRO-LWA Collaboration. 2024b, in American Astronomical Society Meeting Abstracts, Vol. 243, American Astronomical Society Meeting Abstracts, 355.08
De Beck, E., Vlemmings, W., Muller, S., et al. 2015, A&A, 580, A36, doi: 10.1051/0004-6361/201525990
Decin, L., Montargès, M., Richards, A. M. S., et al. 2020, Science, 369, 1497, doi: 10.1126/science.abb1229
Decin, L., Gottlieb, C., Richards, A., et al. 2022, The Messenger, 189, 3, doi: 10.18727/0722-6691/5283
Delgado, L., & Hernanz, M. 2019, MNRAS, 490, 3691, doi: 10.1093/mnras/stz2765
Dent, W. R. F., Harper, G. M., Richards, A. M. S., Kervella, P., & Matthews, L. D. 2024, ApJL, 966, L13, doi: 10.3847/2041-8213/ad3afa
Derdzinski, A. M., Metzger, B. D., & Lazzati, D. 2017, MNRAS, 469, 1314, doi: 10.1093/mnras/stx829
Desmurs, J. F., Bujarrabal, V., Lindqvist, M., et al. 2014, A&A, 565, A127, doi: 10.1051/0004-6361/201423550
Dey, S., Kansabanik, D., & Oberoi, D. 2022, in AGU Fall Meeting Abstracts, Vol. 2022, SH24A–01
Djorgovski, G. 2014, in The Third Hot-wiring the Transient Universe Workshop, ed. P. R. Wozniak, M. J. Graham, A. A. Mahabal, & R. Seaman, 215–215
Doan, L., Ramstedt, S., Vlemmings, W. H. T., et al. 2020, A&A, 633, A13, doi: 10.1051/0004-6361/201935245
Dong, D. Z., Hallinan, G., Nakar, E., et al. 2021, Science, 373, 1125, doi: 10.1126/science.abg6037
Drake, J. J., Cohen, O., Garraffo, C., & Kashyap, V. 2016, in IAU Symposium, Vol. 320, Solar and Stellar Flares and their Effects on Planets, ed. A. G. Kosovichev, S. L. Hawley, & P. Heinzel, 196–201, doi: 10.1017/S1743921316000260
Driessen, L. N., Heald, G., Duchesne, S. W., et al. 2023, PASA, 40, e036, doi: 10.1017/pasa.2023.26
Driessen, L. N., Pritchard, J., Murphy, T., et al. 2024, PASA, 41, e084, doi: 10.1017/pasa.2024.72
Duchesne, S. W., Thomson, A. J. M., Pritchard, J., et al. 2023, PASA, 40, e034, doi: 10.1017/pasa.2023.31

Dulk, G. A. 1985, ARA&A, 23, 169, doi: 10.1146/annurev.aa.23.090185.001125

Dupree, A. K., Strassmeier, K. G., Matthews, L. D., et al. 2020, ApJ, 899, 68, doi: 10.3847/1538-4357/aba516

Eiroa, C., Torrelles, J. M., Curiel, S., & Djupvik, A. A. 2005, AJ, 130, 643, doi: 10.1086/431742

Ellingsen, S. P. 2007, MNRAS, 377, 571, doi: 10.1111/j.1365-2966.2007.11615.x

Erba, C., & Ignace, R. 2022, ApJ, 932, 12, doi: 10.3847/1538-4357/ac6c90

Erickson, P. J., Lind, F. D., Knapp, M., et al. 2019, in AGU Fall Meeting Abstracts, Vol. 2019, SA44A–07

Etoka, S., Baudry, A., Richards, A. M. S., et al. 2022, in IAU Symposium, Vol. 366, The Origin of Outflows in Evolved Stars, ed. L. Decin, A. Zijlstra, & C. Gielen, 199–203, doi: 10.1017/S1743921322000680

Etoka, S., Engels, D., Ullrich, T., González, J. B., & López-Martí, B. 2024, in IAU Symposium, Vol. 380, Cosmic Masers: Proper Motion Toward the Next-Generation Large Projects, ed. T. Hirota, H. Imai, K. Menten, & Y. Pihlström, 371–373, doi: 10.1017/S1743921323002004

Feldman, P. A., & Kwok, S. 1979, JRASC, 73, 271

Filippenko, A. V. 2005, in Astronomical Society of the Pacific Conference Series, Vol. 342, 1604-2004: Supernovae as Cosmological Lighthouses, ed. M. Turatto, S. Benetti, L. Zampieri, & W. Shea, 87

Foing, B. H. 1990, in NATO Advanced Study Institute (ASI) Series C, Vol. 319, Active Close Binaries Proceedings, NATO Advanced Study Institute, 363

Fonfría, J. P., Fernández-López, M., Agúndez, M., et al. 2014, MNRAS, 445, 3289, doi: 10.1093/mnras/stu1968

Forbrich, J., & Berger, E. 2009, ApJL, 706, L205, doi: 10.1088/0004-637X/706/2/L205

Forbrich, J., Dzib, S. A., Reid, M. J., & Menten, K. M. 2021, ApJ, 906, 23, doi: 10.3847/1538-4357/abc68e

Forbrich, J., Reid, M. J., Menten, K. M., et al. 2017, ApJ, 844, 109, doi: 10.3847/1538-4357/aa7aa4

Forbrich, J., Dupuy, T. J., Reid, M. J., et al. 2016a, ApJ, 827, 22, doi: 10.3847/0004-637X/827/1/22

Forbrich, J., Rivilla, V. M., Menten, K. M., et al. 2016b, ApJ, 822, 93, doi: 10.3847/0004-637X/822/2/93

Freytag, B., Steffen, M., Ludwig, H. G., et al. 2012, Journal of Computational Physics, 231, 919, doi: 10.1016/j.jcp.2011.09.026

Gaia Collaboration, Vallenari, A., Brown, A. G. A., et al. 2023, A&A, 674, A1, doi: 10.1051/0004-6361/202243940

Gary, D. E. 2023, ARA&A, 61, 427, doi: 10.1146/annurev-astro-071221-052744

Getman, K. V., Feigelson, E. D., Waggoner, A. R., et al. 2024, ApJ, 976, 195, doi: 10.3847/1538-4357/ad8562

Ginsburg, A., Bally, J., Goddi, C., Plambeck, R., & Wright, M. 2018, ApJ, 860, 119, doi: 10.3847/1538-4357/aac205

Ginsburg, A., McGuire, B., Plambeck, R., et al. 2019, ApJ, 872, 54, doi: 10.3847/1538-4357/aafb71

Giroletti, M., Munari, U., Körding, E., et al. 2020, A&A, 638, A130, doi: 10.1051/0004-6361/202038142

Goedhart, S., Cotton, W. D., Camilo, F., et al. 2024, MNRAS, 531, 649, doi: 10.1093/mnras/stae1166

Golay, W. W., Mutel, R. L., & Abbuhl, E. E. 2024, ApJ, 965, 86, doi: 10.3847/1538-4357/ad29fb

Golay, W. W., Mutel, R. L., Lipman, D., & Güdel, M. 2023, MNRAS, 522, 1394, doi: 10.1093/mnras/stad980

Gonidakis, I., Diamond, P. J., & Kemball, A. J. 2013, MNRAS, 433, 3133, doi: 10.1093/mnras/stt954

Gottlieb, C. A., Decin, L., Richards, A. M. S., et al. 2022, A&A, 660, A94, doi: 10.1051/0004-6361/202140431

Grognard, R. J. M., & McLean, D. J. 1973, SoPh, 29, 149, doi: 10.1007/BF00153446

Grunhut, J. H., Wade, G. A., & MiMeS Collaboration. 2012, in American Institute of Physics Conference Series, Vol. 1429, Stellar Polarimetry: from Birth to Death, ed. J. L. Hoffman, J. Bjorkman, & B. Whitney (AIP), 67–74, doi: 10.1063/1.3701903

Güdel, M. 2002, ARA&A, 40, 217, doi: 10.1146/annurev.astro.40.060401.093806

Guedel, M., & Benz, A. O. 1993, ApJL, 405, L63, doi: 10.1086/186766

Guedel, M., Schmitt, J. H. M. M., & Benz, A. O. 1995, A&A, 302, 775

Guélin, M., Patel, N. A., Bremer, M., et al. 2018, A&A, 610, A4, doi: 10.1051/0004-6361/201731619

Guinan, E. F., Wasatonic, R. J., & Calderwood, T. J. 2019, The Astronomer's Telegram, 13341, 1

Guns, S., Foster, A., Daley, C., et al. 2021, ApJ, 916, 98, doi: 10.3847/1538-4357/ac06a3

Hallinan, G., Littlefair, S. P., Cotter, G., et al. 2015, Nature, 523, 568, doi: 10.1038/nature14619

Harwit, M. 1975, QJRAS, 16, 378

Hess, S., Cecconi, B., & Zarka, P. 2008, Geophys. Res. Lett., 35, L13107, doi: 10.1029/2008GL033656

Heywood, I., Rammala, I., Camilo, F., et al. 2022, ApJ, 925, 165, doi: 10.3847/1538-4357/ac449a

Hjellming, R. M. 1988, in Galactic and Extragalactic Radio Astronomy, ed. K. I. Kellermann & G. L. Verschuur, 381–438

Hjellming, R. M., Rupen, M. P., Shrader, C. R., et al. 1996, ApJL, 470, L105, doi: 10.1086/310312

Höfner, S., Bladh, S., Aringer, B., & Ahuja, R. 2016, A&A, 594, A108, doi: 10.1051/0004-6361/201628424
Höfner, S., Bladh, S., Aringer, B., & Eriksson, K. 2022, A&A, 657, A109, doi: 10.1051/0004-6361/202141224
Höfner, S., & Olofsson, H. 2018, A&A Rv, 26, 1, doi: 10.1007/s00159-017-0106-5
Homan, W., Montargès, M., Pimpanuwat, B., et al. 2020, A&A, 644, A61, doi: 10.1051/0004-6361/202039185
Humphreys, R. M., & Davidson, K. 1994, PASP, 106, 1025, doi: 10.1086/133478
Humphreys, R. M., Richards, A. M. S., Davidson, K., et al. 2024, AJ, 167, 94, doi: 10.3847/1538-3881/ad1dd7
Humphreys, R. M., Ziurys, L. M., Bernal, J. J., et al. 2019, ApJL, 874, L26, doi: 10.3847/2041-8213/ab11e5
Ignace, R. 2024, in American Astronomical Society Meeting Abstracts, Vol. 244, American Astronomical Society Meeting Abstracts, 409.05
Ignace, R., St-Louis, N., & Prinja, R. K. 2020, MNRAS, 497, 1127, doi: 10.1093/mnras/staa2014
Imai, H. 2007, in IAU Symposium, Vol. 242, Astrophysical Masers and their Environments, ed. J. M. Chapman & W. A. Baan, 279–286, doi: 10.1017/S1743921307013130
Iwanek, P., Soszyński, I., Kozłowski, S., et al. 2022, ApJS, 260, 46, doi: 10.3847/1538-4365/ac6676
Kamiński, T., Gottlieb, C. A., Menten, K. M., et al. 2013, A&A, 551, A113, doi: 10.1051/0004-6361/201220290
Kang, J., Kim, M., Kim, K.-T., Hirota, T., & KaVA SF team. 2024, in IAU Symposium, Vol. 380, Cosmic Masers: Proper Motion Toward the Next-Generation Large Projects, ed. T. Hirota, H. Imai, K. Menten, & Y. Pihlström, 218–220, doi: 10.1017/S1743921323003332
Kansabanik, D. 2022, SoPh, 297, 122, doi: 10.1007/s11207-022-02053-x
Kansabanik, D., Bera, A., Oberoi, D., & Mondal, S. 2023a, ApJS, 264, 47, doi: 10.3847/1538-4365/acac79
Kansabanik, D., Mondal, S., & Oberoi, D. 2023b, ApJ, 950, 164, doi: 10.3847/1538-4357/acc385
Kansabanik, D., Mondal, S., & Oberoi, D. 2024a, ApJ, 968, 55, doi: 10.3847/1538-4357/ad43e9
Kansabanik, D., Mondal, S., Oberoi, D., Biswas, A., & Bhunia, S. 2022, ApJ, 927, 17, doi: 10.3847/1538-4357/ac4bba
Kansabanik, D., Mondal, S., Oberoi, D., et al. 2024b, ApJ, 961, 96, doi: 10.3847/1538-4357/ad0b7f
Kao, M. M., Hallinan, G., Pineda, J. S., et al. 2016, ApJ, 818, 24, doi: 10.3847/0004-637X/818/1/24
Kao, M. M., Mioduszewski, A. J., Villadsen, J., & Shkolnik, E. L. 2023, Nature, 619, 272, doi: 10.1038/s41586-023-06138-w
Kao, M. M., & Pineda, J. S. 2022, ApJ, 932, 21, doi: 10.3847/1538-4357/ac660b
Kao, M. M., & Pineda, J. S. 2025, MNRAS, 539, 2292, doi: 10.1093/mnras/stae905
Kao, M. M., & Shkolnik, E. L. 2024, MNRAS, 527, 6835, doi: 10.1093/mnras/stad2272
Karovska, M., Hack, W., Raymond, J., & Guinan, E. 1997, ApJL, 482, L175, doi: 10.1086/310704
Karovska, M., Schlegel, E., Hack, W., Raymond, J. C., & Wood, B. E. 2005, ApJL, 623, L137, doi: 10.1086/430111
Kasper, J. C., Lazio, J., Romero-Wolf, A., et al. 2019, in AGU Fall Meeting Abstracts, Vol. 2019, SH33A–02
Kastner, J. H., Wilner, D. J., Moraga Baez, P., et al. 2024, ApJ, 965, 21, doi: 10.3847/1538-4357/ad2848
Kavanagh, R. D., Vedantham, H. K., Rose, K., & Bloot, S. 2024, A&A, 692, A66, doi: 10.1051/0004-6361/202452094
Kavanagh, R. D., Vidotto, A. A., Klein, B., et al. 2021, MNRAS, 504, 1511, doi: 10.1093/mnras/stab929
Kervella, P., Decin, L., Richards, A. M. S., et al. 2018, A&A, 609, A67, doi: 10.1051/0004-6361/201731761
Keszthelyi, Z., Meynet, G., Martins, F., de Koter, A., & David-Uraz, A. 2021, MNRAS, 504, 2474, doi: 10.1093/mnras/stab893
Keszthelyi, Z., Puls, J., Chiaki, G., et al. 2024, MNRAS, 533, 3457, doi: 10.1093/mnras/stae1855
Keszthelyi, Z., Meynet, G., Shultz, M. E., et al. 2020, MNRAS, 493, 518, doi: 10.1093/mnras/staa237
Kim, H., Lee, H.-G., Mauron, N., & Chu, Y.-H. 2015, ApJL, 804, L10, doi: 10.1088/2041-8205/804/1/L10
Kimball, A. E., Knapp, G. R., Ivezić, Ž., et al. 2009, ApJ, 701, 535, doi: 10.1088/0004-637X/701/1/535
Klement, R., Carciofi, A. C., Rivinius, T., et al. 2017, A&A, 601, A74, doi: 10.1051/0004-6361/201629932
Knapp, M., Paritsky, L., Kononov, E., & Kao, M. M. 2024, arXiv e-prints, arXiv:2404.08432, doi: 10.48550/arXiv.2404.08432
Kobak, A., Bartkiewicz, A., Szymczak, M., et al. 2023, A&A, 671, A135, doi: 10.1051/0004-6361/202244772
Koelemay, L. A., & Ziurys, L. M. 2023, ApJL, 958, L6, doi: 10.3847/2041-8213/ad0899
Kooi, J. E., Ascione, M. L., Reyes-Rosa, L. V., Rier, S. K., & Ashas, M. 2021, SoPh, 296, 11, doi: 10.1007/s11207-020-01755-4
Kooi, J. E., Fischer, P. D., Buffo, J. J., & Spangler, S. R. 2017, SoPh, 292, 56, doi: 10.1007/s11207-017-1074-7
Krucker, S., & Benz, A. O. 2000, SoPh, 191, 341, doi: 10.1023/A:1005255608792
Lacy, M., Baum, S. A., Chandler, C. J., et al. 2020, PASP, 132, 035001, doi: 10.1088/1538-3873/ab63eb

Ladeyschikov, D. 2024, in IAU Symposium, Vol. 380, Cosmic Masers: Proper Motion Toward the Next-Generation Large Projects, ed. T. Hirota, H. Imai, K. Menten, & Y. Pihlström, 230–231, doi: 10.1017/S1743921323003290

Leto, P., Trigilio, C., Buemi, C. S., et al. 2016, MNRAS, 459, 1159, doi: 10.1093/mnras/stw639

Leto, P., Trigilio, C., Oskinova, L., et al. 2017, MNRAS, 467, 2820, doi: 10.1093/mnras/stx267

Leto, P., Trigilio, C., Oskinova, L. M., et al. 2018, MNRAS, 476, 562, doi: 10.1093/mnras/sty244

Leto, P., Trigilio, C., Krtička, J., et al. 2021, MNRAS, 507, 1979, doi: 10.1093/mnras/stab2168

Lewis, M. O., Bhattacharya, R., Sjouwerman, L. O., et al. 2023, A&A, 677, A153, doi: 10.1051/0004-6361/202346568

Lewis, M. O., Pihlström, Y. M., & Sjouwerman, L. O. 2024, in IAU Symposium, Vol. 380, Cosmic Masers: Proper Motion Toward the Next-Generation Large Projects, ed. T. Hirota, H. Imai, K. Menten, & Y. Pihlström, 314–318, doi: 10.1017/S1743921323002375

Lewis, M. O., Pihlström, Y. M., Sjouwerman, L. O., & Quiroga-Nuñez, L. H. 2020a, ApJ, 901, 98, doi: 10.3847/1538-4357/abaf46

Lewis, M. O., Pihlström, Y. M., Sjouwerman, L. O., et al. 2020b, ApJ, 892, 52, doi: 10.3847/1538-4357/ab7920

Lewis, M. O., Pihlström, Y. M., Sjouwerman, L. O., et al. 2020c, ApJ, 892, 52, doi: 10.3847/1538-4357/ab7920

Lim, J., Carilli, C. L., White, S. M., Beasley, A. J., & Marson, R. G. 1998, Nature, 392, 575, doi: 10.1038/33352

Lim, J., & White, S. M. 1996, ApJL, 462, L91, doi: 10.1086/310038

Linford, J. D., Chomiuk, L., & Rupen, M. P. 2018, in Astronomical Society of the Pacific Conference Series, Vol. 517, Science with a Next Generation Very Large Array, ed. E. Murphy, 271

Linsky, J. L. 1996, in Astronomical Society of the Pacific Conference Series, Vol. 93, Radio Emission from the Stars and the Sun, ed. A. R. Taylor & J. M. Paredes, 439

Linsky, J. L., Drake, S. A., & Bastian, T. S. 1992, ApJ, 393, 341, doi: 10.1086/171509

Lorimer, D. R., Bailes, M., McLaughlin, M. A., Narkevic, D. J., & Crawford, F. 2007, Science, 318, 777, doi: 10.1126/science.1147532

Ma, J.-Z., Chiavassa, A., de Mink, S. E., et al. 2024, ApJL, 962, L36, doi: 10.3847/2041-8213/ad24fd

MacGregor, A. M., Osten, R. A., & Hughes, A. M. 2020, ApJ, 891, 80, doi: 10.3847/1538-4357/ab711d

MacGregor, M. A., Weinberger, A. J., Wilner, D. J., Kowalski, A. F., & Cranmer, S. R. 2018, ApJL, 855, L2, doi: 10.3847/2041-8213/aaad6b

MacGregor, M. A., Weinberger, A. J., Loyd, R. O. P., et al. 2021, ApJL, 911, L25, doi: 10.3847/2041-8213/abf14c

Maercker, M., Mohamed, S., Vlemmings, W. H. T., et al. 2012, Nature, 490, 232, doi: 10.1038/nature11511

Magdalenić, J., Marqué, C., Fallows, R. A., et al. 2020, ApJL, 897, L15, doi: 10.3847/2041-8213/ab9abc

Marvel, K. 2004, NewAR, 48, 1349, doi: 10.1016/j.newar.2004.09.042

Matthews, L. D. 2013, PASP, 125, 313, doi: 10.1086/670019

Matthews, L. D. 2019, PASP, 131, 016001, doi: 10.1088/1538-3873/aae856

Matthews, L. D., & Claussen, M. J. 2018, in Astronomical Society of the Pacific Conference Series, Vol. 517, Science with a Next Generation Very Large Array, ed. E. Murphy, 281, doi: 10.48550/arXiv.1810.06666

Matthews, L. D., Dupree, A., & Akiyama, K. 2024, in American Astronomical Society Meeting Abstracts, Vol. 243, American Astronomical Society Meeting Abstracts, 409.01

Matthews, L. D., & Dupree, A. K. 2022, ApJ, 934, 131, doi: 10.3847/1538-4357/ac7726

Matthews, L. D., Greenhill, L. J., Goddi, C., et al. 2010, ApJ, 708, 80, doi: 10.1088/0004-637X/708/1/80

Matthews, L. D., Reid, M. J., Menten, K. M., & Akiyama, K. 2018, AJ, 156, 15, doi: 10.3847/1538-3881/aac491

McCauley, P. I., Cairns, I. H., White, S. M., et al. 2019, SoPh, 294, 106, doi: 10.1007/s11207-019-1502-y

McConnell, D., Hale, C. L., Lenc, E., et al. 2020, PASA, 37, e048, doi: 10.1017/pasa.2020.41

McGuire, B. 2019, BAAS, 51, 233

McGuire, B. A. 2022, ApJS, 259, 30, doi: 10.3847/1538-4365/ac2a48

McGuire, B. A., Carroll, P. B., & Garrod, R. T. 2018a, arXiv e-prints, arXiv:1810.06586, doi: 10.48550/arXiv.1810.06586

McGuire, B. A., Bergin, E., Blake, G. A., et al. 2018b, arXiv e-prints, arXiv:1810.09550, doi: 10.48550/arXiv.1810.09550

McLean, D. J. 1967, PASA, 1, 47, doi: 10.1017/S1323358000010468

Melis, C. 2019, ngVLA Memo Series, 85

Mercier, C., & Trottet, G. 1997, ApJL, 474, L65, doi: 10.1086/310422

Meyer, D. M. A., Vorobyov, E. I., Elbakyan, V. G., et al. 2021, MNRAS, 500, 4448, doi: 10.1093/mnras/staa3528

Meyer, D. M. A., Vorobyov, E. I., Kuiper, R., & Kley, W. 2017, MNRAS, 464, L90, doi: 10.1093/mnrasl/slw187

Mohamed, S., & Podsiadlowski, P. 2012, Baltic Astronomy, 21, 88, doi: 10.1515/astro-2017-0362

Mohan, A., Mondal, S., Oberoi, D., & Lonsdale, C. J. 2019, ApJ, 875, 98, doi: 10.3847/1538-4357/ab0ae5

Molina, I., Chomiuk, L., Linford, J. D., et al. 2024, MNRAS, 534, 1227, doi: 10.1093/mnras/stae2093

Mondal, S. 2021, SoPh, 296, 131, doi: 10.1007/s11207-021-01877-3

Mondal, S., Biswas, A., Oberoi, D., & Kansabanik, D. 2021, in AGU Fall Meeting Abstracts, Vol. 2021, SH15E–2059

Mondal, S., Chen, B., & Yu, S. 2022, in Third Triennial Earth-Sun Summit (TESS), Vol. 54, 2022n7i408p08

Mondal, S., Chen, B., & Yu, S. 2023a, ApJ, 949, 56, doi: 10.3847/1538-4357/acc838

Mondal, S., Mohan, A., Oberoi, D., et al. 2019, ApJ, 875, 97, doi: 10.3847/1538-4357/ab0a01

Mondal, S., Oberoi, D., & Vourlidas, A. 2020, ApJ, 893, 28, doi: 10.3847/1538-4357/ab7fab

Mondal, S., Chen, B., Gary, D., et al. 2023b, in AAS/Solar Physics Division Meeting, Vol. 55, 54th Meeting of the Solar Physics Division, 501.01

Morosan, D. E., Räsänen, J. E., Kumari, A., et al. 2022, SoPh, 297, 47, doi: 10.1007/s11207-022-01976-9

Morris, M., Gilmore, W., Palmer, P., Turner, B. E., & Zuckerman, B. 1975, ApJL, 199, L47, doi: 10.1086/181846

Moscadelli, L., Sanna, A., Beuther, H., Oliva, A., & Kuiper, R. 2022, Nature Astronomy, 6, 1068, doi: 10.1038/s41550-022-01754-4

Munari, U., Giroletti, M., Marcote, B., et al. 2022, A&A, 666, L6, doi: 10.1051/0004-6361/202244821

Murphy, E., ed. 2018, Astronomical Society of the Pacific Conference Series, Vol. 517, Science with a Next Generation Very Large Array

Murphy, T., Kaplan, D. L., Stewart, A. J., et al. 2021, PASA, 38, e054, doi: 10.1017/pasa.2021.44

Mutel, R. L., Lestrade, J. F., Preston, R. A., & Phillips, R. B. 1985, ApJ, 289, 262, doi: 10.1086/162886

Mutel, R. L., Morris, D. H., Doiron, D. J., & Lestrade, J. F. 1987, AJ, 93, 1220, doi: 10.1086/114402

Nyamai, M. M., Chomiuk, L., Ribeiro, V. A. R. M., et al. 2021, MNRAS, 501, 1394, doi: 10.1093/mnras/staa3712

Oberoi, D., Bisoi, S. K., Sasikumar Raja, K., et al. 2023, Journal of Astrophysics and Astronomy, 44, 40, doi: 10.1007/s12036-023-09917-z

Oberoi, D., Matthews, L. D., Cairns, I. H., et al. 2011, ApJL, 728, L27, doi: 10.1088/2041-8205/728/2/L27

O'Gorman, E., Harper, G. M., Brown, A., et al. 2015, A&A, 580, A101, doi: 10.1051/0004-6361/201526136

O'Gorman, E., Kervella, P., Harper, G. M., et al. 2017, A&A, 602, L10, doi: 10.1051/0004-6361/201731171

O'Gorman, E., Harper, G. M., Ohnaka, K., et al. 2020, A&A, 638, A65, doi: 10.1051/0004-6361/202037756

Ohnaka, K., Wong, K. T., Weigelt, G., & Hofmann, K. H. 2024, A&A, 691, L14, doi: 10.1051/0004-6361/202451977

Ordóñez-Toro, J., Dzib, S. A., Loinard, L., et al. 2024, AJ, 167, 108, doi: 10.3847/1538-3881/ad1bd3

Ordóñez-Toro, J., Dzib, S. A., Loinard, L., et al. 2025, MNRAS, 540, 2830, doi: 10.1093/mnras/staf904

Orlando, S., Drake, J. J., & Miceli, M. 2017, MNRAS, 464, 5003, doi: 10.1093/mnras/stw2718

Orrú, E., Norden, M. J., Iacobelli, M., ter Veen, S., & Ahmadi, A. 2024, in Society of Photo-Optical Instrumentation Engineers (SPIE) Conference Series, Vol. 13098, Observatory Operations: Strategies, Processes, and Systems X, ed. C. R. Benn, A. Chrysostomou, & L. J. Storrie-Lombardi, 130980R, doi: 10.1117/12.3019032

Ortiz Ceballos, K. N., Cendes, Y., Berger, E., & Williams, P. K. G. 2024, AJ, 168, 127, doi: 10.3847/1538-3881/ad58be

Ortiz-León, G. N., Dzib, S. A., Kounkel, M. A., et al. 2017, ApJ, 834, 143, doi: 10.3847/1538-4357/834/2/143

Ouyang, X.-J., Zhang, Y., Li, J., et al. 2024, ApJL, 964, L18, doi: 10.3847/2041-8213/ad3338

Owocki, S. P., Shultz, M. E., ud-Doula, A., et al. 2022, MNRAS, 513, 1449, doi: 10.1093/mnras/stac341

Panagia, N., & Felli, M. 1975, A&A, 39, 1

Paredes, J. M. 2005, in EAS Publications Series, Vol. 15, EAS Publications Series, ed. L. I. Gurvits, S. Frey, & S. Rawlings, 187–206, doi: 10.1051/eas:2005153

Parker, E. N. 1958, ApJ, 128, 677, doi: 10.1086/146580

Pattie, E., & Maccarone, T. 2025, in American Astronomical Society Meeting Abstracts, Vol. 245, American Astronomical Society Meeting Abstracts, 346.07D

Pattie, E. C., Maccarone, T. J., Tetarenko, A. J., et al. 2024, ApJ, 970, 126, doi: 10.3847/1538-4357/ad5842

Paulson, S. T., Mallick, K. K., & Ojha, D. K. 2024, MNRAS, 530, 1516, doi: 10.1093/mnras/stae917

Penzias, A. A., Solomon, P. M., Wilson, R. W., & Jefferts, K. B. 1971, ApJL, 168, L53, doi: 10.1086/180784

Pérez-Torres, M., Gómez, J. F., Ortiz, J. L., et al. 2021, A&A, 645, A77, doi: 10.1051/0004-6361/202039052

Phillips, R. B., & Lestrade, J. F. 1988, Nature, 334, 329, doi: 10.1038/334329a0

Pimpanuwat, B., Richards, A. M. S., Gray, M. D., Etoka, S., & Decin, L. 2024, in IAU Symposium, Vol. 380, Cosmic Masers: Proper Motion Toward the Next-Generation Large Projects, ed. T. Hirota, H. Imai, K. Menten, & Y. Pihlström, 386–388, doi: 10.1017/S1743921323002235

Pineda, J. S., Hallinan, G., & Kao, M. M. 2017, ApJ, 846, 75, doi: 10.3847/1538-4357/aa8596

Pineda, J. S., & Villadsen, J. 2023, Nature Astronomy, 7, 569, doi: 10.1038/s41550-023-01914-0

Pineda, J. S., Villadsen, J., Vidotto, A., & Bellotti, S. 2024, in AAS/Division for Extreme Solar Systems Abstracts, Vol. 56, AASTCS10, Extreme Solar Systems V, 617.13

Polidan, R. S., Burns, J. O., Ignatiev, A., et al. 2024, Advances in Space Research, 74, 528, doi: 10.1016/j.asr.2024.04.008

Polisensky, E., Das, B., Peters, W., et al. 2023, ApJ, 958, 152, doi: 10.3847/1538-4357/ad0295

Pritchard, J., Murphy, T., Heald, G., et al. 2024, MNRAS, 529, 1258, doi: 10.1093/mnras/stae127

Pritchard, J., Murphy, T., Zic, A., et al. 2021, MNRAS, 502, 5438, doi: 10.1093/mnras/stab299

Quiroga-Nunez, L. H., Pihlstrom, Y., Sjouwerman, L., Van Langevelde, H., & Brown, A. 2022, in American Astronomical Society Meeting Abstracts, Vol. 240, American Astronomical Society Meeting #240, 216.05

Rahman, M. M., McCauley, P. I., & Cairns, I. H. 2019, SoPh, 294, 7, doi: 10.1007/s11207-019-1396-8

Ramesh, R., Sasikumar Raja, K., Kathiravan, C., & Narayanan, A. S. 2013, ApJ, 762, 89, doi: 10.1088/0004-637X/762/2/89

Ramstedt, S., Mohamed, S., Olander, T., et al. 2018, A&A, 616, A61, doi: 10.1051/0004-6361/201833394

Ramstedt, S., Mohamed, S., Vlemmings, W. H. T., et al. 2014, A&A, 570, L14, doi: 10.1051/0004-6361/201425029

Ramstedt, S., Mohamed, S., Vlemmings, W. H. T., et al. 2017, A&A, 605, A126, doi: 10.1051/0004-6361/201730934

Reid, M. J., & Honma, M. 2014, ARA&A, 52, 339, doi: 10.1146/annurev-astro-081913-040006

Reid, M. J., & Menten, K. M. 1997, ApJ, 476, 327, doi: 10.1086/303614

Reid, M. J., & Menten, K. M. 2007, ApJ, 671, 2068, doi: 10.1086/523085

Richards, A. M. S., Asaki, Y., Baudry, A., et al. 2024, in IAU Symposium, Vol. 380, Cosmic Masers: Proper Motion Toward the Next-Generation Large Projects, ed. T. Hirota, H. Imai, K. Menten, & Y. Pihlström, 389–391, doi: 10.1017/S1743921323003095

Ridgway, S. T., Hall, D. N. B., Wojslaw, R. S., Kleinmann, S. G., & Weinberger, D. A. 1976, Nature, 264, 345, doi: 10.1038/264345a0

Rioja, M. J., Dodson, R., Orosz, G., Imai, H., & Frey, S. 2017, AJ, 153, 105, doi: 10.3847/1538-3881/153/3/105

Robrade, J., & Schmitt, J. H. M. M. 2009, A&A, 496, 229, doi: 10.1051/0004-6361/200811224

Rodriguez, L. F., Canto, J., & Moran, J. M. 1982, ApJ, 255, 103, doi: 10.1086/159808

Rodríguez, L. F., Masqué, J. M., Dzib, S. A., Loinard, L., & Kurtz, S. E. 2014, RMxAA, 50, 3, doi: 10.48550/arXiv.1309.4764

Rose, K., Pritchard, J., Murphy, T., et al. 2023, ApJL, 951, L43, doi: 10.3847/2041-8213/ace188

Saur, J., Grambusch, T., Duling, S., Neubauer, F. M., & Simon, S. 2013, A&A, 552, A119, doi: 10.1051/0004-6361/201118179

Schmid-Burgk, J. 1982, A&A, 108, 169

Seaquist, E. R., & Bode, M. F. 2008, in Classical Novae, ed. M. F. Bode & A. Evans, Vol. 43, 141–166, doi: 10.1017/CBO9780511536168.009

Sharma, R., & Oberoi, D. 2020, ApJ, 903, 126, doi: 10.3847/1538-4357/abb949

Sharma, R., Oberoi, D., Battaglia, M., & Krucker, S. 2022, ApJ, 937, 99, doi: 10.3847/1538-4357/ac87fc

Shiber, S., Chatzopoulos, E., Munson, B., & Frank, J. 2024, ApJ, 962, 168, doi: 10.3847/1538-4357/ad0e0a

Shimwell, T. W., Röttgering, H. J. A., Best, P. N., et al. 2017, A&A, 598, A104, doi: 10.1051/0004-6361/201629313

Shimwell, T. W., Tasse, C., Hardcastle, M. J., et al. 2019, A&A, 622, A1, doi: 10.1051/0004-6361/201833559

Shultz, M. E., Owocki, S. P., ud-Doula, A., et al. 2022, MNRAS, 513, 1429, doi: 10.1093/mnras/stac136

Siebert, M. A., Van de Sande, M., Millar, T. J., & Remijan, A. J. 2022, ApJ, 941, 90, doi: 10.3847/1538-4357/ac9e52

Singh, A. P., Richards, A. M. S., Humphreys, R. M., Decin, L., & Ziurys, L. M. 2023, ApJL, 954, L1, doi: 10.3847/2041-8213/ace7cb

Sjouwerman, L. O., Pihlström, Y. M., Lewis, M. O., et al. 2024, in IAU Symposium, Vol. 380, Cosmic Masers: Proper Motion Toward the Next-Generation Large Projects, ed. T. Hirota, H. Imai, K. Menten, & Y. Pihlström, 292–299, doi: 10.1017/S1743921323002958

Smith, N., Li, W., Foley, R. J., et al. 2007, ApJ, 666, 1116, doi: 10.1086/519949

Sokolovsky, K. V., Johnson, T. J., Buson, S., et al. 2023, MNRAS, 521, 5453, doi: 10.1093/mnras/stad887

Stock, J. W., Kitzmann, D., & Patzer, A. B. C. 2022, MNRAS, 517, 4070, doi: 10.1093/mnras/stac2623

Stock, J. W., Kitzmann, D., Patzer, A. B. C., & Sedlmayr, E. 2018, MNRAS, 479, 865, doi: 10.1093/mnras/sty1531
Stoop, M., de Koter, A., Kaper, L., et al. 2024, Nature, 634, 809, doi: 10.1038/s41586-024-08013-8
Stroh, M. C., Terreran, G., Coppejans, D. L., et al. 2021, ApJL, 923, L24, doi: 10.3847/2041-8213/ac375e
Sun, X., Török, T., & DeRosa, M. L. 2022, MNRAS, 509, 5075, doi: 10.1093/mnras/stab3249
Sundkvist, D. J., Saint-Hilaire, P., Bain, H. M., et al. 2016, in AGU Fall Meeting Abstracts, SH11C–2271
Tandoi, C., Guns, S., Foster, A., et al. 2024, ApJ, 972, 6, doi: 10.3847/1538-4357/ad58db
Tang, J., Tsai, C.-W., & Li, D. 2022, Research in Astronomy and Astrophysics, 22, 065013, doi: 10.1088/1674-4527/ac66bd
Tiede, P. 2022, The Journal of Open Source Software, 7, 4457, doi: 10.21105/joss.04457
Tingay, S. J., Oberoi, D., Cairns, I., et al. 2013, in Journal of Physics Conference Series, Vol. 440, Journal of Physics Conference Series (IOP), 012033, doi: 10.1088/1742-6596/440/1/012033
Townsend, R. H. D., & Owocki, S. P. 2005, MNRAS, 357, 251, doi: 10.1111/j.1365-2966.2005.08642.x
Trigilio, C., Leto, P., Leone, F., Umana, G., & Buemi, C. 2000, A&A, 362, 281, doi: 10.48550/arXiv.astro-ph/0007097
Trigilio, C., Leto, P., Umana, G., Buemi, C. S., & Leone, F. 2008, MNRAS, 384, 1437, doi: 10.1111/j.1365-2966.2007.12749.x
Trigilio, C., Leto, P., Umana, G., Buemi, C. S., & Leone, F. 2011, ApJL, 739, L10, doi: 10.1088/2041-8205/739/1/L10
Trigilio, C., Biswas, A., Leto, P., et al. 2023, arXiv e-prints, arXiv:2305.00809, doi: 10.48550/arXiv.2305.00809
Turner, B. E., & Ziurys, L. M. 1988, in Galactic and Extragalactic Radio Astronomy, ed. K. I. Kellermann & G. L. Verschuur, 200–254
Turner, J. D., Grießmeier, J.-M., Zarka, P., Zhang, X., & Mauduit, E. 2024, A&A, 688, A66, doi: 10.1051/0004-6361/202450095
Turner, J. D., Zarka, P., Grießmeier, J.-M., et al. 2021, A&A, 645, A59, doi: 10.1051/0004-6361/201937201
Tychoniec, Ł., van Dishoeck, E. F., van't Hoff, M. L. R., et al. 2021, A&A, 655, A65, doi: 10.1051/0004-6361/202140692
Umana, G., Buemi, C. S., Trigilio, C., et al. 2011, Bulletin de la Societe Royale des Sciences de Liege, 80, 335, doi: 10.48550/arXiv.1011.3730
Umana, G., Trigilio, C., Cerrigone, L., et al. 2015, in Advancing Astrophysics with the Square Kilometre Array (AASKA14), 118, doi: 10.22323/1.215.0118
Urquhart, J. S. 2024, in IAU Symposium, Vol. 380, Cosmic Masers: Proper Motion Toward the Next-Generation Large Projects, ed. T. Hirota, H. Imai, K. Menten, & Y. Pihlström, 135–151, doi: 10.1017/S1743921323002326
Uscanga, L., Imai, H., Gómez, J. F., et al. 2023, ApJ, 948, 17, doi: 10.3847/1538-4357/acc06f
van den Eijnden, J., Mohamed, S., Carotenuto, F., et al. 2024, MNRAS, 532, 2920, doi: 10.1093/mnras/stae1622
Van den Eijnden, J., Saikia, P., & Mohamed, S. 2022, MNRAS, 512, 5374, doi: 10.1093/mnras/stac823
van den Eijnden, J., Heywood, I., Fender, R., et al. 2022, MNRAS, 510, 515, doi: 10.1093/mnras/stab3395
Vedantham, H. K. 2020, A&A, 639, L7, doi: 10.1051/0004-6361/202038576
Vedantham, H. K., Callingham, J. R., Shimwell, T. W., et al. 2022, ApJL, 926, L30, doi: 10.3847/2041-8213/ac5115
Vedantham, H. K., Dupuy, T. J., Evans, E. L., et al. 2023, A&A, 675, L6, doi: 10.1051/0004-6361/202244965
Velilla-Prieto, L., Cernicharo, J., Agúndez, M., et al. 2019, A&A, 629, A146, doi: 10.1051/0004-6361/201834717
Velilla Prieto, L., Sánchez Contreras, C., Cernicharo, J., et al. 2017, A&A, 597, A25, doi: 10.1051/0004-6361/201628776
Villadsen, J., & Hallinan, G. 2019, ApJ, 871, 214, doi: 10.3847/1538-4357/aaf88e
Villadsen, J., Pineda, J. S., Bellotti, S., & Vidotto, A. 2025, in American Astronomical Society Meeting Abstracts, Vol. 245, American Astronomical Society Meeting Abstracts, 418.07
Vlemmings, W. H. T., Lankhaar, B., Cazzoletti, P., et al. 2019, A&A, 624, L7, doi: 10.1051/0004-6361/201935459
Vogt, S. S., Hatzes, A. P., Misch, A. A., & Kürster, M. 1999, ApJS, 121, 547, doi: 10.1086/313195
Wallström, S. H. J., Danilovich, T., Müller, H. S. P., et al. 2024, A&A, 681, A50, doi: 10.1051/0004-6361/202347632
Walter, H. G., Hering, R., & de Vegt, C. 1990, A&AS, 86, 357
Wang, Y., Murphy, T., Lenc, E., et al. 2023, MNRAS, 523, 5661, doi: 10.1093/mnras/stad1727
Wendker, H. J. 1978, Astronomische Abhandlungen der Hamburger Sternwarte, 10, 3
Wendker, H. J. 1987, A&AS, 69, 87
Wendker, H. J. 1995, A&AS, 109, 177
Wendker, H. J. 2015, VizieR Online Data Catalog: Catalogue of Radio Stars (Wendker, 2001),, VizieR On-line Data Catalog: VIII/99. Originally published in: 1995A&AS..109..177W
Wheeler, J. C., Nance, S., Diaz, M., et al. 2017, MNRAS, 465, 2654, doi: 10.1093/mnras/stw2893

White, S. M. 2000, in Radio interferometry : the saga and the science, ed. D. G. Finley & W. M. Goss, 86
White, S. M., Jackson, P. D., & Kundu, M. R. 1989, ApJS, 71, 895, doi: 10.1086/191401
White, S. M., Shimojo, M., Iwai, K., et al. 2024, ApJ, 969, 3, doi: 10.3847/1538-4357/ad4640
Wild, J. P. 1950, Australian Journal of Scientific Research A Physical Sciences, 3, 399, doi: 10.1071/CH9500399
Williams, M., Linford, J., Sokolovsky, K., et al. 2023, in American Astronomical Society Meeting Abstracts, Vol. 242, American Astronomical Society Meeting Abstracts #242, 109.06
Williams, P. K. G. 2018, in Handbook of Exoplanets, ed. H. J. Deeg & J. A. Belmonte, 171, doi: 10.1007/978-3-319-55333-7_171
Williams, P. K. G., Berger, E., & Zauderer, B. A. 2013, ApJL, 767, L30, doi: 10.1088/2041-8205/767/2/L30
Williams, P. K. G., Cook, B. A., & Berger, E. 2014, ApJ, 785, 9, doi: 10.1088/0004-637X/785/1/9
Williams, P. K. G., Gizis, J. E., & Berger, E. 2017, ApJ, 834, 117, doi: 10.3847/1538-4357/834/2/117
Wood, B. E., Müller, H.-R., Zank, G. P., & Linsky, J. L. 2002, ApJ, 574, 412, doi: 10.1086/340797
Wood, B. E., Müller, H.-R., Redfield, S., et al. 2021, ApJ, 915, 37, doi: 10.3847/1538-4357/abfda5
Wright, A. E., & Barlow, M. J. 1975, MNRAS, 170, 41, doi: 10.1093/mnras/170.1.41
Xia, T.-Y., Shen, J., Li, Z., et al. 2024, ApJ, 976, 139, doi: 10.3847/1538-4357/ad834f
Xu, S., Imai, H., Yun, Y., et al. 2022, ApJ, 941, 105, doi: 10.3847/1538-4357/ac9599
Yadav, R. K., & Thorngren, D. P. 2017, ApJL, 849, L12, doi: 10.3847/2041-8213/aa93fd
Yang, A. Y., Dzib, S. A., Urquhart, J. S., et al. 2023, A&A, 680, A92, doi: 10.1051/0004-6361/202347563
Yanza, V., Dzib, S. A., Palau, A., et al. 2025, MNRAS, 538, 1314, doi: 10.1093/mnras/staf344
Zack, L. N., Halfen, D. T., & Ziurys, L. M. 2011, ApJL, 733, L36, doi: 10.1088/2041-8205/733/2/L36
Zarka, P. 1992, Advances in Space Research, 12, 99, doi: 10.1016/0273-1177(92)90383-9
Zarka, P. 1998, J. Geophys. Res., 103, 20159, doi: 10.1029/98JE01323
Zhang, Q., Hallinan, G., Brisken, W., Bourke, S., & Golden, A. 2020, ApJ, 897, 11, doi: 10.3847/1538-4357/ab9177
Zijlstra, A., Pottasch, S. R., te Lintel Hekkert, P., & Bignell, C. 1989, in IAU Symposium, Vol. 131, Planetary Nebulae, ed. S. Torres-Peimbert, 210
Zijlstra, A. A., Gaylard, M. J., te Lintel Hekkert, P., et al. 1991, A&A, 243, L9
Zirin, H., Baumert, B. M., & Hurford, G. J. 1991, ApJ, 370, 779, doi: 10.1086/169861
Ziurys, L. M., Milam, S. N., Apponi, A. J., & Woolf, N. J. 2007, Nature, 447, 1094, doi: 10.1038/nature05905
Zucker, C., Goodman, A. A., Alves, J., et al. 2022, Nature, 601, 334, doi: 10.1038/s41586-021-04286-5

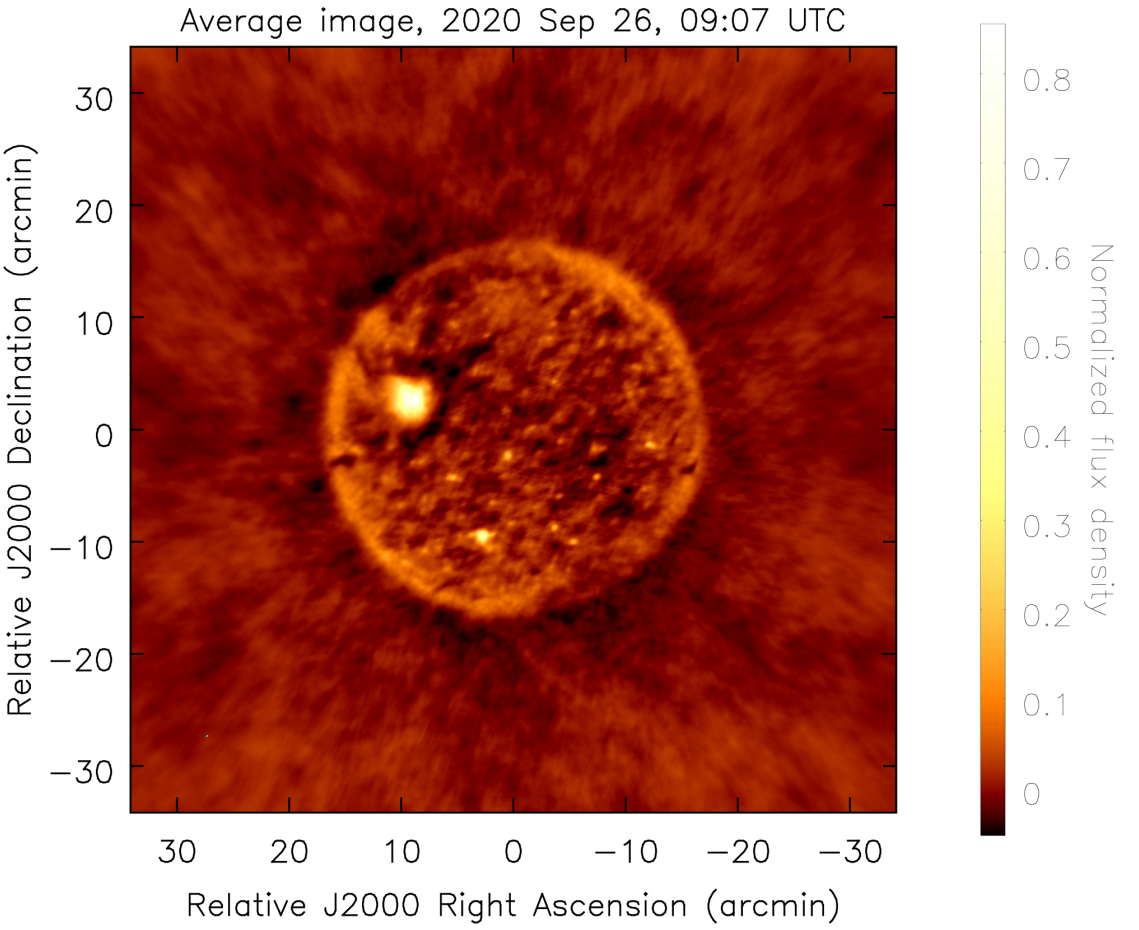

Figure 1. Snapshot image of the Sun obtain with MeerKAT on 2020 September 26 at 09:07 UTC. The image represents a normalized average over a 880–1670 MHz band. The angular resolution is $\sim 8''$, represented by a tiny dot in the bottom left corner of the panel. From D. Kansabanik et al. (2024b).

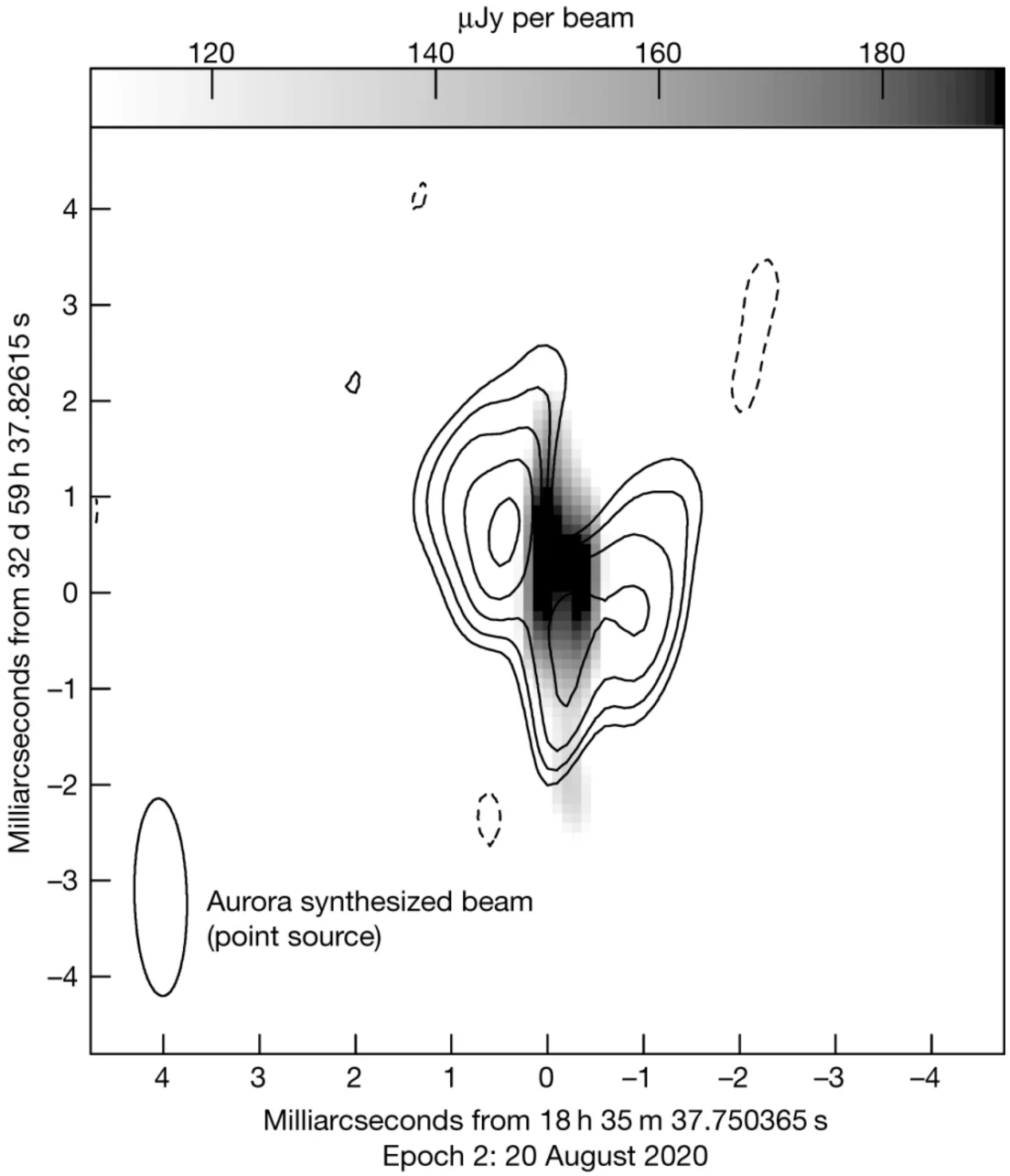

Figure 2. Right-circularly polarized auroral emission (greyscale) from the UCD LSR J1835+3259 as observed with the HSA at 8.4 GHz, overlaid on the separately imaged quiescent emission at the same frequency (contours). The contour levels are $(-1, 1, \sqrt{2}, 2, 2\sqrt{2}, 4) \times \sigma_{\rm RMS}$, where $\sigma_{\rm RMS} \approx 12 - 13 \mu$Jy beam^{-1}. The synthesized beam for the auroral observation is indicated by an ellipse in the lower left corner. The aurora appears centered within the double-lobed structure traced by the quiescent emission. Credit: M. M. Kao et al. (2023).

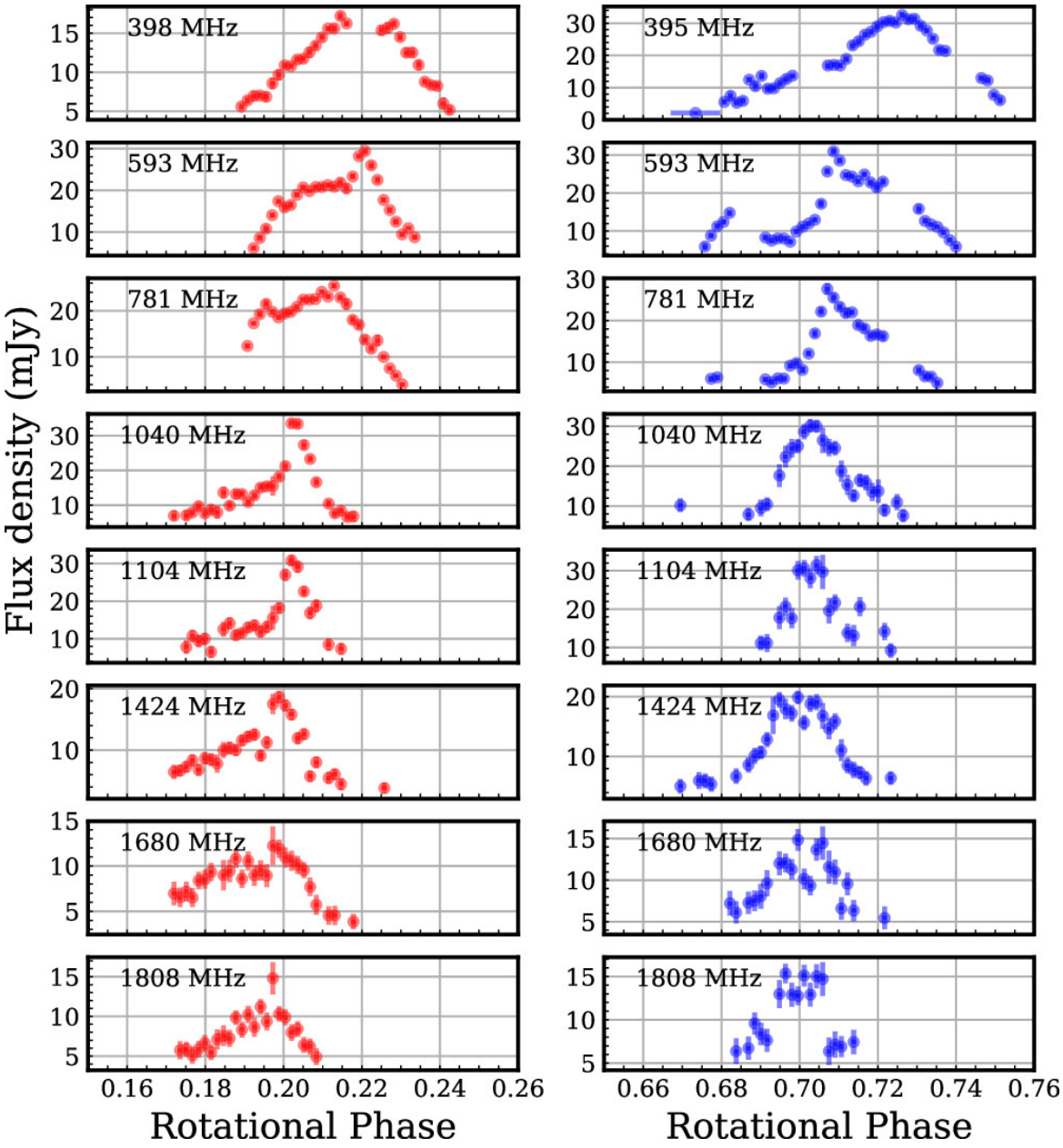

Figure 3. ECM pulses observed at several different frequencies (∼400–1800 MHz) from the magnetic massive star HD 133880. Data were obtained using the uGMRT and the VLA. Right circular polarization emission is shown in red (left panels, observed near the magnetic null at rotational phase 0.175) and left circular polarization is in blue (right panels). The pulses at different frequencies are seen shifted in rotational phase relative to one another, as they originate from different regions of the magnetosphere. Credit: B. Das et al. (2024).

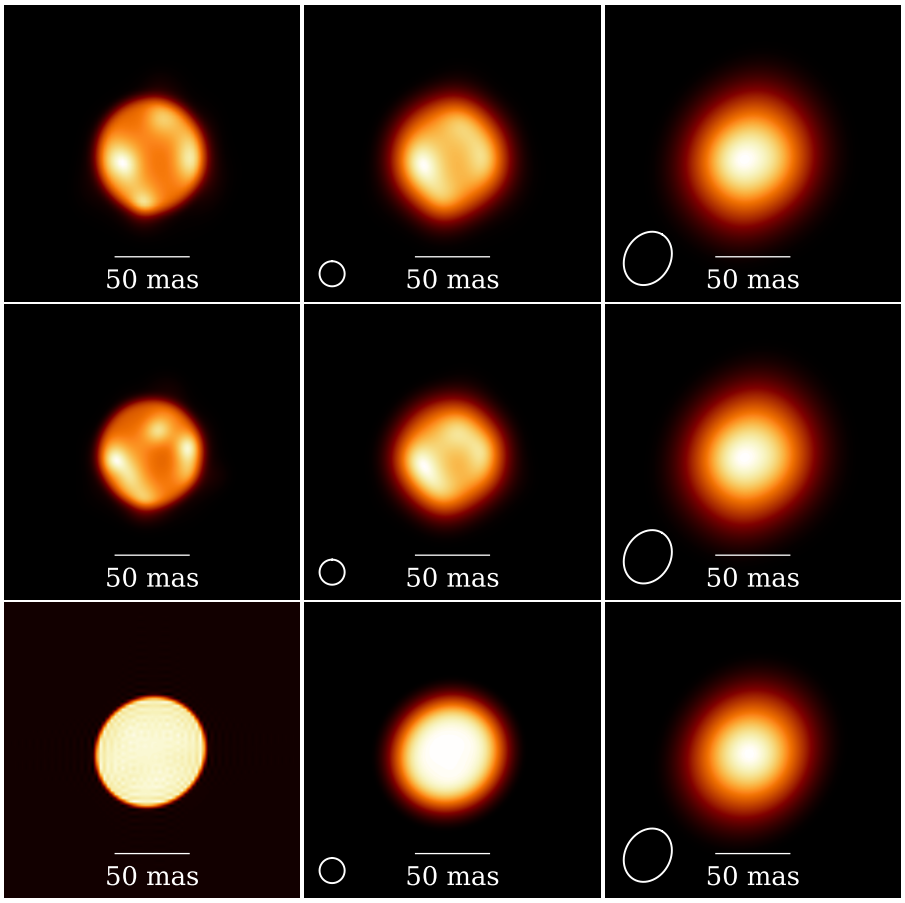

Figure 4. Super-resolved ALMA images of Betelgeuse at 107 GHz (top) and 136 GHz (middle row), obtained with the Bayesian interferometric imaging package Comrade.jl from P. Tiede (2022). Mean posterior images are shown, calculated using a prior based on a stationary Gaussian Markov random field model. The bottom row shows a reconstruction of a uniform disk model (with realistic noise) as a comparison. The center and right panels in each row show the reconstructions blurred by Gaussians. From L. D. Matthews, K. Akiyama, et al., in prep.

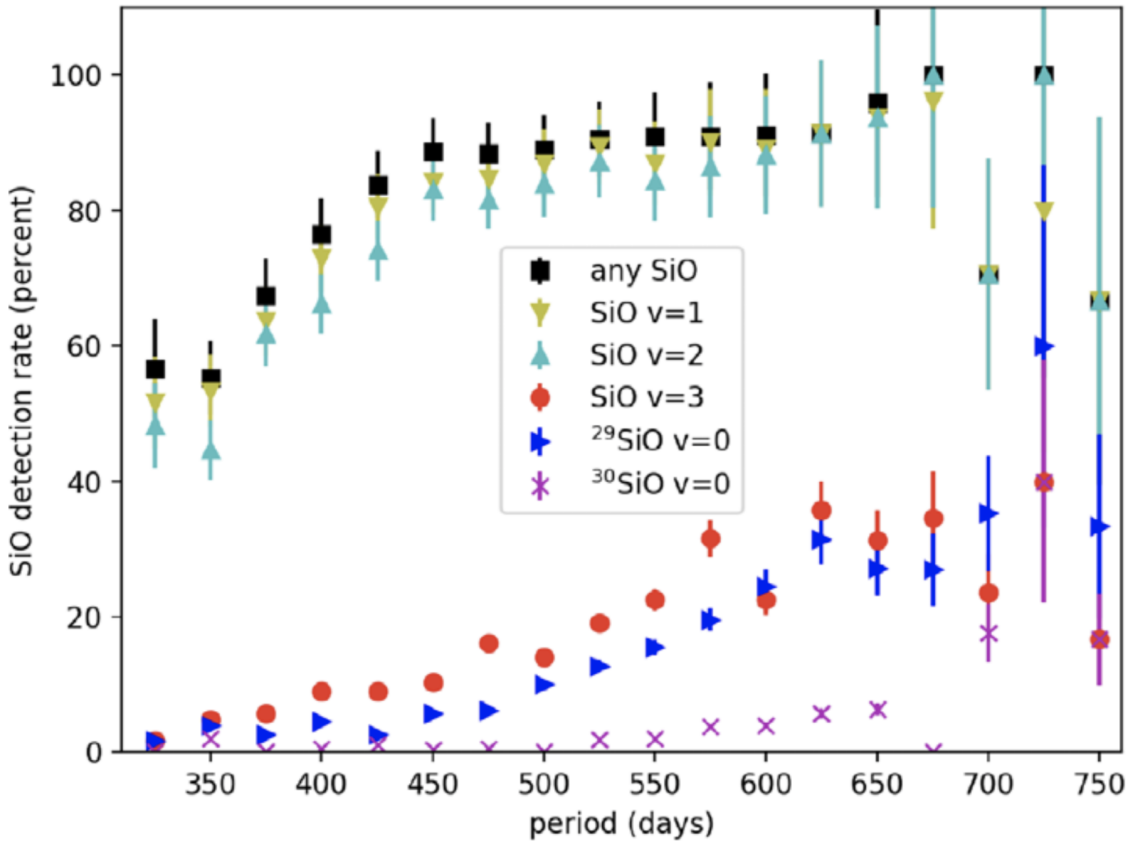

Figure 5. Detection rates as a function of stellar pulsation period of the five most commonly detected SiO transitions covered by the BAaDE survey sample of evolved stars (see Section 16). The SiO transition frequencies range from 42.3 to 43.4 GHz. Credit: M. O. Lewis et al. (2024).

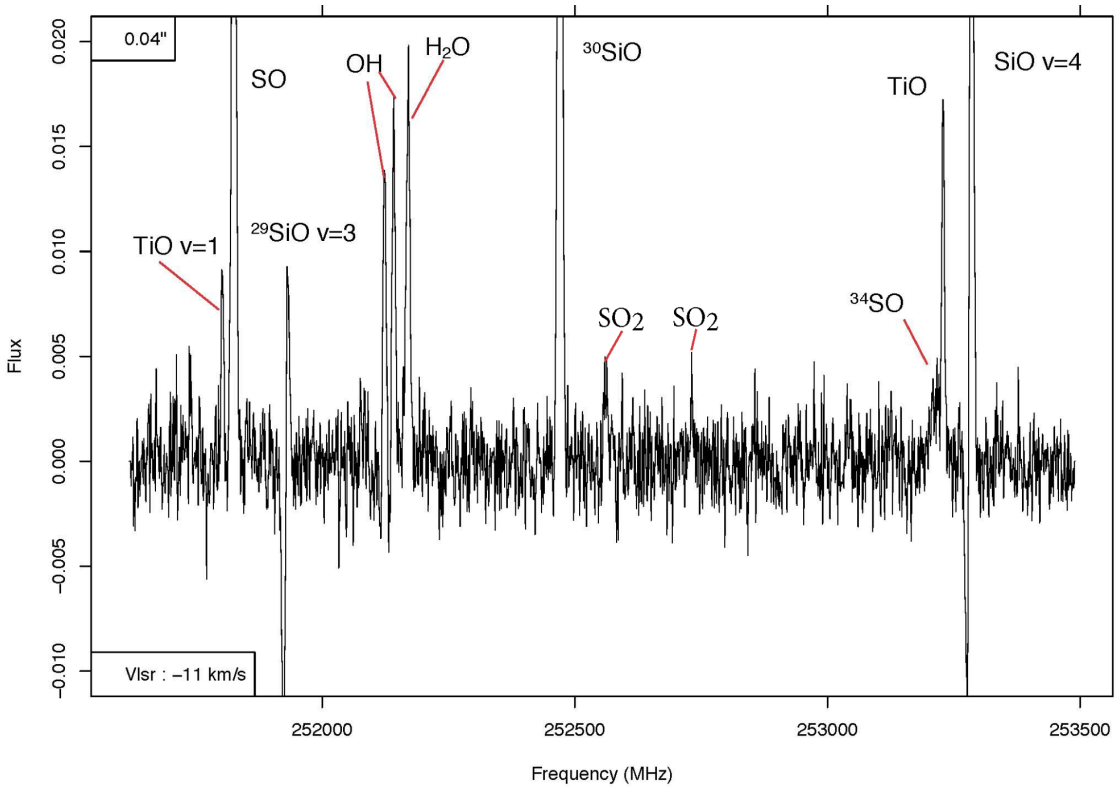

Figure 6. A sample portion of the ALMA spectrum of the oxygen-rich AGB star R Hya, obtained as part of the ATOMIUM project (see Section 9.2). The data were obtained using an extended array configuration, yielding angular resolution of ∼0.″04. Axes are flux density (in Jy) and frequency (in MHz). Identified molecular lines are labeled. Credit: L. Decin, C. A. Gottlieb, & A. M. S. Richards on behalf of the ATOMIUM consortium (see also S. H. J. Wallström et al. 2024).

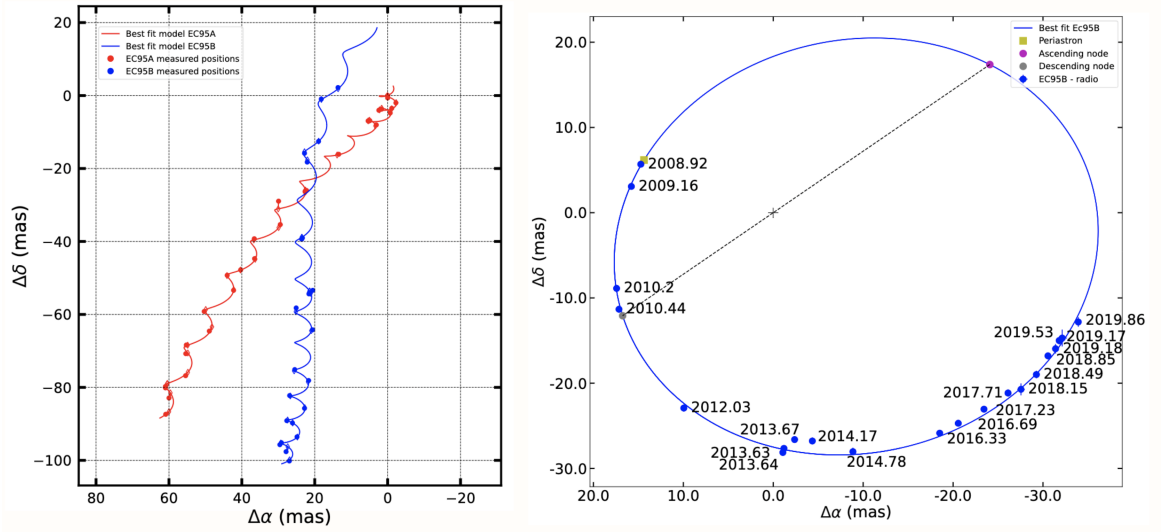

Figure 7. *Left:* Positions of EC95A (red dots) and EC95B (blue dots), two components of a young multiple star system, as measured with the VLBA at 4.9 GHz as part of the DYNAMO-VLBA project. The positions are shown as offsets relative to the position of EC95A as previously measured on 2007 December 22. *Right:* Relative positions together with the resulting orbital fit model. These observations permit mass and orbit determinations for the individual binary components. Credit: J. Ordóñez-Toro et al. (2025).

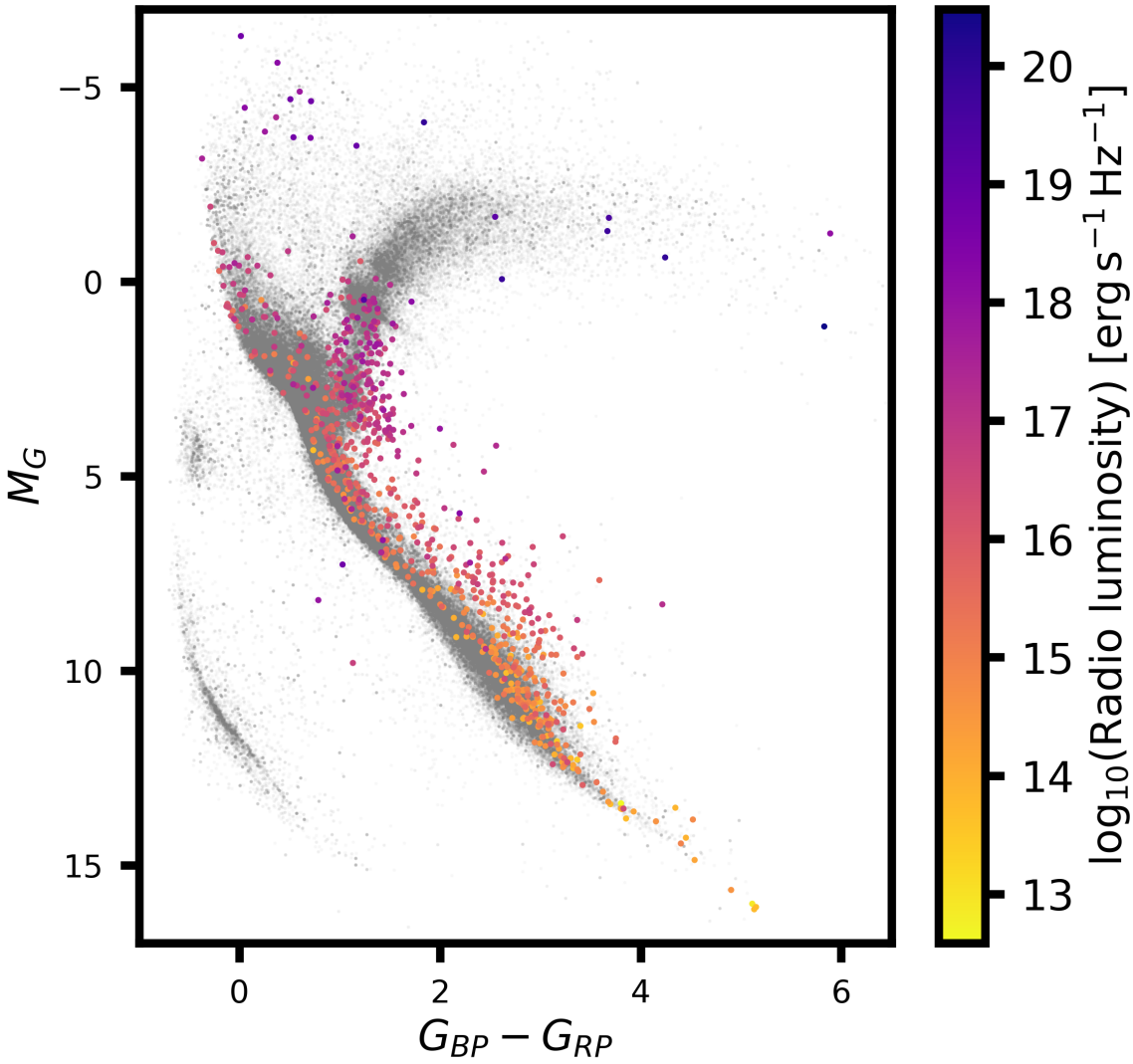

Figure 8. Color magnitude diagram (CMD) showing as colored symbols the radio stars in the SRSC compiled by Driessen et al. (2024). The color scale indicates the radio luminosity of each star assuming distances from *Gaia*. For reference, the grey background points show the CMD from *Gaia* Data Release 2, taken from Pedersen et al. (2019). Credit: L. N. Driessen et al. (2024).

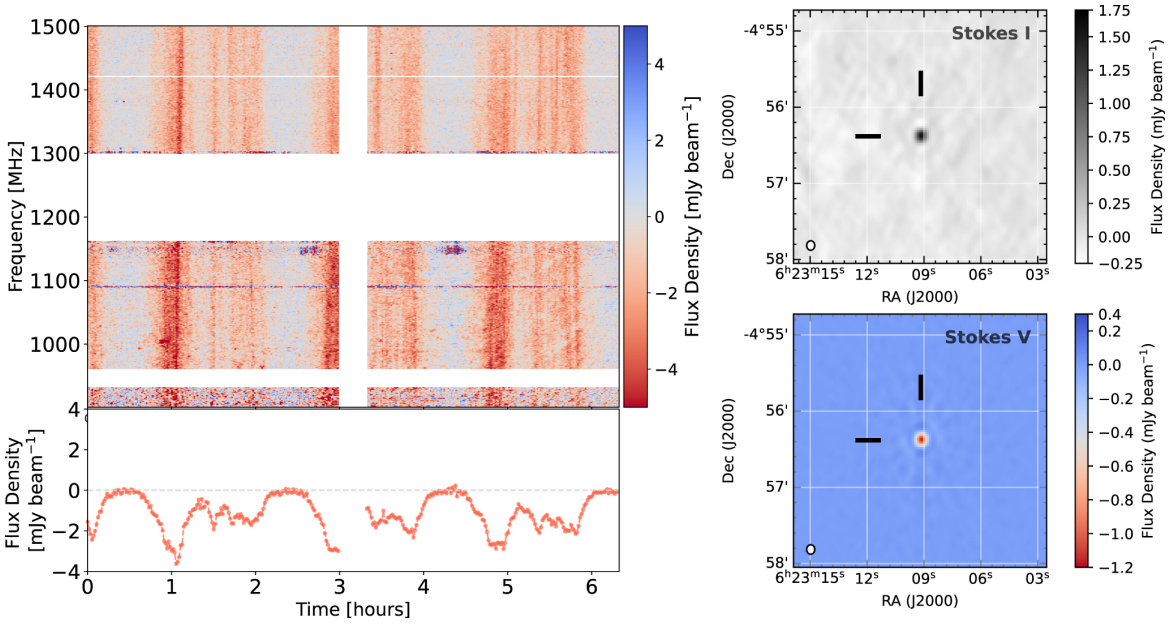

Figure 9. *Left:* Stokes V dynamic spectrum (0.9–1.5 GHz) of the T8 dwarf WISE J062309.94−045624.6, obtained with MeerKAT. The Stokes V light curve is shown in the lower panel (based on 1 MHz frequency bins and 64 s time sampling). Both the light curve and the dynamic spectrum show periodic behavior with additional complex structure. The horizontal gaps correspond to frequencies flagged due to RFI, while the vertical gap corresponds in time to a calibration scan. *Right:* Stokes I (top) and V (bottom) continuum detection images from the same observation. Credit: K. Rose et al. (2023).

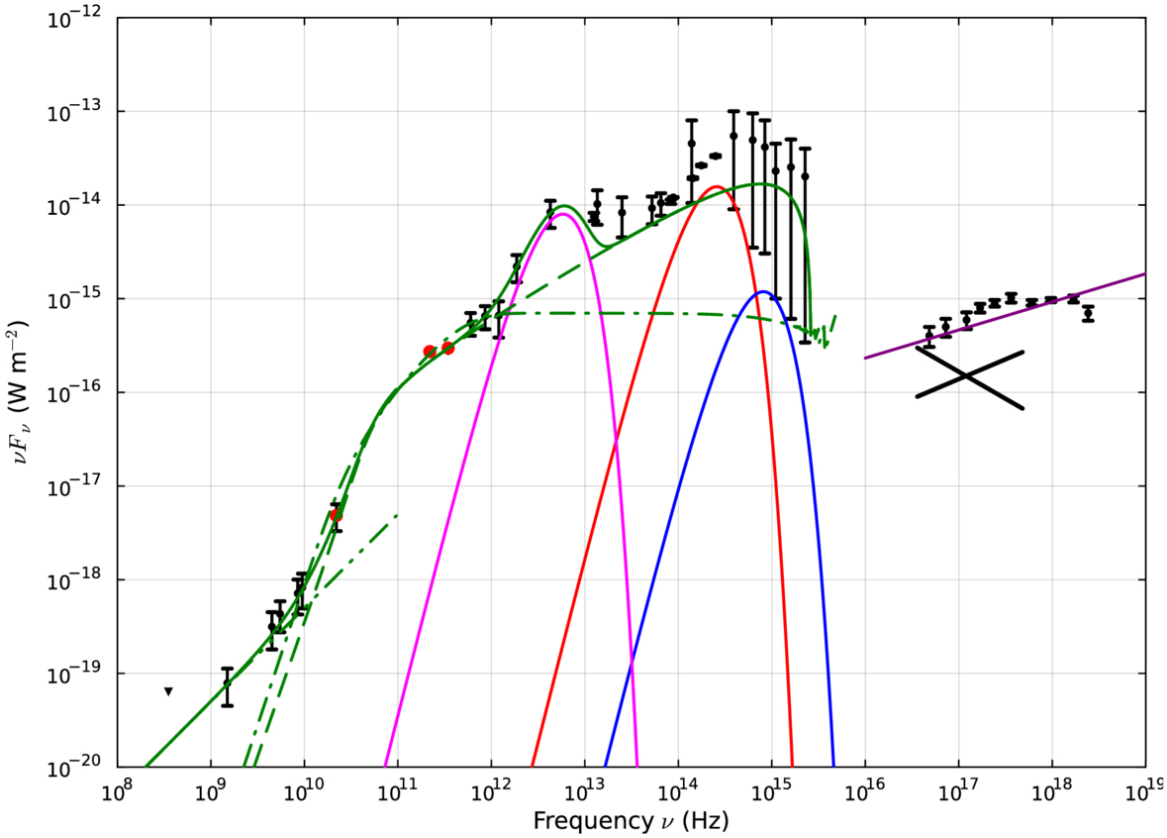

Figure 10. SED of the white dwarf pulsar AR Sco obtained from radio observations. The black points and lines are from previously published observations (see Barrett & Gurwell 2025 for details). The three red points show 22 GHz VLA data along with 220 and 345 GHz SMA data. The magenta, red, and blue curves represent, respectively, blackbody emission from cool (70 K) circumbinary dust, the red dwarf companion ($T_{\rm eff}$=3100 K), and the white dwarf primary ($T_{\rm eff}$=9750 K). The dashed and dot-dash green lines show, respectively, fast- and slow-cooling models for the synchrotron emission at $\nu > 10$ GHz. The dash–double dot green line is the ECM emission at $\nu < 10$ GHz, and the purple line indicates the X-ray emission (a power law). The solid green line shows the sum of all emission components. Credit: P. E. Barrett & M. A. Gurwell (2025).